UNIVERSITY OF CALIFORNIA, MERCED

Contribution of sources and sinks to the photochemistry of the present and past atmosphere of West Antarctica based on air, snow and ice-core records

A dissertation submitted in partial satisfaction of the requirements for the degree of Doctor of Philosophy

in

Environmental Systems

by

Sylvain Masclin

Committee in charge:

Professor Wolfgang F. Rogge, Chair
Professor Roger C. Bales
Professor Martha H. Conklin
Dr. Markus M. Frey

2014

The dissertation of Sylvain Masclin is approved, and it is acceptable in quality and form for publication on microfilm and electronically:

Roger C. Bales, Advisor

Martha H. Conklin

Markus M. Frey, Co-Advisor

Wolfgang F. Rogge, Chair

University of California, Merced

2014

ABSTRACT

A framework is presented for defining the present atmospheric chemistry of West Antarctica and the photochemistry of the atmosphere during the early- to mid-Holocene transition (9,000-6,000 yr BP). Little is known on the contributions of local and regional sources to the photochemical composition of the current atmosphere of West Antarctica and the early- to mid-Holocene atmosphere. Measurements over the West Antarctic continent were scarce in regards of exploring its present photochemical composition, while the contribution of the atmospheric oxidative capacity, namely OH radicals, to the methane decline over the early- to mid-Holocene has been assumed negligible. In this study, investigation of the present atmospheric chemistry was run during Antarctic summer at the WAIS Divide site, through multi-week continuous measurements of photochemical active species: atmospheric NO, O_3, H_2O_2, MHP, and snow NO_3^-, NO_2^- and H_2O_2. Then, estimation of the mixing ratios of past atmospheric oxidants from ice-core records was made possible from the latest findings on air-ice partition equilibrium of reversibly deposited species, HCHO and H_2O_2. Results from the West Antarctic campaign show that the levels of short-lived species above this region, such as NO_X, are driven by local sources, mainly snowpack emissions, whereas regional air mass transport controls the atmospheric concentrations of species with longer lifetime, such as O_3. Atmospheric estimates from the early- to mid-Holocene reveal that both methane sources and sink (low-latitude emissions and oxidation with OH) contributed to the CH_4 budget between 12,000-9,000 yr BP, whereas only the sources drove the decline of CH_4 between 9,000-6,000 yr BP.

DEDICATION

A Morgan
en mon coeur trouve ton refuge
de toi me viennent inspiration et courage
de nous puisons les rêves les plus inimaginables

EPIGRAPH

Fais de ta vie un rêve, et d'un rêve, une réalité.

Antoine de Saint-Exupéry

Happiness only real when shared.

Christopher McCandless, 1992

ACKNOWLEDGEMENTS

I would like first to thank my advisor, Roger Bales, who took me under his wing during this long academic journey. Through his supervision, expertise and guidance, I learnt and developed skills that reveal to be now true assets for the pursuit of my professional experience.

This journey all started with my encounter with Markus Frey at the Laboratoire de Glaciologie et Géophysique de l'Environnement. From then on, his mentoring has never stopped helping me structuring my research. Even if the distance between UC Merced and the British Antarctic Survey was not always easy to handle, I clearly come out of this PhD benefiting from his strong guidance and experience.

I also would like to thank my other committee members, Wolfgang Rogge and Martha Conklin. Wolfgang provided me precious help during the field preparation; his engineering and instrumental knowledge was an essential support to get the detectors ready prior deployment. His frequent visits in the lab have also been appreciated. While Martha is part of my committee, she is also the first professor with who I had the chance to TA for. I am thankful for the support and the trust she provided me along this first teaching experience.

I would like to extend my gratitude to all the people closely or remotely involved in this project. I have special thoughts for all the participants of the 2008-2009 WAIS Divide campaign and of the 2011 WAIS-Divide ice core analysis, especially Joe McConnell and his team of the Ultra-Trace Chemistry laboratory at DRI, Reno. Thanks also to Drew Shindell and his team at GISS, New York, for their significant contribution on the modeling part of this research.

This academic experience would not have been fully complete if I did not have the chance to teach. My acknowledgements go especially to Peggy O'Day, Laura Martin, Angela Winek, Anne Zanzucchi, and Belinda Braunstein who shared their time, their experience, and their teaching philosophy so I could define my own instruction style. Of course, I have a special thought to all the undergraduate students that I had the pleasure to instruct.

Many, Many, many thanks to all the good people, all my friends that have supported me over this experience, and the previous ones. Special thanks to my closest childhood friend, Marie-Hélène, and to the surviving people of the Antarctic overwintering of 2006 (TA56): Ariane, Sylvain and Pascal. Ariane, you were always there when the boat was sinking, thank you for your innumerable rescues! Finally thank you to all the people I met in Merced: the Laguna House people (Ale, John, Pedro, Chris, Marco & Alicia, Jane), Jesus, Alvaro, Shini & Kathrin, Josh, Coty, Sandra, Peter & Elsita, Fred & Lori, Julio & Vero, Joseph, the Shinty team, and all those who like my bread!

I do not have words strong enough to say how grateful I am to my family for all the sacrifices they made, and to let me go so far away from them. To my parents that I love so much and who are the best example I am trying so hard to follow, you give me so much that I won't never be able to pay you back! To my sister Daisy and her family (Damien, Victor and Maurine) that I miss so much; I wish I could spend much more time with them. Vous me manquez terriblement! To my grandmother, the strongest woman I know in this world. And to my "brother" and his family: Pierre-François, Emilie, Paul, Côme, and Noé. You highlight my world every time I am with you!

Finally, all my thanks, admiration and love go to the best outcome this 6 year journey in Merced gave me: my wife Liza and my son Ian (and of course my 4 girls Kyon, Angin, Xina, and Gaia). You opened me your arms and for that, I will eternally owe you. You provided more than the support I needed to complete this PhD, and you're giving me each day the reasons to keep dreaming and make these dreams come true. Je vous aime!

CURRICULUM VITAE

Sylvain Masclin

Environmental Systems
University of California, Merced
5200 North Lake Rd.
Merced, CA 95343

Mail: smasclin@ucmerced.edu
Phone: +1 209 628 7031

EDUCATION

2014 **Ph.D.** Environmental Systems, School of Engineering, UC Merced, Merced. USA.

Dissertation: Quantification of the different contributors in the present and early-mid Holocene atmospheric photochemistry above the West Antarctic Ice Sheet. Advisor: Roger C. Bales; Co-Advisor: Markus M. Frey.

2005 **M.S.** Geological and Environmental Sciences (STUE). Joseph Fourier University. Grenoble (38). France.

Thesis Master year 2: Formaldehyde remobilization during snow metamorphism, using chromatographic analyses, microscopic studies and measurement of apparent specific surfaces of snow grains measurements. Advisor: Florent Dominé; Co-Advisor: Stéphan Houdier. Laboratoire de Glaciologie et Geophysique de l'Environnement (LGGE). Grenoble. France.

Thesis Master year 1: Study of the sampling artefacts of the carbon fraction of aerosols for the POVA program, using Thermo-optical analyses. Advisor: Jean-Luc Jaffrezo. LGGE

2003 **B.S.** Geological and Environmental Sciences (STU). University of Sciences and Technologies of Lille. Villeneuve D'Ascq (59). France.

Report: Thermal calibration of the infrared radiometer CE 312. Advisor: Bahaiddin Damiri Laboratoire d'Optique Atmosphérique (LOA). Villeneuve D'Ascq.

WORKSHOP / INTERNATIONAL COURSE

2011, June: Third Air-Ice Chemical Interactions (AICI) Workshop. Columbia University, New York, USA.

Forum with the purpose to bring together new insights from AICI studies over the last 8 years with topics including: snow (photo)chemistry, the role of halogens in polar regions, tropospheric ozone and mercury depletion, and the resulting chemistry of the lower troposphere and upper snowpack.

2010, Jan. to Feb. European Research Course on Atmospheres (ERCA). Grenoble. France.

High level international course on the Physics and Chemistry of the atmosphere of the Earth plus stellar and non-stellar bodies, on the climate system and climate change, on atmospheric pollution at different scales and on the human dimensions of environmental changes.

PROFESSIONAL EXPERIENCE

2007, June to Dec. — **Chemical analysis engineer.**
Work for Martine De Angelis. Laboratoire de Glaciologie et Geophysique de l'Environnement (LGGE). Grenoble. France.

Setup of a new ionic chromatography (IC) system, contribution to the analytical development and high-resolution chemical analyses of ice samples from deep Greenland ice-cores. Work in cold room for the sample preparation and in clean room for sample analysis.

2007, May to June — **Lab Technician in atmospheric chemistry.**
Work for Michel Legrand, Susanne Preunkert and Bruno Jourdain. LGGE.

Filtration and IC analyses of atmospheric samples collected during prior over wintering campaigns at Dumont D'Urville Station, Antarctica.

2005 to 2007, 15 months — **Lab technician in atmospheric chemistry.**
Work for Michel Legrand, Susanne Preunkert, Joel Savarino and Christophe Genthon. LGGE and IPEV. Dumont D'Urville Station. Antarctica.

Ionic and gas phase chromatography analyses of daily atmospheric samples to study the sulfur cycle in Antarctica. Weekly oxygen and nitrogen isotopic samplings. Monthly mass balance surveys of the glacier surrounding Cap Prud'Homme station.

TEACHING EXPERIENCE

Summer 2014 — **TA for CHEM10: General Chemistry.**
Professor: Thomas Giagou. UC Merced, Merced, USA.

Spring 2014 — **TA for ESS/ENVE10: Earth Resources and Society.**
Professor: Asmeret Asefaw Berhe. UC Merced, Merced, USA.

Fall 2013 — **TA for ESS/ENVE100: Environmental Chemistry.**
Professor: Peggy O'Day. UC Merced, Merced, USA.

Fall 2013 — **Participation in the Council for Graduate Schools program: "Undergraduate learning outcomes assessment: pedagogy and program planning."**
Project leaders: Angela Winek, Anne Zanzucchi, Laura Martin. UC Merced, Merced, USA.

Fall 2012 — **TA for ESS/ENVE100: Environmental Chemistry.**
Professor: Martha Conklin. UC Merced, Merced, USA.

PUBLICATIONS

2014 — Ice-core formaldehyde and hydrogen peroxide: markers of the decline in atmospheric methane over the early- to mid-Holocene, 9,000-6,000 years BP, Masclin, S., Frey, M. M., Shindell, D. T., McConnell, J. R., Bales, R. C., in prep.

2013 — Atmospheric nitric oxide and ozone at the WAIS Divide deep coring site: a discussion of local sources and transport in West Antarctica, Masclin, S., Frey, M. M., Rogge, W. F., Bales, R. C., Atmos. Chem. Phys., 13, 8857–8877, doi:10.5194/acp-13-8857-2013.

2012 — Organics in environmental ices: sources, chemistry, and impacts, McNeill, V. F., Grannas, A. M., Abbatt, J., Ammann, M., Ariya, P., Bartels-Rausch, T., Dominé, F., Donaldson, D. J., Guzman, M. I., Heger, D., Kahan, T., Klán, P., Masclin, S.,

Toubin, C., Voisin, D., Atmos. Chem. Phys., 12, 9653-9778, doi:10.5194/acp-12-9653-2012, 2012.

CONFERENCES AND SYMPOSIA

Feb. 2013 — NO and O_3 in West Antarctica – Contributions of atmospheric circulation and snowpack emissions, Masclin S.
Environmental Systems Seminar, UC Merced, Merced, USA.

Sept. 2011 — Investigation of boundary layer photochemistry at the WAIS-Divide site through measurement of major photochemically active species in snow and air, Masclin, S., Frey, M. M., Rogge, W. F., Bales, R. C.
WAIS Divide meeting, La Jolla, USA.

Aug. 2011 — Estimation of nitrate photolysis in the snowpack of the WAIS-Divide site and its contribution to measured atmospheric nitric oxide budget, Masclin, S., Frey, M. M., Rogge, W. F., Bales, R. C.
ACS Fall National Meeting, Division of Environmental Chemistry, Denver, USA.

Mar. 2009 — Photo exhibition and public seminar on the Antarctic summer field campaign 2008-2009.
UC Merced research week, Merced, USA.

Dec. 2007 — Public seminar describing the 2006 wintering in Antarctica.
LGGE, Grenoble and Merris, France.

POSTERS

June 2011 — Investigation of the boundary layer photochemistry at the WAIS-Divide site through measurement of major photochemically active species in snow and air, Masclin, S., Frey, M. M., Rogge, W. F., Bales, R. C.
3rd Workshop on Air-Ice Chemical Interactions (AICI), New York, USA.

Apr. 2011 — Estimation of the nitrate photolysis in the snowpack of the WAIS-Divide site and its contribution to measured atmospheric nitric oxide budget, Masclin, S., Frey, M. M., Rogge, W. F., Bales, R. C.
UC Merced research week, Merced, USA.

Dec. 2010 — NO_x emission from snowpack at the WAIS-Divide site and its impact on local tropospheric photochemistry, Masclin, S., Frey, M. M., Rogge, W. F., Bales, R. C.
2010 AGU Fall meeting, San Francisco, USA.

Sept. 2010 — Investigation of the boundary layer photochemistry at the WAIS-Divide site, Masclin, S., Frey, M. M., Rogge, W. F., Bales, R. C.
2010 WAIS Divide meeting, La Jolla, USA.

June 2010 — Investigation of the atmospheric chemistry at the WAIS-Divide site in West Antarctica and implications for atmospheric oxidation capacity, Masclin, S., Frey, M. M., Rogge, W. F., Bales, R. C.
2010 International polar year Oslo Science Conference, Oslo, Norway.

Dec. 2009 — First measurements of nitric oxide and ozone at the WAIS-Divide site and implications for atmospheric oxidation, Masclin, S., Frey, M. M., Rogge, W. F., Bales, R. C.
2009 AGU Fall meeting, San Francisco, USA.

Oct. 2009 First measurements of nitric oxide (NO) and ozone (O_3) at the WAIS-Divide site, Masclin, S., Frey, M. M., Rogge, W. F., Bales, R. C.
2009 WAIS Divide meeting, La Jolla, USA.

May 2009 Scientific poster "Atmospheric, snow and firn chemistry studies for interpretation of WAIS Divide Ice-core", Masclin, S., Frey, M. M., Rogge, W. F., Bales, R. C.
2009 UC Merced Commencement Day, Merced, USA.

SKILLS

Software Competencies

Technical programs: Latex, Keynote, Papers, Illustrator, Dreamweaver

Statistical and Analysis tools: Excel, R, Igor Pro, SigmaPlot, Matlab

Atmospheric and Photochemistry models: NOAA Hysplit model, TUV radiation model

GIS and Mapping applications: GMT, NASA GISS Panoply

Language Proficiency

English, French, and Spanish: Fluent (speaking, reading, writing)

TABLE OF CONTENTS

LIST OF FIGURES

Chapter 1:

Chapter 2:

Chapter 3:

LIST OF TABLES

Chapter 2:

Chapter 3:

CHAPTER 1:

INTRODUCTION

1 Context

Atmospheric composition is controlled by the emissions, photochemistry and transport of a wide variety of gas traces. Over the last centuries, greenhouse gases in the atmosphere have significantly changed in response to an increase of anthropogenic emissions and their impact on biogenic emissions. From its isolated geographical location, Antarctica is a unique ice-covered continent free from any significant biogenic and any anthropogenic emissions. It is then the only continent to offer a pristine environment for making measurements of a natural and remote atmosphere. Long- and short-lived atmospheric-oxidation products over the continent can also be deposited into the snowpack and preserved in the ice (e.g. formaldehyde (HCHO) or hydrogen peroxide (H_2O_2)), or directly trapped in air bubbles enclosed in ice (e.g. methane (CH_4) or carbon dioxide (CO_2)), providing potential markers of a past atmospheric composition.

Campaigns of atmospheric and snow measurements have been done over the Antarctic continent, including at coastal sites (Halley, Neumayer, Dumont D'Urville) and the interior of the continent (South Pole, Dome C) (Grannas et al., 2007).

Though these investigations, the shallow boundary layer overlying the East Antarctic Plateau was identified as a strongly oxidizing environment where high levels of NO_X – nitric oxide (NO) + nitrogen dioxide (NO_2) – from snowpack emissions (Davis et al., 2004) cause the conversion of peroxyradicals (HO_2) to hydroxyl radicals (OH) (Mauldin et al., 2004), and enhance ozone (O_3) production through NO_2 to NO conversion (Helmig et al., 2008).

Halogens released within the Sea Ice Zone of coastal Antarctica modify the atmospheric oxidizing capacity by driving O_3 depletion, increasing the NO_2 to NO ratio and decreasing the HO_2/OH ratio (Saiz-Lopez et al., 2007).

The only investigation of the boundary-layer photochemistry of West Antarctica's interior revealed that changes in stratospheric ozone modulate the NO_X chemistry, which in return controls the production rate of OH and H_2O_2 (Frey et al., 2005). Their photochemical modeling suggest that atmospheric H_2O_2 is sensitive to atmospheric NO concentrations, indicating the potential to use ice-core records of H_2O_2 to infer the oxidative capacity of past atmospheres by constraining past NO_X and OH levels. This study, carried out during the ITASE-Traverses, did not include measurements of NO_X, however, and investigated the atmospheric composition of the West Antarctic Ice Sheet (WAIS) at dispersed locations during three consecutive summers.

Few attempts have been made to reconstruct from the ice-core-records past atmospheric concentrations of photochemical active species such as H_2O_2. From the analysis of the H_2O_2 preserved in 23 shallow ice-cores between WAIS and South Pole, Frey et al. (2006) tested their air-snow transfer model previously applied at Summit, Greenland and South Pole, and showed that changes in the accumulation rate control the

H_2O_2 ice-core record, while recent changes in annual temperature had a negligible effect on its preservation. Computing their semi-empirical model of air-snow H_2O_2 transfer with estimates of effective annual mean atmospheric mixing ratio of H_2O_2, the authors were able to reconstruct the H_2O_2 ice-core records measured at almost all sites, concluding that their semi-empirical model could be applied for any Antarctic sites with a high accumulation rate and low temperature. In their study, Lamarque et al. (2011) did not directly infer the atmospheric H_2O_2 from its record in ice, but they investigated the changes of ice-core H_2O_2 with the H_2O_2 outputs from the atmospheric chemistry and climate models CAM-Chem and G-PUCCINI. Their results show that ice-core H_2O_2 is driven by changes in the total O_3 column, mainly related to changes in stratospheric O_3.

Assuming a steady state between chemical production and loss of HCHO, Staffelbach et al. (1991) proposed a formula that leads us to calculate the concentrations of atmospheric OH, knowing those of HCHO and CH_4. Based on the changes in the HCHO/CH_4 ratio observed in Greenland ice-cores, the authors estimated a decrease of OH concentrations from the pre-industrial period to today. While this relationship raised a lot of interest in the use of ice-core records of HCHO and CH_4 as markers of the oxidative capacity of past atmospheres, the post-depositional processes affecting HCHO – revolatilization and photochemical production – make its interpretation difficult (Levine et al., 2011; Wolff et al., 2007). Both studies concluded that even if a correct atmospheric HCHO and OH were estimated, it would not provide information on the changes in oxidative capacity on a global scale.

While the estimation of HCHO production in the surface snowpack remains a challenge, several studies have investigated or vapor-ice equilibriums of HCHO. Betterton and Hoffmann (1988) determined the vapor-liquid equilibrium of HCHO by calculating a Henry's Law constant for a HCHO concentration of 1.1×10^{-3} mol L^{-1}, but the concentration dependence of this constant limits its application. Burkhart et al. (2002) calculated an ice-air partitioning coefficient of HCHO by exposing laboratory-made snow to a HCHO atmosphere over a 2-day period, but results from Perrier et al. (2003) suggest that this snow had not reached thermodynamic equilibrium. In a recent study, Barret et al. (2011b) investigated the thermodynamics of the partitioning of HCHO between the gas phase and the ice and liquid water phase. They proposed a new formulation of the thermodynamic equilibrium of HCHO in ice to predict the mole fraction of HCHO in ice, and its application to the existing data on air-ice partitioning confirmed that the snow analyzed by Burkhart et al. (2002) was not at thermodynamic equilibrium. While the authors point to the need for determining the physical properties of snow such as specific surface area (SSA), their atmospheric HCHO estimates from daily snow samples match the actual measured atmospheric concentrations. With additional measurements of SSA of snow samples, Barret et al. (2011a) calculated estimates of atmospheric HCHO in good agreement with observations, suggesting that the air-ice partitioning equilibrium of Barret et al. (2011a) and Burkhart et al. (2002) could be a potential tool for inferring past atmospheric HCHO concentrations from ice-core records, and evaluating the oxidative capacity of past atmospheres.

The application of these tools from ice-core records of H_2O_2 and HCHO can provide further and additional interpretation of changes in past atmospheric composition, such as the changes in CH_4 concentrations over the Holocene illustrated in Figure 1.

For the period between the Last Glacial Maximum (~20,000 years before present (yr BP)) and the Pre-Industrial period (~200 yr BP), the contributors of the CH_4 increase are still debated (Murray et al., 2014, and references therein). All the studies point however to a major contribution of the CH_4 sources, such as orbitally driven emissions from tropical wetlands, rather than a contribution of its sinks, mainly CH_4 oxidation with OH.

For the mid- to late-Holocene period (~5,000 yr BP to present), there is still debate on a possible contribution of early anthropogenic activities in the rise of CH_4 concentrations (Ruddiman, 2013, and references therein; Schmidt et al., 2005).

Finally, only few studies have focused on the early- to mid-Holocene (~10,000 to ~6,000 yr BP). Blunier et al. (1995) and Mayewski et al. (2004) mainly suggested that the decrease of atmospheric CH_4 over this period was caused by a reduction of its sources during an arid low-latitude climate, and they considered negligible the contribution of its sink with OH.

2 Objectives

The purpose of this work was to develop a better understanding of the current and past atmospheric chemistry in the interior of West Antarctica, its current interactions with the snowpack and its response to regional contributions. This research was first motivated by the sparseness of the spatial data coverage of the boundary layer in Antarctica. Second, recent findings on the air-ice equilibrium of HCHO and H_2O_2 may offer the potential of evaluating the changes in oxidative capacity of paleoatmospheres from ice-core records. Finally, the interpretation of these proxies can possibly lead to a more detailed investigation of the CH_4 decrease over the early- to mid-Holocene. Four key questions will be addressed in the following chapters:

1) What is the summer composition of the boundary layer in the interior of West Antarctica? (Chapter 2)

2) How do local sources and regional sources contribute to the atmospheric chemistry of short and long-lived atmospheric species in the WAIS region? (Chapter 2)

3) Can reliable past-atmospheric concentrations of HCHO and H_2O_2 be inferred from ice-core records? (Chapter 3)

4) How can HCHO and H_2O_2 ice-core records be used to interpret changes in past atmospheric CH_4? (Chapter 3)

3 Methods

The investigation of the West Antarctic atmospheric chemistry took place at the WAIS Divide ice-core site (79.467° S, 112.085° W, 1766 m a.m.s.l.) with deployment between December 2008 and January 2009. The WAIS Divide site is a seasonal field campsite that opened in 2005 with the main objective of drilling a deep ice-core with resolution equivalent to those from Greenland, allowing for detailed study of greenhouse-gas concentrations of paleoatmospheres and exhaustive comparison of the climatic and environmental conditions between the southern and northern hemispheres. Its closing is scheduled for 2018. The temporary laboratory, a Polarhaven tent, was set up in the clean area, about 5 km NW of the main campsite, and vehicle access was tightly restricted. The electric generators were located about 30 m downwind from the tent, and the exhaust from the preway heater was located on the top of the tent.

Continuous atmospheric measurements of NO, O_3, ROOH and HCHO were made with the ambient air sampled 1 m above snow, 12 m upwind from the tent for ROOH and 20 m upwind for NO and O_3. The ambient air was pulled at about 1.4 STP L min^{-1} through an insulated and heated PFA (1/4" I.D.) before analytical detection in the ~20°C heated tent. Concentrations of NO_3^-, NO_2^- and H_2O_2 in snow were measured from top 1-cm surface snow sampled on a daily basis and from shallow snow pits of about 30-cm depth. All of the snow samples were stored in 100-mL SCHOTT bottles and kept frozen until their analysis in the laboratory at UC Merced after the campaign.

A detailed description of the instruments is given in Chapter 2 for NO, O_3, ROOH, NO_3^- and NO_2^-. The analytical instrument used to measured atmospheric HCHO is similar to the one that Hutterli et al. (1999) used at Summit, Greenland, but the instability of the coil temperature interfered with the acquisition of reliable data, so they were discarded. In brief, all of the instruments were calibrated daily (every 2 hours for the NO instrument) and limits of detection were 5 pptv, 1ppbv, 87 pptv and 167 pptv for NO, O_3, H_2O_2 and MHP, respectively. For the snow-sample analysis, the limit of detection was 0.4 ppbw for NO_3^-, NO_2^- and H_2O_2.

The 462.05 m section of the WAIS Divide ice-core, between a depth of 1,301.92 and 1,763.97m, was analyzed at the Ultra Trace Chemistry Laboratory at the Desert Research Institute (DRI, Reno, Nevada) in March 2011, after its processing at the National Ice-core Laboratory (NICL, Colorado). The ice-core section was analyzed using the Continuous Flow Analysis-Trace Elements Dual coupled to a single particle soot photometer, described by Sigl et al. (2013) and Banta et al. (2008). These instruments were also coupled to our formaldehyde detector, which is described in Chapter 3. The instruments were calibrated on a daily basis and their limits of detection were 0.29 ppbw and less than 1 ppbw for HCHO and H_2O_2, respectively.

Paleoatmospheric concentrations of photochemically active species and atmospheric oxidants were estimated from the ice-core records of the 462.05 m section, and from model runs at 6,000 and 9,000 ka. Estimation of past atmospheric HCHO and H_2O_2 from the ice-core was based on the recent air-ice equilibrium functions of HCHO (Barret et al., 2011b) and of H_2O_2 (Frey et al., 2006); paleoatmospheric OH was inferred using the atmospheric concentrations of HCHO and CH_4 in the formula proposed by Staffelbach et al. (1991) (see Chapter 3). Estimation of the past atmospheric chemistry

from the model was obtained the runs of the latest Goddard Institute for Space Studies Global Climate Model ModelE2 described in Chapter 3.

4 References

Banta, J. R., Mcconnell, J. R., Frey, M. M., Bales, R. C. and Taylor, K.: Spatial and temporal variability in snow accumulation at the West Antarctic Ice Sheet Divide over recent centuries, J Geophys Res, 113(D23), 1–8, doi:10.1029/2008JD010235, 2008.

Barret, M., Domine, F., Houdier, S., Gallet, J.-C., Weibring, P., Walega, J., Fried, A. and Richter, D.: Formaldehyde in the Alaskan Arctic snowpack: Partitioning and physical processes involved in air-snow exchanges, J Geophys Res- Atmos, 116(D18), n–a–n–a, doi:10.1029/2011JD016038, 2011a.

Barret, M., Houdier, S. and Domine, F.: Thermodynamics of the Formaldehyde-Water and Formaldehyde-Ice Systems for Atmospheric Applications, J Phys Chem A, 115(3), 307–317, doi:10.1021/jp108907u, 2011b.

Betterton, E. A. and Hoffmann, M. R.: Henry's law constants of some environmentally important aldehydes, Environ Sci Technol, 22(12), 1415–1418, doi:doi: 10.1021/es00177a004, 1988.

Blunier, T., Chappellaz, J., Schwander, J., Stauffer, B. and Raynaud, D.: Variations in Atmospheric Methane Concentration During the Holocene Epoch, Nature, 374(6517), 46–49, 1995.

Burkhart, J. F., Hutterli, M. A. and Bales, R. C.: Partitioning of formaldehyde between air and ice at-35 degrees C to-5 degrees C, Atmos Environ, 36(13), 2157–2163, 2002.

Davis, D. D., Chen, G., Buhr, M., Crawford, J. H., Lenschow, D., Lefer, B., Shetter, R., Eisele, F., Mauldin, L. and Hogan, A.: South Pole NO_x chemistry: an assessment of factors controlling variability and absolute levels, Atmos Environ, 38(32), 5375–5388, doi:10.1016/j.atmosenv.2004.04.039, 2004.

Frey, M. M., Bales, R. C. and Mcconnell, J. R.: Climate sensitivity of the century-scale hydrogen peroxide (H_2O_2) record preserved in 23 ice cores from West Antarctica, J Geophys Res- Atmos, 111(D21), D21301, doi:10.1029/2005JD006816, 2006.

Frey, M. M., Stewart, R. W., Mcconnell, J. R. and Bales, R. C.: Atmospheric hydroperoxides in West Antarctica: Links to stratospheric ozone and atmospheric oxidation capacity, J Geophys Res, 110(D23), 1–17, doi:10.1029/2005JD006110, 2005.

Grannas, A. M., Jones, A. E., Dibb, J., Ammann, M., Anastasio, C., Beine, H. J., Bergin, M., Bottenheim, J., Boxe, C. S., Carver, G., Chen, G., Crawford, J. H., Dominé, F., Frey, M. M., Guzman, M. I., Heard, D. E., Helmig, D., Hoffmann, M. R., Honrath, R. E., Huey, L. G., Hutterli, M., Jacobi, H.-W., Klan, P., Lefer, B., McConnell, J., Plane, J., Sander, R., Savarino, J., Shepson, P. B., Simpson, W. R., Sodeau, J. R., Glasow, Von, R., Weller, R., Wolff, E. W. and Zhu, T.: An overview of snow photochemistry: evidence, mechanisms and impacts, Atmos Chem Phys, 7(16), 4329–4373, 2007.

Helmig, D., Johnson, B., Oltmans, S. J., Neff, W., Eisele, F. and Davis, D. D.: Elevated ozone in the boundary layer at South Pole, Atmos Environ, 42(12), 2788–2803, doi:10.1016/j.atmosenv.2006.12.032, 2008.

Hutterli, M. A., Rothlisberger, R. and Bales, R. C.: Atmosphere-to-snow-to-firn transfer studies of HCHO at Summit, Greenland, Geophys Res Lett, 26(12), 1691–1694, 1999.

Lamarque, J.-F., McConnell, J. R., Shindell, D. T., Orlando, J. J. and Tyndall, G. S.: Understanding the drivers for the 20th century change of hydrogen peroxide in Antarctic ice-cores, Geophys Res Lett, 38, –, doi:10.1029/2010GL045992, 2011.

Levine, J. G., Wolff, E. W., Jones, A. E., Hutterli, M. A., Wild, O., Carver, G. D. and Pyle, J. A.: In search of an ice core signal to differentiate between source-driven and sink-driven changes in atmospheric methane, J Geophys Res, 116(D5), n–a–n–a, doi:10.1029/2010JD014878, 2011.

Mauldin, L., Kosciuch, E., Henry, B., Eisele, F., Shetter, R., Lefer, B., Chen, G., Davis, D. D., Huey, G. and Tanner, D.: Measurements of OH, HO_2+RO_2, H_2SO_4, and MSA at the South Pole during ISCAT 2000, Atmos Environ, 38(32), 5423–5437, doi:10.1016/j.atmosenv.2004.06.031, 2004.

Mayewski, P. A., Rohling, E. E., Curt Stager, J., Karlén, W., Maasch, K. A., David Meeker, L., Meyerson, E. A., Gasse, F., van Kreveld, S., Holmgren, K., Lee-Thorp, J., Rosqvist, G., Rack, F., Staubwasser, M., Schneider, R. R. and Steig, E. J.: Holocene climate variability, Quaternary Research, 62(3), 243–255, doi:10.1016/j.yqres.2004.07.001, 2004.

Murray, L. T., Mickley, L. J., Kaplan, J. O., Sofen, E. D., Pfeiffer, M. and Alexander, B.: Factors controlling variability in the oxidative capacity of the troposphere since the Last Glacial Maximum, Atmos Chem Phys, 14(7), 3589–3622, doi:10.5194/acp-14-3589-2014-supplement, 2014.

Perrier, S., Sassin, P. and Domine, F.: Diffusion and solubility of HCHO in ice: preliminary results, Canadian journal of physics, 81(1-2), 319–324, 2003.

Ruddiman, W. F.: The Anthropocene, Annual Review of Earth and Planetary Sciences, 41, 45–68, 2013.

Saiz-Lopez, A., Mahajan, A. S., Salmon, R. A., Bauguitte, S. J. B., Jones, A. E., Roscoe, H. K. and Plane, J. M. C.: Boundary Layer Halogens in Coastal Antarctica, Science, 317(5836), 348–351, doi:10.1126/science.1141408, 2007.

Schmidt, G., DTT, S. and Harder, S.: Reply to comment by W.F. Ruddiman on "A note on the relationship between ice core methane concentrations and insolation", Geophys Res Lett, 32(15), –, doi:10.1029/2005GL022982, 2005.

Sigl, M., Mcconnell, J. R., Layman, L., Maselli, O., McGwire, K., Pasteris, D., Dahl-Jensen, D., Steffensen, J. P., Vinther, B., Edwards, R., Mulvaney, R. and Kipfstuhl, S.: A new bipolar ice core record of volcanism from WAIS Divide and NEEM and implications for climate forcing of the last 2000 years, J Geophys Res- Atmos, 118(3), 1151–1169, 2013.

Staffelbach, T., Neftel, A., Stauffer, B. and Jacob, D.: A record of the atmospheric methane sink from formaldehyde in polar ice cores, Nature, 349(6310), 603–605, doi:10.1038/349603a0, 1991.

Wolff, E. and Spahni, R.: Methane and nitrous oxide in the ice core record, Philosophical Transactions of the Royal Society A: Mathematical, Physical and Engineering Sciences, 365(1856), 1775–1792, doi:10.1038/nature01525, 2007.

Wolff, E. W., Hutterli, M. A. and Jones, A. E.: Past atmospheric composition and chemistry from ice cores – progress and prospects, Environ Chem, 4(4), 211–216, doi:10.1071/EN07031, 2007.

5 Figures

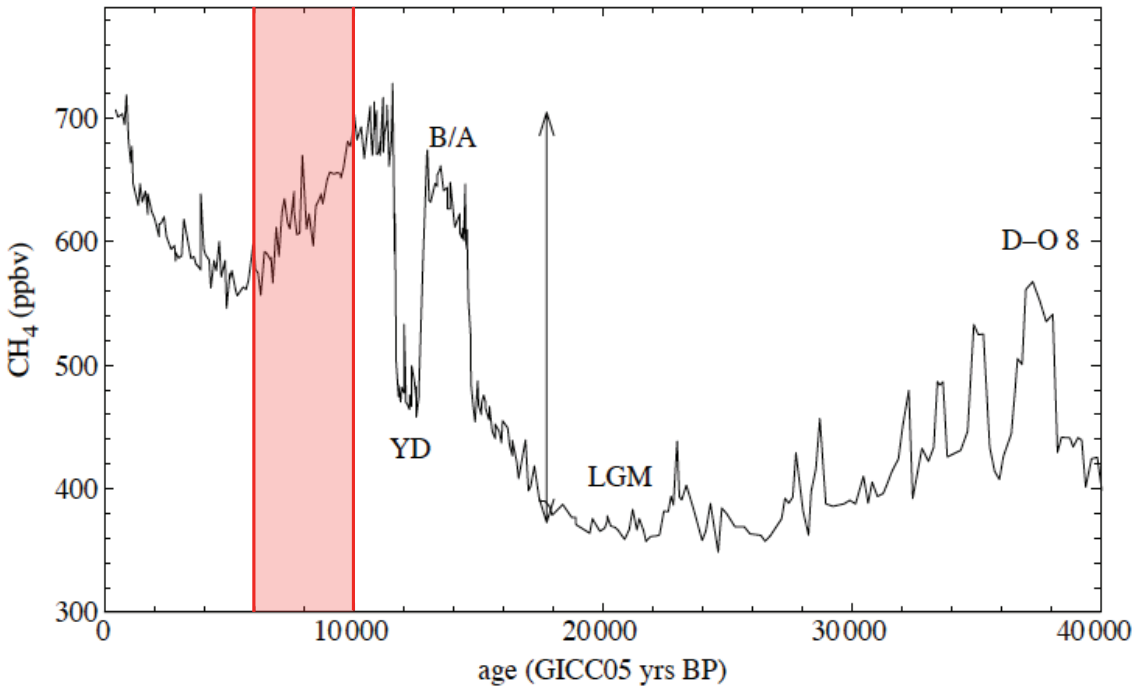

Figure 1. CH_4 over the last 40 kyr from the GRIP and NGRIP ice-core measurements (Wolff and Spahni, 2007). The period of this study, characterized by a decrease of CH_4 between 10,000 to 6,000 yr BP, is highlighted in red. Timing of important climatic features are also reported as follow: D-O 8, Dansgaard-Oeschger warm event number 8; LGM, last glacial maximum; B/A, Bølling-Allerød warm period; YD, Younger Dryas cold period.

CHAPTER 2:

ATMOSPHERIC NITRIC OXIDE AND OZONE AT THE WAIS DIVIDE DEEP CORING SITE: A DISCUSSION OF LOCAL SOURCES AND TRANSPORT IN WEST ANTARCTICA

S. Masclin[1], M. M. Frey[2,1], W. F. Rogge[1,3], and R. C. Bales[1,3]

[1]Environmental Systems, University of California, Merced, California, USA
[2]British Antarctic Survey, Natural Environment Research Council, Cambridge, UK
[3]Sierra Nevada Research Institute, University of California, Merced, California, USA

Published in Atmospheric Chemistry and Physics: 5 September 2013.

1 Abstract

The first measurements of atmospheric nitric oxide (NO) along with observations of ozone (O_3), hydroperoxides (H_2O_2 and MHP) and snow nitrate (NO_3^-), on the West Antarctic Ice Sheet (WAIS) were carried out at the WAIS Divide deep ice-coring site between 10 December 2008 and 11 January 2009. Average ±1σ mixing ratios of NO were 19±31 pptv and confirmed prior model estimates for the summer boundary layer above WAIS. Mean ±1σ mixing ratios of O_3 of 14±4 ppbv were in the range of previous measurements from overland traverses across WAIS during summer, while average ±1σ concentrations of H_2O_2 and MHP revealed higher levels with mixing ratios of 743±362 and 519±238 pptv, respectively.

An upper limit for daily average NO_2 and NO emission fluxes from snow of 8.6×10^8 and 33.9×10^8 molecule cm^{-2} s^{-1}, respectively, were estimated based on photolysis of measured NO_3^- and nitrite (NO_2^-) in the surface snowpack. The resulting high NO_X emission flux may explain the little preservation of NO_3^- in snow (~30%) when compared to Summit, Greenland (75-93%). Assuming rapid and complete mixing in to the overlying atmosphere, and steady state of NO_X, these snow emissions are equivalent to an average (range) production of atmospheric NO_X of 30 (21-566) pptv hr^{-1} for a typical atmospheric boundary-layer depth of 250 (354-13) m. These upper bounds indicate that local emissions from the snowpack are a significant source of short-lived nitrogen oxides above the inner WAIS.

The net O_3 production of 0.8 ppbv day^{-1} triggered with NO higher than 2 pptv is too small to explain the observed O_3 variability. Thus, the origins of the air masses reaching WAIS Divide during this campaign were investigated with a 4-day back-trajectory analysis every 4 hr. The resulting 168 back trajectories revealed that in 75% of all runs air originated from the Antarctic coastal slopes (58%) and the inner WAIS (17%). For these air sources O_3 levels were on average 13±3 ppbv. The remaining 25% are

katabatic outflows from the East Antarctic Plateau above 2500 m. When near-surface air from the East Antarctic Plateau reaches WAIS Divide through a rapid transport of less than 3 days, O_3 levels are on average 19±4 ppbv with maximum mixing ratios of 30 ppbv. Episodes of elevated ozone at WAIS Divide are therefore linked to air mass export off the East Antarctic Plateau, demonstrating that outflows from the highly oxidizing summer atmospheric boundary layer in the interior of the continent can episodically raise the mixing ratios of long-lived atmospheric chemical species such as O_3 and enhance the oxidative capacity of the atmosphere above WAIS.

2 Introduction

Over the last decade, a large number of field and lab studies have provided evidence of the importance of snow photochemistry on the chemical composition of air above snow-covered surfaces in the polar and mid-latitudes (Grannas et al., 2007, and references therein). The upper snowpack is seen not only as a chemical reservoir but as a chemical reactor. Trace gases emitted by the snowpack include hydrogen peroxide (H_2O_2), formaldehyde (CH_2O) and nitrogen oxides ($NO_X = NO + NO_2$), and increase the oxidizing potential of the atmospheric boundary layer through production of the hydroxyl radical (OH) and ozone (O_3) (Grannas et al., 2007; Thomas et al., 2012). Measurements of atmospheric and snow concentrations and also fluxes from snow surfaces indicate that the polar snowpack emits NO_X mainly through the photolysis of nitrate (NO_3^-) in near-surface snow (Grannas et al., 2007; Bauguitte et al., 2012; Frey et al., 2013). Snowpack emissions of NO_X can contribute significantly to the NO_Y (NO_X + other oxidized nitrogen species) budget above snow, as observed in continental and coastal Antarctica (Jones et al., 2000; Frey et al., 2013). Bauguitte et al. (2012) reached a similar conclusion at Halley station by highlighting that halogen chemistry over the Antarctic coast controls the lifetime of NO_X species and reduces the nitric oxide (NO) mixing ratios. When atmospheric turbulence is low or atmospheric boundary layer depths are shallow, these emissions contribute to high NO_X levels, several hundred pptv, as observed at South Pole and over the East Antarctic Plateau (Davis et al., 2004, 2008; Slusher et al., 2010; Frey et al., 2013). Chen et al. (2004) and Mauldin et al. (2004) showed that at South Pole these high levels of NO_X shift the HO_X ($OH + HO_2$) partitioning towards OH:

$$NO + HO_2 \rightarrow NO_2 + OH \qquad \text{(R1)}$$

NO_X emissions from snow can also lead to net production of O_3 over the East Antarctic Plateau (Helmig et al., 2008a, and references therein), and thereby shift HO_X partitioning of the overlying atmosphere.

Above the West Antarctic Ice Sheet (WAIS), enhanced snowpack emissions of NO_X associated with events of stratospheric O_3 depletion may lower the formation rate of atmospheric H_2O_2 (Frey et al., 2005). Photochemical modeling suggests that atmospheric H_2O_2 is sensitive to the NO background, opening up the possibility of

constraining past NO_X and OH levels using the H_2O_2 ice-core record (Frey et al., 2005, 2006). Therefore, investigation of the current atmospheric boundary-layer photochemistry at a WAIS ice-core drilling site is essential to interpret ice-core records of photochemically active species such as H_2O_2 and NO_3^-. This can also provide information regarding the contribution of air advection from the East Antarctic Plateau to levels of oxidants above WAIS, similar to Legrand et al. (2009) who observed outflows from the Antarctic Plateau increasing O_3 concentrations at the East Antarctic coastal site Dumont D'Urville.

So far, atmospheric-sampling campaigns in the Antarctic have taken place at existing stations on the coast (Dumont D'Urville, Halley, Neumayer) and on the East Antarctic Plateau (South Pole, Dome C). Only recent airborne campaigns (Eisele and Davis, 2008; Slusher et al., 2010) or scientific overland traverses (Frey et al., 2005) provided information on the composition of the lower atmosphere across the interior of the continent. Thus, spatial data coverage of the lower atmosphere in Antarctica is still sparse and little is known about the variability of O_3 and its precursors above WAIS. For example, the first ground-based measurements across WAIS lasting several days included atmospheric records of H_2O_2, methyl hydroperoxide (MHP), CH_2O, O_3 but not NO_X (Frey et al., 2005).

The current study includes multi-week first observations of NO and complementary measurements of atmospheric O_3, H_2O_2, MHP and of surface-snow H_2O_2, NO_3^- and nitrite (NO_2^-) in the WAIS region. The aims were to determine the summer composition of the lower atmosphere in the interior of West Antarctica and the relative importance of local production versus air mass transport on the local atmospheric budgets of NO_X and O_3.

3 Methods

From 10 December 2008 to 11 January 2009, atmospheric concentrations of NO and O_3 were continuously measured at WAIS Divide (local time: LT = UTC − 07:30). Mixing ratios of ROOH (H_2O_2 and MHP) were recorded between 31 December 2008 to 7 January 2009. Snow samples were collected daily from the surface and weekly from 30 cm snow pits for chemical analysis of NO_3^-, NO_2^- and H_2O_2.

Atmospheric sampling took place 5 km NW of the WAIS Divide drilling camp (79.467° S, 112.085° W, 1766 m a.m.s.l., http://www.waisdivide.unh.edu). All instruments were run out of a Polarhaven tent heated by a preway heater. Atmospheric measurements were made 1 m above the snow, 10 m upwind (prevailing winds from NE) from the tent, with ambient air drawn through an insulated and heated PFA (1/4" I.D.) intake line (typically 1.4 STP − L min^{-1}) of 12 m for ROOH, and of 20 m for NO and O_3. In an attempt to minimize artifacts in our atmospheric records, the two generator (3.5 and 5 KW) that provided electricity to the lab were located about 30 m downwind from the sampling lines, and all activities around the site were restricted. However, the heater exhaust was located on the top of the Polarhaven tent.

3.1 Atmospheric sampling

NO was measured using a modified chemiluminescence instrument used previously at South Pole (Davis et al., 2001, 2004). NO mixing ratios recorded at 1 Hz were aggregated to 1 min averages. The limit of detection (LOD), defined as 2-σ of the background count rate, was 5 pptv. A two-minute background signal was monitored every 20 min and an automatic 4 min calibration was performed every 2 h by addition of a 2 ppmv NO standard. Due to late delivery of this NO gas standard to the site, calibration was only run during the last 3 days of the campaign. The instrument sensitivity remained fairly constant over the three days, with an average over 16 calibrations of 7.10 ± 0.18 Hz $pptv^{-1}$, similar to the preseason value of 7.00 Hz $pptv^{-1}$ determined in the lab. We therefore used the 3-day average value of these calibrations to process the overall dataset. NO spikes related to pollution from generators and heater exhaust were removed using a moving standard deviation filter with a maximum standard deviation of 30 (1.5 times the interquartile range of the dataset). This led to the removal of 25 % from the raw NO record.

Surface O_3 was monitored at 1 min resolution using a 2B Technologies (Golden, Colorado) O_3 monitor, model 205, similar to those previously used in the remote Antarctic such as on the ITASE traverses (Frey et al., 2005) and in an O_3 monitoring network (Bauguitte et al., 2011). LOD was 1 ppbv.

Atmospheric ROOH were measured based on continuous scrubbing of sample air followed by separation in an HPLC column and fluorescence detection, described in detail by Frey et al. (2005, 2009a). The detector was calibrated 1–2 times per day with H_2O_2 solution and MHP standards synthesized in our lab following the protocol described by Frey et al. (2009a). The LOD, 2-σ of the baseline, were 87 pptv for H_2O_2 and 167 pptv for MHP. Unexpected variations of the coil-scrubber temperatures may have caused higher LOD than those reported by Frey et al. (2005, 2009a).

3.2 Snow sampling

All surface snow and snow pits were sampled in a 7200 m^2 clean area upwind from the Polarhaven tent. The top 1 cm of the non-cohesive surface snow, referred to as the skin layer (Frey et al., 2009b; Erbland et al., 2013), was collected daily with a 10 mL glass test tube to assess temporal changes in snow chemistry. Twice during the campaign, the skin layer was sampled simultaneously at five different spots inside the clean area to assess possible local spatial variability of NO_3^-, NO_2^- and H_2O_2.

Weekly snow pits were sampled at 2 cm resolution to a depth of 30 cm, covering the snowpack zone where 85 % of NO_3^- photolysis is expected to occur (France et al., 2011). Snowflakes were collected on aluminum foil during the only snow precipitation event observed during the campaign, on 12 December 2008.

All snow samples were collected in 100 mL SCHOTT bottles and kept frozen during storage and transport until analysis 14 months later. The analysis involved melting the snow 1 hour before injecting the sample into a self-built continuous flow analysis (CFA) system, as described by Frey et al. (2006). The LOD, defined as 3σ of the

baseline, was 0.4 ppbw for NO_3^-, NO_2^- and H_2O_2. Only values above LOD were used for further calculations. Some loss of NO_2^- in the samples may have occurred between the time of collection and analysis, as Takenayr BPand Bandow (2007) and O'Driscoll et al. (2012) showed that NO_2^- may be oxidized during freezing and storage.

4 Results

4.1 Atmospheric concentrations

The average $\pm 1\sigma$ (median) of NO over the campaign was 19 $\pm$ 31 (10) pptv (Table 1). Some noise remained in the NO dataset after filtering; however, the 4 h running median (Fig. 1a) shows very little change in the overall trend of the data due to filtering, with the median value after filtering similar to that of the raw dataset (6 pptv). One-minute data did not exhibit any clear diel cycle (Fig. 1), but 1 h binned data centered on each hour for the measurement period revealed a diel cycle that can be interpreted with the variations of the average solar elevation angle (Fig. 2b). NO mixing ratios increased at 07:00–08:00 LT with a maximum rise of 36 % from the daily median of 10 pptv. A decrease was observed afterwards and followed by a second increase of 20 % above the median value at 19:00 LT. These peaks in NO occurred as solar elevation angle increased and decreased, with lower values of NO at the maxima and minima of solar elevation angle.

Average $\pm 1\sigma$ (median) mixing ratios of O_3 at WAIS Divide were 14 $\pm$ 4 (13) ppbv (Table 1). The mean is two thirds of the 20 $\pm$ 2 ppbv average mixing ratio observed at Byrd Station in summer 2002, but is in the range of values from previous measurements between 79.06° S and 85.00° S above the WAIS (Frey et al., 2005) (Fig. 3). Two events of elevated O_3 levels were recorded between 24 and 25 December, and between 27 and 29 December, with concentrations in the range of 20 to 30 ppbv (Fig. 1). Concentrations above 25 ppbv were only observed for winds blowing from ENE to SWS. This 135° sector represents 67 % of all the wind directions observed during the field campaign (Fig. 4). The hourly binned O_3 data (Fig. 2b) show a small diel cycle in phase with solar elevation angle and wind speed. The mixing ratios rose by 5 % of the median value (13 ppbv) in the morning, reaching a maximum at 14:00 LT and dropping thereafter in the afternoon.

Concentrations of H_2O_2 and MHP were measured between 31 December 2008 and 5 January 2009 (Fig. 1). Averages $\pm 1\sigma$ (medians) were 743 $\pm$ 362 (695) and 519 $\pm$ 238 (464) pptv for H_2O_2 and MHP, respectively. Our records are closer to values observed at West Antarctic sites below 1500 m a.m.s.l. and higher than measurements made in the surrounding area (Fig. 3), with mixing ratios of H_2O_2 that were twice those observed at Byrd station in late November 2002 (Table 1) (Frey et al., 2005). Average $\pm 1\sigma$ (range) of the MHP : (H_2O_2 + MHP) ratios were 0.42 $\pm$ 0.10 (0.12–0.76). These values are in the range of those previously recorded over WAIS (Frey et al., 2005). Binned values suggest, for both H_2O_2 and MHP, a diel cycle with respective

maximum 44 and 37 % above their medians (695 and 464 pptv) observed in the morning (Fig. 2c).

4.2 Concentrations in snow

Average $\pm 1\sigma$ (median) concentrations of NO_2^-, NO_3^- and H_2O_2 in the skin layer at WAIS Divide were 0.6 ± 0.4 (0.5), 137 ± 37 (142) and 238 ± 37 (238) ppbw, respectively (Table 1). Daily concentrations of NO_2^- in the skin layer showed a decrease of 30 pptw per day (R^2 = 0.36) over the campaign (Fig. 5). This decrease represents a rate of 5 % per day of the average concentration of NO_2^- measured in all of the snow-surface samples. Unlike NO_2^-, NO_3^- and H_2O_2 exhibited some variation but no trend was observed for these species.

The coefficients of variation of concentrations of NO_2^-, NO_3^- and H_2O_2 in the skin layer are 49 %, 26 % and 17 %, respectively. The coefficients of variation for samples collected simultaneously on 1 and 8 January 2009 (Fig. 5) are 17 %, 31 % and 7 % for NO_2^-, NO_3^- and H_2O_2, respectively. The similar coefficients of variation for NO_3^- concentrations in snow imply that spatial variability contributes significantly to the overall variability and thus a temporal trend may be difficult to detect. For NO_2^- and H_2O_2, the coefficients of temporal variability (49 % and 17 %, respectively) are more than double those calculated from spatial variability (17 % and 7 %, respectively). The variations of daily concentrations of NO_2^- and H_2O_2 in near-surface snow may then be interpreted as temporal trends. Concentrations of H_2O_2 in the top 5–15 cm of the profile (Fig. 6) may also indicate a temporal trend; seasonal increase in concentrations measured over this period was apparent not only in the top 5 cm of snow, but also down to at least 15 cm. Although there was no new snow accumulation during this period, there was wind redistribution and atmosphere–snow exchange of H_2O_2 and other atmospheric gas species, or nighttime deposition of fog.

The 30 cm deep profiles of NO_2^-, NO_3^- and H_2O_2 illustrated in Fig. 6 represent concentration changes of these species in snow over the last 6 months of 2008, based on local mean annual snow accumulation rate of 0.20 $m_{weq}\,yr^{-1}$ (Banta et al., 2008) and an average snow density of 0.37. Total concentrations of NO_3^- in the snow column dropped by about 19 % between the first and last snow-pit samplings. NO_3^- concentrations decrease by 94–188 ppbw over the top 5 cm of snow, reaching ~ 30 ppbw below. Total NO_2^- stored in the 30 cm column decreased by about 65 % across the three snow-pit samplings. Unlike NO_2^- and NO_3^-, total concentrations of H_2O_2 in the top 30 cm of snowpack doubled over the 18 days of sampling. A 233–298 ppbw decrease of H_2O_2 concentrations in the first 10 cm of each snow pit was generally observed.

5 Discussion

5.1 Local photochemistry

5.1.1 Factors controlling atmospheric levels of ROOH, NO, O_3 and snow content of NO_3^-, NO_2^- and H_2O_2

Levels of NO and O_3 measured at WAIS Divide during summer 2008–2009 are slightly higher than coastal values but lower than observed concentrations on the Antarctic Plateau (Fig. 3). The observed mean of NO mixing rates are close to the 10 pptv modeled by Frey et al. (2005) at Byrd, about 160 km from WAIS Divide. Their potential NO concentrations were computed with the NASA Goddard Flight Center (GSFC) point photochemical model that included a snow- pack source of H_2O_2 and CH_2O.

The diel cycle of NO (Fig. 2b) does not compare well with either measurements from the East Antarctic Plateau (Dome C) (Frey et al., 2013) or from the West Antarctic coast (Halley) (Bauguitte et al., 2012). Data show a symmetry of the NO diel cycle with respect to local noon that is similar to predictions and observations from Summit/Greenland (Thomas et al., 2012), but with lower mixing ratios and a diel amplitude of 6.5 pptv. The NO variability is mainly in phase with solar radiations but presents two minima around local noon and midnight and two daily maxima around 07:00 and 19:00 LT. The 36 % rise from the NO median of 10 pptv ob- served in the morning along with the increase of solar elevation angle suggests that the increase of solar elevation angle enhances the photolytic production of NO from the snow- pack. The 2 h binned data of NO and wind speed (data not shown) suggest that higher NO mixing ratios were observed for wind speeds less than 3 m s^{-1}, indicating a potential local production of NO from surface snow. The decrease observed after 09:00 LT at high solar elevation angle may result from the increase of the atmospheric boundary layer height and of the wind speed. Higher wind speeds would result in an increase of turbulent mixing and therefore in efficient vertical upward transport and dilution of surface emissions into a growing volume given by the developing boundary layer (Frey et al., 2013). The increase of NO levels by 20 % of the median value around 19:00 LT may result from the decrease of the atmospheric boundary layer height and wind speed along with solar elevation angle. However, no measurements of the diel variability of the atmospheric boundary layer height were performed during the campaign to confirm this point. These data suggest that both snow photochemistry and physical mixing control the diel cycle of NO at WAIS Divide. Through its different sinks and sources, the NO_X photochemistry may also drive the NO variability but this contribution cannot be defined here as it requires a more detailed analysis using a 1-D model (Thomas et al., 2012).

The interpretation of the 1 month record of O_3 in terms of seasonal trend is made difficult given the short period of measurement. However, its comparison with the annual cycles of O_3 observed at other Antarctic stations, with concentrations between those observed at Halley and South Pole, suggests a possible influence of both marine and

continental air on the WAIS Divide level, and shows characteristic low mixing ratios around the Austral solstice.

The O_3 diel cycle (Fig. 2b) is similar to observations from Dome C (Legrand et al., 2009) but with lower amplitude and concentrations. The increase of 5 % of the median value is consistent with O_3 produced locally from the snowpack NO_X emissions and confined into a shallow atmospheric boundary layer. Similarly to the NO diel cycle, the following decrease of O_3 in the afternoon can be attributed to a deeper atmospheric boundary layer and higher wind speeds that dilute all the produced O_3. Because the chemical lifetime of O_3 in polar regions is in the order of days (Grannas et al., 2007), it is not expected that photochemical loss is a main driver of the diel cycle of O_3. Lack of higher mixing ratios during periods with wind speed less than 3 m s^{-1} (data not shown) suggests that local production of O_3 over the surface snow is not the predominant process at WAIS Divide during the austral summer. The amplitude of the diel cycle is relatively low in comparison with the average daily O_3 which indicates that another source may be considered to explain the change of O_3 over the campaign. The ENE to SWS wind directions associated with high O_3 values (Fig. 4) point to a possible contribution of air mass transport of this chemical species at WAIS Divide, e.g. outflow from the East Antarctic Plateau (see Sect. 4.2). A similar conclusion was reached by Helmig et al. (2007a) from the review of other Antarctic station data. H_2O_2 concentrations at WAIS Divide are similar to those observed above WAIS at lower latitudes (below 1500 m a.m.s.l.) but 3 times the mixing ratios measured at South Pole (Frey et al., 2009a). As shown in Table 1 and in Fig. 3, the concentrations of H_2O_2 measured at WAIS Divide are higher than those measured at nearby sites (Frey et al., 2005). A similar comparison between our average MHP mixing ratios and prior measurements across WAIS (Frey et al., 2005, 2009a) is also observed. The average specific humidity of 1.1 g kg^{-1} calculated for the period of ROOH measurement is higher than previous records from nearby sites (Frey et al., 2005). This high value may explain the elevated mixing ratios of H_2O_2 and MHP measured at WAIS Divide, as water vapor is an important precursor for both species.

H_2O_2 and MHP exhibited a simultaneous increase with solar elevation angle between 03:00–13:00 LT, followed by a decrease (Fig. 2). The maximum amplitude of H_2O_2 is observed at 05:00 LT, with a rise of 43 % above the median value of 695 pptv. For MHP, mixing ratios rose to a maximum of 37 % above the median (464 pptv) at 05:00 and 13:00 LT. These results also suggest that both H_2O_2 and MHP may be affected by photochemistry and an increase of the atmospheric boundary layer depth during the day. Unlike NO, ROOH did not show an increase in the second part of the day but the levels remained low, consistent with an increased uptake by the snowpack when the temperature decreased in the evening (Hutterli, 2003, and references therein). The temperature record at the WAIS Divide camp was, however, too intermittent to further investigate the influence of temperature on atmospheric H_2O_2. A source from the snowpack is not considered significant for MHP since it has a solubility only 0.1 % that of H_2O_2 (Lind and Kok, 1994) and because no MHP has been detected in snow and ice above the current LOD (Frey et al., 2005, 2009a). The change of MHP may depend on the photochemistry of its precursors such as CH_4, NMHCs and water vapor, which may decrease with solar elevation angle. Higher H_2O_2 and MHP levels at low wind speeds

(less than 4 m s^{-1}) (data not shown) suggest that ROOH are produced locally, coherent with a local photochemical production of MHP and a physical snow-air ex- change controlling H_2O_2 (Frey et al., 2009a). They are then diluted through turbulent transport after production.

NO_3^- values are closer to those measured at coastal sites such as Halley or Neumayer stations (Mulvaney et al., 1998), than to the values observed at higher-altitude sites such as South Pole and Concordia stations (Dibb et al., 2004; France et al., 2011). Concentrations of skin-layer NO_3^- present short-term and local spatial variations as Jarvis et al. (2009) and Wolff et al. (2008) also observed at Summit and Halley. These variations cannot be explained with a scenario of fresh snowfall since only one snow precipitation occurred during the campaign (Fig. 5). Part of these variations of NO_3^- in the skin layer as H_2O_2 may be caused by processes such as nighttime deposition of NO_3^-, in the form of nitric oxide (HNO_3) and H_2O_2 or HNO_3 and H_2O_2 gas exchange. Other part can be attributed to some events of snow removed by the wind since this snow removal would also impact on chemical species other than NO_3^- (such as H_2O_2, which presents similar variations to NO_3^-) on 26–27 December 2008 and on 1–2 January 2009. However, these events are too episodic to explain the overall variations of skin-layer NO_3^-. It is suggested that part of NO_3^- in the top snowpack undergoes some possible post-depositional processes such as photolysis.

The contents of NO_3^- and H_2O_2 in fresh snowfall are in the range of skin-layer concentrations, while previous observations showed that fresh snowfall contains higher concentrations of these species than does aged snow (e.g., Mulvaney et al., 1998). In addition to post-depositional equilibrium with the atmosphere, it is possible that either the snow may have degassed during its collection or prior to analysis. Anastasio and Robles (2007) showed that NO_3^- and H_2O_2 contribute to half the light absorption in polar snow for wavelengths of 280 nm and above. Since the snowflakes from this diamond-dust-like precipitation stayed exposed to the sun under a clear sky until their collection at the end of the event – over 5 h – it is possible that photochemical loss of NO_3^- and H_2O_2 may have occurred during the collection process.

The NO_3^- and H_2O_2 profiles measured in the 30 cm snow pits show a summer peak, as observed in earlier studies (Kreutz et al., 1999, and references therein). The increase over the campaign of H_2O_2 concentrations in the top 15 cm of snow (Fig. 6) may point to a significant deposition of H_2O_2 during summer, and may also reflect changes in the overlying atmospheric H_2O_2 levels, as discussed in Hutterli (2003). NO_3^- in the skin layer does not show a constant increase with time, unlike H_2O_2. However, a 70 % decrease of NO_3^- concentrations with increasing depth in the snow is observed, unlike reported snow-pit measurements from polar sites with similar surface temperature and snow accumulation rate, such as Summit, Greenland (e.g., Burkhart et al., 2004). These NO_3^- profiles are similar to those observed at Dome C (e.g., Frey et al., 2009b; France et al., 2011). Based on the interpretation of these authors, this sharp decrease may therefore indicate that NO_3^- in the top snowpack can be significantly reduced by photolysis. A similar photochemical depletion can be suggested to explain the slight decrease of NO_2^- concentration observed in the 30 cm deep profiles over the campaign.

5.1.2 Post-depositional loss of NO_3^- in surface snowpack

WAIS Divide and Summit, Greenland, have similar latitudes, surface temperature and snow accumulation rate (Table 2 and Fig. 7a). Concentrations of NO_3^- in the skin layer are also in the same range for both sites, between 24– 206 ppbw for WAIS Divide and 61–207 ppbw for Summit (Fig. 8a, b).

However, the median NO_3^- concentrations in the top 1 m of snow at WAIS Divide is lower than at Summit, 38 vs. 138 ppbw. At very dry and cold sites on the East Antarctic Plateau such as Dome C, mean NO_3^- concentrations are as low as 10–20 ppbw if one excludes the surface layer (Fig. 8c). Note that at Dome C most NO_3^- is concentrated in the top layer with levels 1–2 orders of magnitude larger than at depth (Frey et al., 2009b; Erbland et al., 2013). Comparison of concentrations at the surface and at depth allows estimating net preservation of NO_3^- in snow, which is about 30 % at WAIS Divide, 75–93 % at Summit (Burkhart et al., 2004; Dibb et al., 2007) and less than 10 % at Dome C (Rothlisberger et al., 2002; Frey et al., 2009b).

Differences in average NO_3^- concentrations in the skin layer and preserved at depth between WAIS Divide and Summit can be attributed to (a) a lower background of atmospheric reactive nitrogen in Antarctica compared to the Arctic due to a larger distance from anthropogenic pollution sources, and (b) differences in processes occurring during and after deposition.

Regarding (b), the relative contributions of the processes involved may vary significantly between different locations, i.e., both physical (evaporation and adsorption of HNO_3) and photochemical (photolysis of NO_3^-) processes have been put forward to explain NO_3^- net preservation (sum of gain and loss) in polar snow (Rothlisberger et al., 2002; Frey et al., 2009b). Both processes will be sensitive to accumulation rate and timing. For example, little snowfall in the sunlit season implies longer exposure of surface snow to UV radiation, leading to significant loss of NO_3^- at some sites from photolysis (Frey et al., 2009b; Erbland et al., 2013).

In general, NO_3^- concentration is preserved in polar snow scales with mean annual temperature and accumulation rate (Rothlisberger et al., 2002, Fig. 7). Comparison shows that NO_3^- concentrations at WAIS Divide are not unusual at all since they do fall into the range expected in Antarctica (Fig. 7b, c). They are, however, still lower than those in pre-1940 snow at Greenlandic sites of similar accumulation rate and temperature. The slightly lower accumulation and thus slower burial rate of annual snow deposition at WAIS Divide vs. Summit may contribute to this difference in NO_3^- preservation

But, as suggested by the recent literature, variables linked to (post)depositional processes other than accumulation rate may contribute as well to the observed difference and include micro-physical properties and chemical heterogeneity in the snow matrix. Regarding the latter, observations of atmospheric and snow NO_3^- in coastal Antarctica showed that deposition of NO_3^- spikes is linked to sea salt aerosol, i.e., by conversion of gas-phase NO_3^- to NO_3^- aerosol and enhanced trapping of gas-phase NO_3^- on salty surfaces (Wolff et al., 2008). This enhanced deposition efficiency will be less important further inland. However, higher NO_3^- concentrations were also associated with

higher dust content (i.e., calcium (Ca^{2+})), suggesting reduced post-depositional loss of NO_3^- by photolysis or evaporation (Rothlisberger et al., 2000). In comparison with Summit, the lower dust content in WAIS Divide snow, ~ 20 % as alkaline and ~ 30 % as much Ca^{2+} (Table 2), may reduce the preservation of NO_3^- in snow and enhance the NO_X emission flux in summer. Systematic differences of NO_X emissions from surface snow could indeed further support increased loss rates and thus less preservation of NO_3^- in surface snow at WAIS Divide. At Summit, Honrath et al. (2002) measured 24 h average NO_X fluxes of 2.5×10^8 molecule cm^{-2} s^{-1}, significantly less than what we calculated for WAIS Divide (see Sec. 4.1.5). However, based on a similar approach to our study, Zatko et al. (2013) recently modeled an NO_X flux at Summit 5–10 times that reported by Honrath et al. (2002). These results point to significant NO_X emissions from NO_3^- in the snowpack at both sites. Our calculations suggest high loss rates, higher than at Summit (see Sect. 4.1.5), but uncertainties in available measurements and model estimates prevent concluding that emission rates are significantly higher at WAIS Divide than at Summit.

Further, the stable isotopic composition of NO_3^- in snow and provide information on the amount of post-depositional NO_3^- loss (e.g., Frey et al., 2009b; Erbland et al., 2013). At Summit, the N and O isotopes of NO_3^- showed that most of the NO_X emitted from the surface snow is recycled back to the snow as NO_3^-, explaining high NO_3^- preservation (Hastings, 2004). It can be speculated that if the NO_3^- loss rate was similar at WAIS Divide, then some of the emitted gas phase species may be lost through lateral export, implying a lower recycling efficiency and therefore lower NO_3^- preservation. Thus, NO_3^- post-depositional loss is a nonlinear combination of both accumulation and temperature, but other parameters need also to be considered including snow chemistry to get a more complete process understanding.

5.1.3 Steady-state estimation of atmospheric NO_2

Considering the $NO–NO_2–O_3$ system, it is reasonable to assume a photo-stationary steady state between NO and NO_2 at 1 m above the snowpack (Frey et al., 2013) to infer the potential atmospheric NO_2 concentrations from reactions:

$$NO_2 + h\nu \rightarrow NO + O(^3P) \quad \text{(R2)}$$

$$O(^3P) + O_2 + M \rightarrow O_3 + M \quad \text{(R3)}$$

$$NO + O_3 \rightarrow NO_2 + O_2 \quad \text{(R4)}$$

The conversion of NO to NO_2 described in Reaction (R4) is also achieved through different channels (Reactions R1, R5–R6) with the presence of oxidants such as HO_X, peroxy (RO_2) or halogen (XO = ClO, BrO, IO) radicals:

$$NO + RO_2 \rightarrow NO_2 + RO \quad \text{(R5)}$$

$$NO + XO \rightarrow NO_2 + X \quad \text{(R6)}$$

NO_2 mixing ratios can therefore be estimated from the extended Leighton ratio as derived in Ridley et al. (2000):

$$[NO_2] = [NO]\frac{k_{R4}[O_3]+k_{R1}[OX]}{j_{R2}} \quad (1)$$

with OX the total radical concentration ([OX] = [HO_2] + [RO_2] + 2[XO]) as XO represents the halogen radicals (Ridley et al., 2000). The photolytic rate constant j_{R2} was calculated from the NCAR/ACD radiative-transfer model TUV version 5.0 (Lee-Taylor and Madronich, 2002) with O_3 columns measured by total ozone mapping spectrometer (TOMS) (http://ozoneaq.gsfc.nasa.gov/ozone_overhead_current_v8.md) and assuming clear-sky conditions. k_{R4} and k_{R1} were estimated through the temperature-dependent expressions from Sander et al. (2006). An NO_2 concentration of 5 pptv was computed based on the averages of NO and O_3 observed at WAIS Divide, and on 4.9×10^7 molecule cm^{-3} HO_2 + RO_2 mixing ratios derived from the 1.3×10^6 molecule cm^{-3} OH radical concentrations computed for Byrd (Frey et al., 2005). Because the mixing ratios of HO_X for WAIS Divide are estimates, we calculated the steady-state NO_2 concentrations with reported HO_X levels from Halley (2.3×10^7 molecule cm^{-3}) (Bloss et al., 2007) and South Pole (8.3×10^7 molecule cm^{-3}) (Eisele and Davis, 2008), resulting in NO_2 concentrations of 5.1 and 6.1 pptv, respectively. These results show that this steady state relationship depends essentially on NO and O_3 mixing ratios.

Note that halogen radicals were not considered in these calculations, and no records have yet been reported above WAIS. Coastal sea ice is the main source of active halogen (Saiz-Lopez and von Glasow, 2012, and references therein) and measurements from Antarctic coastal sites showed a strong spatial variability in concentrations of halogens and their potential impact on boundary layer photochemistry. Summertime measurements of IO and BrO ranged from 0.7 to 5.5 pptv at Halley (Saiz-Lopez et al., 2007), while mixing ratios at Dumont D'Urville were observed between 0.04 and 0.15 pptv for IO and below or equal to 2 pptv for BrO (Grilli et al., 2013). The back-trajectory analysis described in Sect. 4.2.1 shows that marine intrusions over WAIS are frequent (58 % of all back trajectories) and have therefore the potential to export halogen compounds over the ice sheet. However, from measurements by the satellite spectrometer SCIAMACHY (Schönhardt et al., 2012), monthly mean IO and BrO vertical column amounts averaged over 2004 to 2009 revealed insignificant concentrations of both species over WAIS Divide between December and January. Thus, it is reasonable to assume that little or insignificant halogen chemistry is occurring at WAIS Divide.

The NO : NO_2 ratio of 3.8 is significantly higher than the ratios of 1.3–2 and 1.5 observed respectively at Halley (Bauguitte et al., 2012, and references therein) and Dome C (Frey et al., 2013). These studies showed evidence of large discrepancies between observed and steady-state estimated ratios that are attributed to halogen chemistry for the coastal station and to the presence of HO_2 + RO_2 on the plateau. Therefore, the estimated atmospheric NO_2 from the steady-state assumption has to be considered as a lower limit of true value.

5.1.4 Potential NO_x lifetime

The NO_X lifetime was calculated to investigate the factors controlling its atmospheric concentration. Assuming that halogen chemistry is not significant at WAIS Divide, Reactions (R7)–(R8) are the main sink of NO_2 during polar day:

$$NO_2 + OH + M \rightarrow HNO_3 + M \quad \text{(R7)}$$

$$NO_2 + HO_2 + M \rightarrow HNO_4 + M \quad \text{(R8)}$$

Based on these reactions, the lifetime of NO_2 (τ_{NO_2}) was estimated with $[OH] = 1.3\times10^6$ molecule cm^{-3} and $[HO_2] = 4.9\times10^7$ molecule cm^{-3} (Sect. 4.1.3). The lifetime of NO_X (τ_{NO_x}) was then deduced through Eq. (2) (Seinfeld and Pandis, 1998):

$$\tau_{NO_X} = \tau_{NO_2} \times \left(1 + \frac{[NO]}{[NO_2]}\right) \quad (2)$$

The resulting lifetime of NO_X at WAIS Divide of 15 h represents an upper bound, given that the $NO : NO_2$ ratio of 3.8 is an upper limit. This value is less than the 24 h estimated by Jones et al. (2000) from a snow block at Neumayer, but it is longer than the 6.4 h estimated at Halley (Bauguitte et al., 2012) and 8 h at South Pole (Davis et al., 2004). Bauguitte et al. (2012) showed that NO_2 lifetime at Halley is mainly controlled by halogen oxidation processes, while low temperatures at South Pole prevent thermal decomposition of pernitric acid and therefore enhance NO_2 removal through its oxidation with HO_2 (Slusher et al., 2002). Thus, our potential NO_X lifetime seems plausible since we expect to observe none of these conditions at WAIS Divide. NO_x lifetimes computed with reported HO_x concentrations from South Pole and Halley (Sect. 4.1.3) are respectively 9 and 33 h and represent the potential lower and upper bounds for the NO_X lifetime in the inner WAIS.

Considering a photochemical lifetime of other NO_X precursors, such as HNO_4 and HNO_3 (HNO_3 compared to dry deposition), of less than a day above the East Antarctic Plateau (Davis et al., 2008; Slusher et al., 2002) and an air mass transport between WAIS Divide and the Plateau longer than 33 h (Sect. 4.2), outflows from this region are not expected to be a major NO_X source for the boundary layer at WAIS.

5.1.5 Calculation of upper-limit NO_x emission from NO_3^- and NO_2^- photolysis

The simplified reaction scheme (R9) to (R12) summarizes the currently known NO_3^- photochemistry in near-surface

$$NO_3^- + h\nu \rightarrow NO_2 + O^- \quad \text{(R9)}$$

$$NO_3^- + h\nu \rightarrow NO_2^- + O\left(^3P\right) \quad \text{(R10)}$$

$$NO_2^- + h\nu \rightarrow NO + O^- \quad \text{(R11)}$$

$$NO_2^- + OH \rightarrow NO_2 + OH^- \quad \text{(R12)}$$

While NO_3^- photolysis is the major source of NO_2 (Reaction R9) (Grannas et al., 2007), recent studies also pointed at the potential contribution of the photolysis of NO_2^- to produce nitric oxide (Reaction R11) (France et al., 2012, and references therein). Therefore, calculations of the NO_x emission flux in snow were based on Reactions (R9) and (R11) for the respective wavelengths 280–360 nm and 280–400 nm (Chu and Anastasio, 2003, 2007, and references therein). The first-order rate constants for the photolysis of NO_3^- at the snowpack surface $j_{NO3^-,z0}$ were calculated as defined in Seinfeld and Pandis (1998):

$$j_{NO_3^-,z_0} = \int_{\lambda_1}^{\lambda_2} \sigma_{NO_3^-}(\lambda,T)\, \phi_{NO_3^-}(\lambda,T)\, I(\lambda,\theta,z_0)\, d\lambda \quad (3)$$

Based on the results of Chu and Anastasio (2003), the spectral UV absorptivity $\sigma_{NO3^-}(\lambda, T)$ was derived between 280 to 360 nm from the measured molar absorption coefficients of aqueous NO_3^- at 278 K and a quantum yield $\varphi_{NO3^-}(\lambda, T)$ of 2.79×10^{-3} was estimated for T = 259 K, the average temperature over the three sampling days. The first-order rate constants for the photolysis of NO_2^- at the snow surface $j_{NO2^-,z0}$ were calculated with the same approach. $\sigma_{NO2^-}(\lambda, T)$ was calculated between 280 to 400 nm from reported molar absorptivities for aqueous NO_2^- at 274 K and a range of $\varphi_{NO2^-}(\lambda, T)$ of $3.4\times10^{-2} - 0.9\times10^{-2}$ for λ between 280 and 400 nm was also determined for T = 259 K (Chu and Anastasio, 2007). The actinic fluxes I(λ, θ, z_0) were computed with the NCAR/ACD radiative transfer model TUV version 5.0 under clear-sky conditions for a 23° solar elevation angle (SEA = $90^\circ - \theta$, with θ the solar zenith angle) averaged over the three sampling days.

The transmission of light in snow that drives the photochemistry in the top snowpack is controlled by optical processes: scattering and absorption (Dominé et al., 2008; Grannas et al., 2007, and references therein). These processes are summarized in the parameter *e*-folding depth (EFD), which in turn depends on snow physical properties – grain size, density, liquid water content – and the concentration of light-absorbing impurities such as black carbon. Studies at Dome C (France et al., 2011) and Barrow, Alasyr BP(Reay et al., 2012), showed that absorption in snow layers, and therefore EFD, is inversely proportional to the content of black carbon in snow. Reported concentrations of black carbon in snow at WAIS Divide of 0.08 ± 0.4 ng g^{-1} (average±1σ) are in the range of those measured at South Pole, 0.2–0.3 ng g^{-1} (Bisiaux et al., 2012, and references therein). Values of $j_{NO3^-,z0}$ and $j_{NO2^-,z0}$ were then scaled as a function of depth (z) using an EFD of 30 cm (Table 3), based on the similar value calculated for South Pole by Zatko et al. (2013):

$$j_{NO_3^-} = j_{NO_3^-,z_0} \times \exp\left(\frac{-z}{EFD}\right) \quad (4)$$

The depth-integrated emission flux of NO_X was calculated for 18 and 28 December 2008 and 4 January 2009 with

$$F_{NO_2} = \int_{z=0cm}^{z=30cm} \left[NO_3^-\right] j_{NO_3^-,z} \, dz \quad (5)$$

$$F_{NO} = \int_{z=0cm}^{z=30cm} \left[NO_2^-\right] j_{NO_2^-,z} \, dz \quad (6)$$

with respectively $[NO_3^-]_z$ and $[NO_2^-]_z$ in molecule cm^{-3} measured at each depth z (Fig. 6).

In order to convert flux F_{NOx} (molecule $cm^{-2} s^{-1}$) into a volumetric production rate P_{NOx} (pptv h^{-1}), F_{NOx} was multiplied by the height of the boundary layer estimated from prior balloon soundings above the West Antarctic Ice Sheet in summer, with an average height of 250 m (range 13–354 m) between morning and late afternoon (Frey et al., 2005). Note that atmospheric boundary layer height as low as 13 m may be infrequent at WAIS Divide. Therefore, estimation of the potential NO_X production from snow for an atmospheric boundary layer height of 13 m will be an upper bound.

Recent studies (Chu and Anastasio, 2007; Boxe and Saiz-Lopez, 2008, and references therein) suggest that only NO_3^- and NO_2^- in quasi-liquid layers are available for photolysis as photochemistry of these species does not occur in the bulk ice. Because the distribution of NO_3^- and NO_2^- between the quasi-liquid layers and the lattice ice is unknown, these calculations assumed that all NO_3^- and NO_2^- can be photolyzed. It is also assumed that the totality of the NO_X produced escapes from the snowpack and is released into the overlying atmosphere without considering any chemical loss. These fluxes and production rates are therefore an upper limit of the potential NO_X source from the snow.

5.1.6 Potential NO_x production from top snowpack

The resulting potential daily NO_2 emission fluxes from NO_3^- photolysis in the surface snowpack were 8.6×10^8 molecule $cm^{-2} s^{-1}$ (Table 3). This value is in agreement with previous reported NO_2 emission fluxes on the Antarctic continent (Table 4). For NO, the estimated value is 33.9×10^8 molecule $cm^{-2} s^{-1}$. Maximum daily NO_X emission fluxes from snow are therefore F_{NOx} of 42.5×10^8 molecule $cm^{-2} s^{-1}$, with 20 % and 80 % from NO_3^- and NO_2^- photolysis, respectively. This contribution is similar to that found by France et al. (2012) at Barrow.

The resulting local NO_X production is 30 pptv h^{-1} for a mean atmospheric boundary layer height of 250 m (Table 3). Average production rates of 21 and

566-pptv h^{-1} were calculated for boundary layer depths of 354 and 13 m, respectively. Comparison between the potential NO_X production rate and the mixing ratios of NO_X estimated from the extended Leighton mechanism with measured NO (Sect. 4.1.3) indicates that the snow source contributes significantly to the NO_X budget at WAIS Divide. However, values of P_{NOx} suggest that the estimated production rates are an upper limit since the observed levels of NO (19 pptv) and the estimated NO_2 mixing ratios (5 pptv) are inconsistent with an NO_X production rate of 566 pptv h^{-1} for atmospheric boundary layer height of 13 m.

These calculated NO_X emissions are higher than reported values from other Antarctic sites, where modeled and measured fluxes reached between 2.4×10^8 and 22×10^8 molecule cm^{-2} s^{-1} (Table 4). In a recent study, Zatko et al. (2013) suggested that local contamination from nearby stations increases the content of impurities in snow, therefore reducing the EFD of the actinic flux in the top snowpack, resulting in a possible underestimation of the NO_X emissions modeled or measured nearby stations by a factor of 1.4–2.4. Thus, high NO_X emissions could be expected in our study since the sampling site was 5 km upwind of the main WAIS camp emissions (Sect. 2). However, the results from Zatko et al. (2013) can be discussed since most of the measurements or estimations of NO_X nearby Antarctic stations were from sites located in clean air sector, upwind of the stations (Table 4). With said precautions, local contamination from nearby stations should not reach these sites and impact on the measured or calculated snowpack emissions.

The above estimates do have uncertainties: a) daily surface-snow samples revealed that the local-scale spatial variability of NO_3^- in the near-surface snowpack is significant, and b) our calculations assume that all of the NO_3^- and NO_2^- in snow is available for photolysis followed by emission into the atmosphere of all the photo-produced NO and NO_2. Concerning b), Anastasio and Chu (2009) suggested that 30 % of the NO_2 produced from NO_3^- photolysis may be converted to NO_2^- within the snow matrix before being released into the atmosphere. Also, the decrease of 5 % per day of NO_2^- in surface snow (Sect. 3.2) indicates that only a small amount of NO_2^- may actually undergo photolysis to produce NO. Nevertheless, these results show the key role of the boundary-layer depth in determining the contribution of snowpack emissions to the overlying photochemistry. Our estimates imply that both the variability of boundary layer height with an observed range in summer of 13 to 354 m and local NO_X emissions from snow impact the atmospheric NO_X mixing ratios.

5.1.7 Local production of O_3

The oxidation of methane is the main in situ chemical source of tropospheric O_3. Thus, Reaction (R1) leads to production of O_3 while Reaction (R13) leads to its destruction (Seinfeld and Pandis, 1998):

$$HO_2 + O_3 \rightarrow OH + 2O_2 \qquad \text{(R13)}$$

The ratio between theses two rates indicates whether WAIS Divide is an O_3 production or destruction site:

$$\frac{(R_{13})}{(R_1)} = \frac{k_{R13}}{k_{R1}} \frac{[O_3]}{[NO]} \quad (7)$$

This ratio was calculated with $k_{R1} = 9.49 \times 10^{-12}$ cm^3 molecule^{-1} s^{-1} and $k_{R13} = 1.62 \times 10^{-15}$cm^3 molecule^{-1} s^{-1}, derived from Sander et al. (2006), and an average temperature of 255.6 K measured during the campaign. Note that this estimation from the photo stationary state relation accounts for the NO_X emit- ted from the snowpack. In the case of Summit, Thomas et al. (2012) showed that NO_X emitted from the snowpack can increase the boundary layer O_3 by an additional 2–3 ppbv. Frey et al. (2013) show that under calm conditions typical for Dome C, East Antarctica, NO and NO_2 emitted by surface snow reach steady-state at 1 m. Thus, it is expected that our measured mixing ratios of O_3 at 1 m above surface snow already reflect the contribution from the NO_X emissions. Also, it is assumed that halogen chemistry does not occur at WAIS Divide, otherwise the reaction of BrO with O_3 and NO_X in the snowpack would reduce the local O_3 production (Thomas et al., 2012).

The ratio (R13) : (R1) equals 0.216 and confirms that WAIS Divide is a surface ozone production site (Sect. 4.1.1).

From Eq. (7), a threshold value of 2 pptv for NO is found to trigger O_3 production at WAIS Divide, whereas this threshold is reached at 5 pptv in the remote continental troposphere of mid-latitude regions (Seinfeld and Pandis, 1998) and of high latitude sites, such as Dome C (derived from Chen et al., 2007). An atmospheric HO_2 concentration of 4.9×10^7 molecule cm^{-3} leads to a potential O_3 production of 0.8 ppbv day^{-1}. This is about 5% of the observed O_3 mixing ratios and respectively 20 % and 50 % of the rates calculated above the East Antarctic Plateau. O_3 production rates are ~ 4 ppbv day^{-1} at South Pole (Chen et al., 2004, and references therein) and ~ 1.5 ppbv day^{-1} at Dome C (Legrand et al., 2009). Our result is consistent with these previous studies since WAIS Divide is a lower-altitude site with a deeper atmospheric boundary layer that is influenced by a diel cycle of UV irradiance.

It is apparent that local O_3 production is too small to account for the observed increases between 24–25 and 27–29 December of 0.3 ppbv h^{-1}. We therefore consider the impact of air mass transport, as detailed below.

5.2 Impacts of air mass transport

Analysis of wind direction and O_3 mixing ratios indicate that air masses from the ENE-SWS sector have typically the highest O_3 concentrations (Sect. 2, Fig. 4). O_3 can be considered a long-lived chemical species compared to NO_X (Sect. 4.1.5) with a lifetime of about 22 days in the polar regions (Grannas et al., 2007). It is therefore expected that local O_3 is affected by transport, so the origin and transport of air at WAIS Divide were further investigated using 4-day back trajectories.

A total 168 trajectories were computed with the NOAA Hysplit (HYbrid Single-Particle Lagrangian Integrated Trajectory; see http://ready.arl.noaa.gov/hysplit4.html) model (R. R. Draxler and G. D. Rolph, 2003) every 4 h using global meteorological data from the NCEP Global Data Assimilation System (GDAS) with a 3 h temporal resolution, a $1^\circ \times 1^\circ$ (latitude x longitude) spatial resolution, an endpoint at the latitude and longitude of WAIS Divide and 10 m above ground level from 10 December 2008 to 8 January 2009. A comparison of the resulting 168 trajectories with another set generated from the NCEP-NCAR archived data shows similar results (Fig. 9), while Sinclair et al. (2013) showed that back trajectories from NCEP-NCAR and ECMWF Interim Re-Analysis (ERA-Interim) were comparable during austral summer. Therefore, the following discussion is based on trajectories produced from the GDAS archives. The back trajectories were combined to create daily maps (Fig. 10) and we distinguish three regions of air mass origin based on elevation, slope and previous O_3 and temperature measurements (Fig. 9).

We refer to the East Antarctic Plateau as the East Antarctic region above 2500 m a.m.s.l. with a slope of less than 1° since elevated O_3 has not been observed below 2500 m a.m.s.l. during the Antarctic summer (Frey et al., 2005). Surface O_3 is produced over the East Antarctic Plateau and possibly exported through air outflow (Sect. 4.2.2). The inner WAIS refers to the West Antarctic area above 1750 m a.m.s.l. with a slope inferior to 1°. An average temperature of about $-25\ ^\circ C$ was reported in the inner WAIS compared to $-15\ ^\circ C$ in the lower-elevated regions (Frey et al., 2005). Finally, based on a slope higher than 1° and on the previous observations, the areas below 2500 m a.m.s.l. in East Antarctica and 1750 m a.m.s.l. in West Antarctica are referred to as Antarctic coastal slopes.

Figure 9 shows that over the campaign, 58 % of the air masses originated from the Antarctic coastal slopes with 2 % possibly flowing from the distant King Haakon VII coast. An estimated 17 % was transported from the inner WAIS and 25 % of the air was advected from the East Antarctic Plateau. About 71 % of the air reaching WAIS Divide flowed from East Antarctica and 29 % from West Antarctica.

5.2.1 Air mass origins related to low O_3 levels

Except for outflows from the East Antarctic Plateau, all air mass origins are associated with low O_3, averaging 13 ± 3 ppbv (Fig. 11). This represents therefore 75 % of the air mass reaching WAIS Divide, which includes air from the coastal slopes (Fig. 10a, b) and the inner WAIS (Fig. 10e). In coastal Antarctica, halogen-catalyzed chemistry has been found to prevent O_3 production in summer and even leads to the well-known episodic O_3 depletion events during spring (Jones et al., 2008, and references therein). The little vertical- column amounts of IO and BrO observed at WAIS Divide from satellite in December and January 2004–2009 (Schönhardt et al., 2012) suggest that contribution of halogens from intrusions of coastal air (58 % of all back trajectories) to the WAIS Divide photochemistry is not significant. Thus, reduction of O_3 levels at WAIS Divide by halogen chemistry may not occur, as assumed in the previous sections

Air masses from the interior of WAIS (17 % of all back trajectories, Fig. 10e) are also associated with low O_3 mixing ratios. Influence from local halogen chemistry or halogens exported from the Antarctic coasts is not consistent with observations of Schönhardt et al. (2012).

It is therefore suggested that the O_3 levels of the air masses from the coastal slopes and the interior of WAIS are low, so these airflows can reduce the O_3 levels of WAIS Divide when reaching the site. From these results and the wind-speed record (Fig. 11), it is also expected that O_3 production over WAIS is less than or equal to our estimated O_3 production rate for WAIS Divide.

Airflows from long-distance sources such as King Haakon VII sea coast (2 % of all back trajectories, Fig. 10f) appear infrequently, with no obvious impact on local O_3. The O_3 signature of these air masses likely disappeared during their transport over more than 2500 km.

5.2.2 Air mass origins associated with elevated O_3 levels

Approximately 25 % of all back trajectories point to airflows from the East Antarctic Plateau (Fig. 10c, d and Fig. 9), which are mainly related to the highest O_3 measured at WAIS Divide, with an average $\pm 1\sigma$ of 19 ± 4 ppbv (Fig. 11).

This is consistent with the O_3 production above the East Antarctic Plateau (Helmig et al., 2008a, and references therein) that enhances the O_3 levels of WAIS through air transport, as previously reported by Legrand et al. (2009), who only observed high O_3 mixing ratios at Dumont D'Urville for air masses originating from the Antarctic Plateau. Such an oxidizing environment is confirmed by the O_3 observations at South Pole (S. J. Oltmans, http://ds.data. jma.go.jp/gmd/wdcgg) over the same period that shows an average concentration of 31 ppbv, 17 ppbv more than the average observed at WAIS Divide (Fig. 11).

Further back-trajectory analysis reveals two conditions in which high O_3 concentrations are observed above WAIS Divide. First, elevated O_3 mixing ratios were only observed for lower atmosphere air coming from the East Antarctic Plateau (below 1500 m above ground level). The trajectories of these near-surface airflows are in good agreement with the katabatic streamlines described by Parish and Bromwich (2007). This suggests that air exported off the East Antarctic Plateau via katabatic outflows raises significantly the O_3 mixing ratios at WAIS Divide. The ozone depletion recorded between 25 and 27 December 2008 (Fig. 10d and Fig. 11) is attributed to an air mass coming from altitude as high as ~ 3000 m above ground level.

Secondly, high O_3 was only observed at WAIS Divide when the transport time from the East Antarctic Plateau was less than 3 days (Fig. 10c and d). To investigate this condition, the total O_3 loss during transport from the Antarctic Plateau to WAIS Divide was estimated. The back trajectories indicate that O_3 maxima during 24–28 December at WAIS Divide are due to rich O_3 air originating from the South Pole region, as local records show similar but higher peaks about 2 days before (Fig. 11). From this delay, a loss rate of 0.25 ($\pm$0.04) ppbv h^{-1} was calculated. This represents an O_3 loss rate

of 5.5 (±0.9) ppbv day^{-1} when averaged O_3 mixing ratios were 30 and 14 ppbv, respectively, at South Pole and WAIS Divide over the campaign. If these loss rates (from dilution, net destruction, etc.) are typical, then it follows that O_3 export off the Plateau has to be rapid (less than 3 days) in order to have an impact on WAIS Divide's levels.

Observations of elevated O_3 levels are frequently related to vertical transport from the free troposphere/lower stratosphere at Summit, Greenland (Helmig et al., 2007b) and other Arctic sites (Helmig et al., 2007a, and references therein). These stratospheric-intrusion events are promoted by boundary-layer instabilities, which are caused by significant diel radiation cycles and by the size of the Greenland ice sheet (Helmig et al., 2007b). All of the vertical O_3 profiles over the East Antarctic Plateau from tethered-balloon measurements (Helmig et al., 2008a; Johnson et al., 2008; Oltmans et al., 2008) and an airborne study (Slusher et al., 2010) present higher O_3 mixing ratios in the atmospheric boundary layer than in the free troposphere, indicating that no contribution of stratospheric O_3 occurs over the Antarctic Plateau. Enhancement of the O_3 levels at WAIS Divide from vertical transport is neither supported by the back-trajectory analysis nor by the vertical O_3 profiles measured at South Pole during this period (http://www.esrl.noaa.gov/gmd/dv/data/index.php), confirming the previous observations from the East Antarctic Plateau.

However, not all elevated O_3 mixing ratios at this site could be explained with the air origin. This is the case for the 5 h rise of O_3 mixing ratios that reached 24 ppbv on 12 December and occurred during the only snowfall observed during the campaign (Fig. 5). With low wind speeds (Fig. 11) and airflow from the inner WAIS observed during this event, it is possible that more O_3 accumulated in the boundary layer from local production. However, given the O_3 production rate we estimated previously (Sect. 4.1.7), it seems unlikely that only the local production of O_3 could cause this specific increase.

6 Conclusions

Being from a geographically intermediate site between the Antarctic coast and the East Antarctic Plateau, our results show that concentrations of atmospheric NO, O_3, H_2O_2 and skin-layer NO_3^- at WAIS Divide during summer 2008–2009 are similar to coastal levels.

Comparison of local potential NO_X production from daily average depth-integrated emission fluxes of NO_X and the NO_X mixing ratios estimated from a steady-state assumption shows that NO_3^- and NO_2^- photolysis in the local snowpack are a significant source of NO_X at WAIS Divide. The upper limit of 15 h NO_X lifetime confirms that short-lived NO_X species are more sensitive to local production above WAIS than to outflows from the East Antarctic Plateau. Lower NO_3^- preservation in snow at WAIS Divide than at Summit is coherent with the potential NO_X emission flux and suggests stronger lateral export of emitted NO_X than local recycling.

O_3 production at WAIS Divide can be triggered with NO mixing ratios higher than 2 pptv, but the small O_3 production rate cannot explain the observed O_3 variability, which suggests a significant air mass transport contribution. Air flows from the East Antarctic Plateau are only associated with high O_3 mixing ratios if the air transport is near surface by gravity driven winds and less than 3 days from the East Antarctic Plateau. With levels of O_3 over the East Antarctic Plateau twice those observed at WAIS Divide, outflows from the interior of the continent therefore have the potential to enhance the mixing ratios of long-lived atmospheric chemical species such as O_3 over WAIS. During this 28-day campaign, outflows from the Antarctic Plateau were observed over 7.5 days, raising the summer O_3 average by about 20 % (2 ppbv). The possibility of halogen chemistry above inland WAIS that would impact the atmospheric photochemistry is not consistent with satellite observations and cannot therefore explain the low O_3 levels that are associated with air mass origins from the interior of WAIS.

Results from the back-trajectory analysis over December 2008 and January 2009 at WAIS Divide (Fig. 9) compare well with those of Markle et al. (2012) calculated over thirty years in the Ross Sea region. For the same months, the authors found that 45 % of the air mass trajectories have an oceanic/West Antarctic origin and 55 % a continental/East Antarctic source, while we observed respective values of 29 % and 71 % at WAIS Divide. These results confirm the minor contribution of oceanic/West Antarctic inflows to the WAIS atmosphere during austral summer shown by Nicolas and Bromwich (2011), and the predominance of continental/East Antarctic air masses that may significantly impact the oxidative capacity of the atmosphere above the interior of WAIS.

Acknowledgements. This work was supported by the National Science Foundations Office of Polar Programs (OPP-0636929). We thank G. Huey for the use of the nitric oxide detector. We also thank S. J. Oltmans for using his O_3 measurements from South Pole, as well as B. Alexander and E. D. Sofen for their insight concerning the EFD and NO_3^- photolysis at WAIS Divide.

7 References

Anastasio, C. and Chu, L.: Photochemistry of Nitrous Acid (HONO) and Nitrous Acidium Ion (H_2ONO^+) in Aqueous Solution and Ice, Environ. Sci. Technol., 43, 1108–1114, doi:10.1021/es802579a, 2009.

Anastasio, C. and Robles, T.: Light absorption by soluble chemical species in Arctic and Antarctic snow, J. Geophys. Res.-Atmos., 112, D24304, doi:10.1029/2007JD008695, 2007.

Banta, J. R., Mcconnell, J. R., Frey, M. M., Bales, R. C., and Taylor, K.: Spatial and temporal variability in snow accumulation at the West Antarctic Ice Sheet Divide over recent centuries, J. Geophys. Res., 113, D23102, doi:10.1029/2008JD010235, 2008.

Bauguitte, S. J.-B., Brough, N., Frey, M. M., Jones, A. E., Maxfield, D. J., Roscoe, H. K., Rose, M. C., and Wolff, E. W.: A network of autonomous surface ozone monitors in Antarctica: technical description and first results, Atmos. Meas. Tech., 4, 645–658, doi:10.5194/amt-4-645-2011, 2011.

Bauguitte, S. J.-B., Bloss, W. J., Evans, M. J., Salmon, R. A., Anderson, P. S., Jones, A. E., Lee, J. D., Saiz-Lopez, A., Roscoe, H. K., Wolff, E. W., and Plane, J. M. C.: Summertime NO_x measurements during the CHABLIS campaign: can source and sink estimates unravel observed diurnal cycles?, Atmos. Chem. Phys., 12, 989–1002, doi:10.5194/acp-12-989-2012, 2012.

Bisiaux, M. M., Edwards, R., McConnell, J. R., Curran, M. A. J., Van Ommen, T. D., Smith, A. M., Neumann, T. A., Pasteris, D. R., Penner, J. E., and Taylor, K.: Changes in black carbon deposition to Antarctica from two high-resolution ice-core records, 1850–2000 AD, Atmos. Chem. Phys., 12, 4107–4115, doi:10.5194/acp-12-4107-2012, 2012.

Bloss, W. J., Lee, J. D., Heard, D. E., Salmon, R. A., Bauguitte, S. J.-B., Roscoe, H. K., and Jones, A. E.: Observations of OH and HO_2 radicals in coastal Antarctica, Atmos. Chem. Phys., 7, 4171–4185, doi:10.5194/acp-7-4171-2007, 2007.

Boxe, C. S. and Saiz-Lopez, A.: Multiphase modeling of nitrate photochemistry in the quasi-liquid layer (QLL): implications for NO_x release from the Arctic and coastal Antarctic snowpack, Atmos. Chem. Phys., 8, 4855–4864, doi:10.5194/acp-8-4855-2008, 2008.

Burkhart, J. F., Hutterli, M. A., Bales, R. C., and Mcconnell, J. R.: Seasonal accumulation timing and preservation of nitrate in firn at Summit, Greenland, J. Geophys. Res.-Atmos., 109, D19302, doi:10.1029/2004JD004658, 2004.

Chen, G., Davis, D. D., Crawford, J. H., Hutterli, M. A., Huey, G., Slusher, D., Mauldin, L., Eisele, F., Tanner, D., Dibb, J. E., Buhr, M., Mcconnell, J. R., Lefer, B., Shetter, R., Blake, D. R., Song, C., Lombardi, K., and Arnoldy, J.: A reassessment of HO_x South Pole chemistry based on observations recorded during ISCAT 2000, Atmos. Environ., 38, 5451–5461, 2004.

Chen, G., Huey, G., Crawford, J. H., Olson, J. R., Hutterli, M. A., Sjostedt, S. J., Tanner, D., Dibb, J. E., Lefer, B., Blake, N. J., Davis, D. D., and Stohl, A.: An assessment of the polar HO_x photochemical budget based on 2003 Summit Greenland field observations, Atmos. Environ., 41, 7806–7820, doi:10.1016/j.atmosenv.2003.07.018, 2007.

Chu, L. and Anastasio, C.: Quantum yields of hydroxyl radical and nitrogen dioxide from the photolysis of nitrate on ice, J. Phys. Chem. A, 107, 9594–9602, doi:10.1021/jp0349132, 2003.

Chu, L. and Anastasio, C.: Temperature and wavelength dependence of nitrite photolysis in frozen and aqueous solutions, Environ. Sci. Technol., 41, 3626–3632, doi:10.1021/es062731q, 2007.

Davis, D. D., Nowak, J., Chen, G., Buhr, M., Arimoto, R., Hogan, A., Eisele, F., Mauldin, L., Tanner, D., Shetter, R., Lefer, B., and McMurry, P.: Unexpected high levels of NO observed at South Pole, Geophys. Res. Lett., 28, 3625–3628, doi:10.1029/2000GL012584, 2001.

Davis, D. D., Chen, G., Buhr, M., Crawford, J. H., Lenschow, D., Lefer, B., Shetter, R., Eisele, F., Mauldin, L., and Hogan, A.: South Pole NO_x chemistry: an assessment of factors controlling variability and absolute levels, Atmos. Environ., 38, 5375–5388, doi:10.1016/j.atmosenv.2004.04.039, 2004.

Davis, D. D., Seelig, J., Huey, G., Crawford, J. H., Chen, G., Wang, Y., Buhr, M., Helmig, D., Neff, W., Blake, D. R., Arimoto, R., and Eisele, F.: A reassessment of Antarctic plateau reactive nitrogen based on ANTCI 2003 airborne and ground based measurements, Atmos. Environ., 42, 2831–2848, doi:10.1016/j.atmosenv.2007.07.039, 2008.

Dibb, J. E., Huey, G., Slusher, D., and Tanner, D.: Soluble reactive nitrogen oxides at South Pole during ISCAT 2000, Atmos. Envi- ron., 38, 5399–5409, 2004.

Dibb, J. E., Whitlow, S. I., and Arsenault, M.: Seasonal variations in the soluble ion content of snow at Summit. Greenland: Constraints from three years of daily surface snow samples, Atmos. Environ., 41, 5007–5019, doi:10.1016/j.atmosenv.2003.01.001, 2007.

Dibb, J. E., Ziemba, L. D., Luxford, J., and Beckman, P.: Bromide and other ions in the snow, firn air, and atmospheric boundary layer at Summit during GSHOX, Atmos. Chem. Phys., 10, 9931– 9942, doi:10.5194/acp-10-9931-2010, 2010.

Domine, F., Albert, M., Huthwelker, T., Jacobi, H.-W., Kokhanovsky, A. A., Lehning, M., Picard, G., and Simpson, W. R.: Snow physics as relevant to snow photochemistry, Atmos. Chem. Phys., 8, 171–208, doi:10.5194/acp-8-171-2008, 2008.

Eisele, F. L. and Davis, D. D.: Antarctic tropospheric chemistry investigation (ANTCI) 2003, Atmos. Environ., 42, 2747–2748, doi:10.1016/j.atmosenv.2007.09.074, 2008.

Erbland, J., Vicars, W. C., Savarino, J., Morin, S., Frey, M. M., Frosini, D., Vince, E., and Martins, J. M. F.: Air-snow transfer of nitrate on the East Antarctic Plateau – Part 1: Isotopic evidence for a photolytically driven dynamic equilibrium in summer, Atmos. Chem. Phys., 13, 6403–6419, doi:10.5194/acp-13- 6403-2013, 2013.

France, J., Reay, H., King, M., Voisin, D., Jacobi, H., Dominé, F., Beine, H., Anastasio, C., MacArthur, A., and Lee-Taylor, J.: Hydroxyl radical and NO_x production rates, black carbon concentrations and light-absorbing impurities in snow from field measurements of light penetration and nadir reflectivity of on- shore and offshore coastal Alaskan snow, J. Geophys. Res., 117, D00R12, doi:10.1029/2011JD016639, 2012.

France, J. L., King, M. D., Frey, M. M., Erbland, J., Picard, G., Preunkert, S., MacArthur, A., and Savarino, J.: Snow optical properties at Dome C (Concordia), Antarctica; implications for snow emissions and snow chemistry of reactive nitrogen, Atmos. Chem. Phys., 11, 9787–9801, doi:10.5194/acp-11-9787-2011, 2011.

Frey, M. M., Stewart, R. W., Mcconnell, J. R., and Bales, R. C.: Atmospheric hydroperoxides in West Antarctica: Links to stratospheric ozone and atmospheric oxidation capacity, J. Geophys. Res., 110, D23301, doi:10.1029/2005JD006110, 2005.

Frey, M. M., Bales, R. C., and Mcconnell, J. R.: Climate sensitivity of the century-scale hydrogen peroxide (H_2O_2) record preserved in 23 ice-cores from West Antarctica, J. Geophys. Res.-Atmos, 111, D21301, doi:10.1029/2005JD006816, 2006.

Frey, M. M., Hutterli, M. A., Chen, G., Sjostedt, S. J., Burkhart, J. F., Friel, D. K., and Bales, R. C.: Contrasting atmospheric boundary layer chemistry of methylhydroperoxide (CH_3OOH) and hydrogen peroxide (H_2O_2) above polar snow, Atmos. Chem. Phys., 9, 3261–3276, doi:10.5194/acp-9-3261-2009, 2009a.

Frey, M. M., Savarino, J., Morin, S., Erbland, J., and Martins, J. M. F.: Photolysis imprint in the nitrate stable isotope signal in snow and atmosphere of East Antarctica and implications for reactive nitrogen cycling, Atmos. Chem. Phys., 9, 8681–8696, doi:10.5194/acp-9-8681-2009, 2009b.

Frey, M. M., Brough, N., France, J. L., Anderson, P. S., Traulle, O., King, M. D., Jones, A. E., Wolff, E. W., and Savarino, J.: The diurnal variability of atmospheric nitrogen oxides (NO and NO_2) above the Antarctic Plateau driven by atmospheric stability and snow emissions, Atmos. Chem. Phys., 13, 3045–3062, doi:10.5194/acp-13-3045-2013, 2013.

Grannas, A. M., Jones, A. E., Dibb, J., Ammann, M., Anastasio, C., Beine, H. J., Bergin, M., Bottenheim, J., Boxe, C. S., Carver, G., Chen, G., Crawford, J. H., Dominé, F., Frey, M. M., Guzmán, M. I., Heard, D. E., Helmig, D., Hoffmann, M. R., Honrath, R. E., Huey, L. G., Hutterli, M., Jacobi, H. W., Klán, P., Lefer, B., McConnell, J., Plane, J., Sander, R., Savarino, J., Shepson, P. B., Simpson, W. R., Sodeau, J. R., von Glasow, R., Weller, R., Wolff, E. W., and Zhu, T.: An overview of snow photochemistry: evidence, mechanisms and impacts, Atmos. Chem. Phys., 7, 4329– 4373, doi:10.5194/acp-7-4329-2007, 2007.

Grilli, R., Legrand, M., Kukui, A., Méjean, G., Preunkert, S., and Romanini, D.: First investigations of IO, BrO, and NO_2 summer atmospheric levels at a coastal East Antarctic site using mode- locked cavity enhanced absorption spectroscopy, Geophys. Res. Lett., 40, 791–796, doi:10.1002/grl.50154, 2013.

Hastings, M. G.: Seasonal variations in N and O isotopes of nitrate in snow at Summit, Greenland: Implications for the study of nitrate in snow and ice-cores, J. Geophys. Res., 109, D20306, doi:10.1029/2004JD004991, 2004.

Helmig, D., Oltmans, S. J., Carlson, D., Lamarque, J.-F., Jones, A. E., Labuschagne, C., Anlauf, K., and Hayden, K.: A review of surface ozone in the polar regions, Atmos. Environ., 41, 5138– 5161, doi:10.1016/j.atmosenv.2006.09.053, 2007a.

Helmig, D., Oltmans, S. J., Morse, T. O., and Dibb, J. E.: What is causing high ozone at Summit, Greenland?, Atmos. Environ., 41, 5031–5043, doi:10.1016/j.atmosenv.2006.05.084, 2007b.

Helmig, D., Johnson, B., Oltmans, S. J., Neff, W., Eisele, F., and Davis, D. D.: Elevated ozone in the boundary layer at South Pole, Atmos. Environ., 42, 2788–2803, doi:10.1016/j.atmosenv.2006.12.032, 2008.

Honrath, R., Lu, Y., Peterson, M., Dibb, J., Arsenault, M., Cullen, N., and Steffen, K.: Vertical fluxes of NO_x, HONO, and HNO_3 above the snowpack at Summit, Greenland, Atmos. Environ., 36, 2629–2640, doi:10.1016/S1352-2310(02)00132-2, 2002.

Hutterli, M. A.: Sensitivity of hydrogen peroxide (H_2O_2) and formaldehyde (HCHO) preservation in snow to changing environmental conditions: Implications for ice-core records, J. Geo- phys. Res., 108, 4023, doi:10.1029/2002JD002528, 2003.

Jacobi, H.-W., Weller, R., Jones, A. E., Anderson, P. S., and Schrems, O.: Peroxyacetyl nitrate (PAN) concentrations in the Antarctic troposphere measured during the photochemical experiment at Neumayer (PEAN'99), Atmos. Environ., 34, 5235– 5247, doi:10.1016/S1352-2310(00)00190-4, 2000.

Jarvis, J. C., Hastings, M. G., Steig, E. J., and Kunasek, S. A.: Isotopic ratios in gas-phase HNO_3 and snow nitrate at Summit, Greenland, J. Geophys. Res., 114, D17301, doi:10.1029/2009JD012134, 2009.

Jefferson, A., Tanner, D., Eisele, F., Davis, D., Chen, G., Crawford, J., Huey, J., Torres, A., and Berresheim, H.: OH photochemistry and methane sulfonic acid formation in the coastal Antarctic boundary layer, J. Geophys. Res.-Atmos., 103, 1647–1656, doi:10.1029/97JD02376, 1998.

Johnson, B., Helmig, D., and Oltmans, S. J.: Evaluation of ozone measurements from a tethered balloon-sampling platform at South Pole Station in December 2003, Atmos. Environ., 42, 2780–2787, doi:10.1016/j.atmosenv.2007.03.043, 2008.

Jones, A., Weller, R., Minikin, A., Wolff, E., Sturges, W., McIntyre, H., Leonard, S., Schrems, O., and Bauguitte, S.: Oxidized nitrogen chemistry and speciation in the Antarctic troposphere, J. Geophys. Res.-Atmos., 104, 21355–21366, doi:10.1029/1999JD900362, 1999.

Jones, A., Weller, R., Anderson, P., Jacobi, H., Wolff, E., Schrems, O., and Miller, H.: Measurements of NO_x emissions from the Antarctic snowpack, Geophys. Res. Lett., 28, 1499–1502, doi:10.1029/2000GL011956, 2001.

Jones, A. E., Weller, R., Wolff, E. W., and Jacobi, H.-W.: Speciation and rate of photochemical NO and NO_2 production in Antarctic snow, Geophys. Res. Lett., 27, 345–348, doi:10.1029/1999GL010885, 2000.

Jones, A. E., Wolff, E. W., Salmon, R. A., Bauguitte, S. J.-B., Roscoe, H. K., Anderson, P. S., Ames, D., Clemitshaw, K. C., Fleming, Z. L., Bloss, W. J., Heard, D. E., Lee, J. D., Read, K. A., Hamer, P., Shallcross, D. E., Jackson, A. V., Walker, S. L., Lewis, A. C., Mills, G. P., Plane, J. M. C., Saiz-Lopez, A., Sturges, W. T., and Worton, D. R.: Chemistry of the Antarctic Boundary Layer and the Interface with Snow: an overview of the CHABLIS campaign, Atmos. Chem. Phys., 8, 3789–3803, doi:10.5194/acp-8-3789-2008, 2008.

Jones, A. E., Wolff, E. W., Ames, D., Bauguitte, S. J.-B., Clemitshaw, K. C., Fleming, Z., Mills, G. P., Saiz-Lopez, A., Salmon, R A., Sturges, W. T., and Worton, D. R.: The multi-seasonal NO_y budget in

coastal Antarctica and its link with surface snow and ice-core nitrate: results from the CHABLIS campaign, Atmos. Chem. Phys., 11, 9271–9285, doi:10.5194/acp-11-9271-2011, 2011.

Kreutz, K. and Koffman, B.: WAIS Divide Snowpit Chemical and Isotope Measurements, Antarctica, Boulder, Colorado USA: Na- tional Snow and Ice Data Center, 2011.

Kreutz, K. J., Mayewski, P. A., Twickler, M. S., Whitlow, S. I., White, J., Shuman, C. A., Raymond, C. F., Conway, H., and McConnell, J. R.: Seasonal variations of glaciochemical, isotopic and stratigraphic properties in Siple Dome (Antarctica) surface snow, Ann. Glaciol., 29, 38–44, doi:10.3189/172756499781821193, 1999.

Lee-Taylor, J. and Madronich, S.: Calculation of actinic fluxes with a coupled atmosphere-snow radiative transfer model, J. Geophys. Res.-Atmos., 107, 4796, doi:10.1029/2002JD002084, 2002.

Legrand, M., Preunkert, S., Jourdain, B., Gallée, H., Goutail, F.,Weller, R., and Savarino, J.: Year-round record of surface ozone at coastal (Dumont d'Urville) and inland (Concor- dia) sites in East Antarctica, J. Geophys. Res., 114, D20306, doi:10.1029/2008JD011667, 2009.

Legrand, M. R. and Delmas, R. J.: Soluble impurities in four Antarctic ice-cores over the last 30,000 years, Ann. Glaciol., 10, 116–120, 1988.

Lind, J. A. and Kok, G. L.: Correction to Henry's law determinations for aqueous solutions of hydrogen peroxide, methylhydroperoxide, and peroxyacetic acid, J. Geophys. Res., 99, 21119– 21119, doi:10.1029/94JD01155, 1994.

Markle, B. R., Bertler, N. A. N., Sinclair, K. E., and Sneed, S. B.: Synoptic variability in the Ross Sea region, Antarctica, as seen from back-trajectory modeling and ice-core analysis, J. Geophys. Res., 117, D02113,doi:10.1029/2011JD016437, 2012.

Mauldin, L., Kosciuch, E., Henry, B., Eisele, F., Shetter, R., Lefer, B., Chen, G., Davis, D. D., Huey, G., and Tanner, D.: Measurements of OH, HO_2+RO_2, H_2SO_4, and MSA at the South Pole during ISCAT 2000, Atmos. Environ., 38, 5423–5437, doi:10.1016/j.atmosenv.2004.06.031, 2004.

Mayewski, P. A. and Dixon, D.: US International Trans Antarctic Scientific Expedition (US ITASE) glaciochemical data, Boulder, CO, USA, National Snow and Ice Data Center, 2005.

Mayewski, P. A., Spencer, M. J., Twickler, M. S., and Whitlow, S.: A glaciochemical survey of the Summit region, Greenland, Ann. Glaciol., 14, 186–190, 1990.

Mulvaney, R., Wagenbach, D., and Wolff, E. W.: Postdepositional change in snowpack nitrate from observation of year-round near-surface snow in coastal Antarctica, J. Geophys. Res.-Atmos., 103, 11021–11031, doi:10.1029/97JD03624, 1998.

Nicolas, J. P. and Bromwich, D. H.: Climate of West Antarctica and Influence of Marine Air Intrusions, J. Climate, 24, 49–67, doi:10.1175/2010JCLI3522.1, 2011.

O'Driscoll, P., Minogue, N., Takenaka, N., and Sodeau, J.: Release of Nitric Oxide and Iodine to the Atmosphere from the Freezing of Sea-Salt Aerosol Components, J. Phys. Chem. A, 112, 1677– 1682, doi:10.1021/jp710464c, 2012.

Oltmans, S. J., Johnson, B. J., and Helmig, D.: Episodes of high surface-ozone amounts at South Pole during summer and their impact on the long-term surface-ozone variation, Atmos. Environ., 42, 2804–2816, doi:10.1016/j.atmosenv.2007.01.020, 2008.

Oncley, S., Buhr, M., Lenschow, D., Davis, D., and Semmer, S.: Observations of summertime NO fluxes and boundary-layer height at the South Pole during ISCAT 2000 using scalar similarity, Atmos. Environ., 38, 5389–5398, doi:10.1016/j.atmosenv.2004.05.053, 2004.

Parish, T. R. and Bromwich, D. H.: Reexamination of the Near- Surface Airflow over the Antarctic Continent and Implica- tions on Atmospheric Circulations at High Southern Latitudes, Mon. Weather. Rev., 135, 1961–1973, doi:10.1175/MWR3374.1, 2007.

Preunkert, S., Ancellet, G., Legrand, M., Kukui, A., Kerbrat, M., Sarda-Estève, R., Gros, V., and Jourdain, B.: Oxidant Produc- tion over Antarctic Land and its Export (OPALE) project: An overview of the 2010–2011 summer campaign, J. Geophys. Res., 117, D15307, doi:10.1029/2011JD017145, 2012.

Reay, H. J., France, J. L., and King, M. D.: Decreased albedo, e- folding depth and photolytic OH radical and NO_2 production with increasing black carbon content in Arctic snow, J. Geophys. Res.-Atmos., 117, D00R20, doi:10.1029/2011JD016630, 2012.

Ridley, B., Walega, J., Montzka, D., Grahek, F., Atlas, E., Flocke, F., Stroud, V., Deary, J., Gallant, A., Boudries, H., Bottenheim, J., Anlauf, K., Worthy, D., Sumner, A., Splawn, B., and Shepson, P.: Is the Arctic surface layer a and sink of NO_x in winter/spring?, J. Atmos. Chem., 36, 1–22, doi:10.1023/A:1006301029874, 2000.

Rothlisberger, R., Hutterli, M., Sommer, S., Wolff, E., and Mulvaney, R.: Factors controlling nitrate in ice-cores: Evidence from the Dome C deep ice-core, J. Geophys. Res.-Atmos., 105, 20565– 20572, doi:10.1029/2000JD900264, 2000.

Rothlisberger, R., Hutterli, M., Wolff, E., Mulvaney, R., Fischer, H., Bigler, M., Goto-Azuma, K., Hansson, M., Ruth, U., Siggaard-Andersen, M., and Steffensen, J.: Nitrate in Greenland and Antarctic ice-cores: a detailed description of post-depositional processes, Ann. Glaciol., 35, 209–216, doi:10.3189/172756402781817220, 2002.

Saiz-Lopez, A. and von Glasow, R.: Reactive halogen chemistry in the troposphere, Chem. Soc. Rev., 41, 6448–6472, doi:10.1039/c2cs35208g, 2012.

Saiz-Lopez, A., Mahajan, A. S., Salmon, R. A., Bauguitte, S. J. B., Jones, A. E., Roscoe, H. K., and Plane, J. M. C.: Boundary Layer Halogens in Coastal Antarctica, Science, 317, 348–351, doi:10.1126/science.1141408, 2007.

Sander, S., Friedl, R., Golden, D., Kurylo, M., Moortgat, G., Keller- Rudek, H., Wine, P., Kolb, C., Molina, M., Finlayson-Pitts, B., Huie, R., and Orkin, V.: Chemical kinetics and photochemical data for use in atmospheric studies, Evaluation number 15, JPL publication, 2006.

Schönhardt, A., Begoin, M., Richter, A., Wittrock, F., Kaleschke, L., Gómez Martín, J. C., and Burrows, J. P.: Simultaneous satel- lite observations of IO and BrO over Antarctica, Atmos. Chem. Phys., 12, 6565–6580, doi:10.5194/acp-12-6565-2012, 2012.

Seinfeld, J. H. and Pandis, S. N.: Atmospheric chemistry and physics: from air pollution to climate change, from air pollution to climate change, Wiley, 1998.

Sinclair, K. E., Bertler, N. A. N., Trompetter, W. J., and Baisden, W. T.: Seasonality of Airmass Pathways to Coastal Antarctica: Ramifications for Interpreting High-Resolution Ice-core Records, J. Climate, 26, 2065–2076, doi:10.1175/JCLI-D-12-00167.1, 2013.

Slusher, D., Huey, G., Tanner, D., Chen, G., Davis, D. D., Buhr, M., Nowak, J., Eisele, F., Kosciuch, E., Mauldin, L., Lefer, B., Shetter, R., and Dibb, J. E.: Measurements of pernitric acid at the South Pole during ISCAT 2000, Geophys. Res. Lett., 29, 2011, doi:10.1029/2002GL015703, 2002.

Slusher, D. L., Neff, W. D., Kim, S., Huey, L. G., Wang, Y., Zeng, T., Tanner, D. J., Blake, D. R., Beyersdorf, A., Lefer, B. L., Crawford, J. H., Eisele, F. L., Mauldin, R. L., Kosciuch, E., Buhr, M. P., Wallace, H. W., and Davis, D. D.: Atmospheric chemistry results from the ANTCI 2005 Antarctic plateau airborne study, J. Geophys. Res.-Atmos., 115, D07304, doi:10.1029/2009JD012605, 2010.

Takenaka, N. and Bandow, H.: Chemical kinetics of reactions in the unfrozen solution of ice, J. Phys. Chem. A, 111, 8780–8786, doi:10.1021/jp0738356, 2007.

Thomas, J. L., Dibb, J. E., Huey, L. G., Liao, J., Tanner, D., Lefer, B., von Glasow, R., and Stutz, J.: Modeling chemistry in and above snow at Summit, Greenland – Part 2: Impact of snowpack

chemistry on the oxidation capacity of the boundary layer, Atmos. Chem. Phys., 12, 6537–6554, doi:10.5194/acp-12-6537-2012, 2012.

Traversi, R., Becagli, S., Castellano, E., Cerri, O., Morganti, A., Severi, M., and Udisti, R.: Study of Dome C site (East Antartica) variability by comparing chemical stratigraphies, Microchem. J., 92, 7–14, doi:10.1016/j.microc.2008.08.007, 2009.

Wang, Y., Choi, Y., Zeng, T., Davis, D., Buhr, M., Huey, L. G., and Neff, W.: Assessing the photochemical impact of snow NO_x emissions over Antarctica during ANTCI 2003, Atmos. Environ., 42, 2849–2863, doi:10.1016/j.atmosenv.2007.07.062, 2008.

Wolff, E. W., Jones, A. E., Bauguitte, S. J.-B., and Salmon, R. A.: The interpretation of spikes and trends in concentration of nitrate in polar ice-cores, based on evidence from snow and atmospheric measurements, Atmos. Chem. Phys., 8, 5627–5634, doi:10.5194/acp-8-5627-2008, 2008.

Zatko, M. C., Grenfell, T. C., Alexander, B., Doherty, S. J., Thomas, J. L., and Yang, X.: The influence of snow grain size and impurities on the vertical profiles of actinic flux and associated NO_x emissions on the Antarctic and Greenland ice sheets, Atmos. Chem. Phys., 13, 3547–3567, doi:10.5194/acp-13-3547-2013, 2013.

8 Tables & Figures

Table 1. Averages $\pm 1\sigma$ (medians) of atmospheric and snow concentrations of the chemical species observed at WAIS Divide and nearby sites.

Site	atmospheric				skin layer		
	NO (pptv)	O_3 (ppbv)	H_2O_2 (pptv)	MHP (pptv)	H_2O_2 (ppbw)	NO_3^- (ppbw)	NO_2^- (ppbw)
WAIS Divide	19 ± 31 (10)	14 ± 4 (13)	743 ± 362 (695)	519 ± 238 (464)	238 ± 37 (238)	137 ± 37 (142)	0.6 ± 0.4 (0.5)
ITASE 00-1[a]	–	–	303 ± 159	–	175	–	–
Byrd[b]	10 –	20 ± 2 (20)	364 ± 138 (348)	422 ± 162 (411)	25 ± 4 (25)	– –	– –

[a] 79.38° S, 111.23° W, 1791 m a.m.s.l. (from Frey et al., 2005)

[b] 80.02° S, 119.60° W, 1537 m a.m.s.l. (from Frey et al., 2005); NO based on optimum model runs; atmospheric H_2O_2 from sampling at site RIDS-C (80.00° S, 119.53° W, 1575 m a.m.s.l.); H_2O_2 in snow from sampling at site RIDS-B in 1996 (79.46° S, 118.04° W, 1650 m a.m.s.l.)

Table 2. Concentrations of major ions (in ppbw) measured in surface snow at WAIS Divide and Summit, Greenland, and the respective estimated pH and alkalinity.

Sampling year	Na^+	NH_4^+	K^+	Mg^{2+}	Ca^{2+}	Cl^-	NO_3^-	SO_2^-	pH[a]	Alk.[b]
WAIS Divide (T_{air} = −28.5 ˚C; Acc = 20 cm_{weq} yr^{-1})										
2000[c]	13	–	16	1	8	24	24	24	6.1	0.37
2006[d]	6	4	2	1	1	33	61	43	5.6	0.34
2006[g]	4	2	0.4	1	2	31	62	42	5.6	0.27
2008[e]	31	–	2	5	5	54	67	41	5.8	0.29
								Average	5.8	0.32
Summit (T_{air} = = −29.5 ˚C; Acc =24 cm_{weq} yr^{-1})										
1987[f]	2	6	1 1		15	8	40	40	5.6	1.2
2003–2009[g]	8	21	10	2	18	42	234	107	5.2	2.4
2007[h]	4	10	3	2	19	23	195	72	5.3	1.6
2008[e]	3	5	3	1	6	19	239	54	5.3	0.65
								Average	5.3	1.5

[a] Based on [H+] = ([SO42−] - 0.12 × [Na+]) + [NO3+] + ([Cl−] - 1.17 × [Na+]) (Legrand and Delmas, 1988).
[b] In µeq L^{-1}, derived from the ionic balance and attributing the missing part of anions to dissolved carbonate.
[c] Site ITASE 00-1, top 2 cm of surface snow; unpublished data (Mayewski and Dixon, 2005).
[d] Top 3 cm of surface snow with the first cm removed, unpublished data from http://www.waisdivide.unh.edu.
[e] Top 3 cm of surface snow, unpublished data (Kreutz and Koffman, 2011).
[f] Top 3 cm of surface snow (Mayewski et al., 1990).
[g] Top 1 cm of surface snow, unpublished data from http://niflheim.nilu.no/geosummit/.
[h] Top 0.5 cm of surface snow (range 0.1–6 cm, Dibb et al., 2010).

Table 3. Potential depth integrated NO_X emission fluxes and equivalent NO_X production rates from NO_3^- and NO_2^- photolysis for an EFD of 30 cm, a solar elevation angle of 23° and three different atmospheric boundary layer heights (ABL) from previous measurements (Frey et al., 2005).

Compound	Potential emission fluxes	Potential production rates (pptv h^{-1})		
	(10^8 molecule cm^{-2} s^{-1})	ABL = 13 m	ABL = 250 m	ABL = 354 m
NO_2	8.6	114	6	4
NO	33.9	452	24	17

Table 4. Potential emission flux of NO_X from NO_3^- and NO_2^- photolysis in snow at WAIS Divide compared to other Antarctic sites.

Site & reference	$F_{NOx} \pm 1\sigma$ (10^8 molecule cm^{-1} s^{-1})		Period	Notes
	Measured	Modeled		
WAIS Divide				
This study		$F_{NOx} = 42.5$[a]	12/08–01/09	Daily average, 23˚ SEA
Neumayer				
Jones et al. (2001)	3(+0.3/−0.9)[b]		05–07/02/99	Noon maxima
Halley				
Jones et al. (2011)		2.42[a]	18/01/05	Daily average
Bauguitte et al. (2012)	12.6[b]	3.48[c]	2/2/05	Noon maxima
	7.3[b]			(07:05–15:05 UTC) average
South Pole				
Oncley et al. (2004)		3.9 ± 0.4[d]	26–30/11/00	Overall average
Wang et al. (2008)		3.2–4.2[e]	11–12/03	
Zatko et al. (2013)		3.3–9.8[f]	January	Noon maxima, near station
		7.7–22[f]		Noon maxima, remote
Dome C				
Frey et al. (2013)	6.9 ± 7.2[b]		12/09–01/10	
Zatko et al. (2013)		3.2–12[f]	January	Noon maxima, near station
		4.4–17[f]		Noon maxima, remote
WAIS Divide				
This study		$F_{NO2} = 8.6$	12/08–01/09	Daily average, 23˚ SEA
		$F_{NO} = 33.9$[a]		
South Pole				
Oncley et al. (2004)		$F_{NO} = 2.6 \pm 0.3$[d]	26–30/11/00	Overall average
Dome C				
France et al. (2011)		$F_{NO2} = 2.4$–3.8[g]	12/09–01/10	Values for 22˚ SEA

[a] Depth-integrated FNOx with spectral irradiance from the TUV model.
[b] From measured gradients of NOx concentrations and turbulent diffusivity.
[c] From 1-D model of NOx concentrations based on production from NO− photolysis and chemical loss.
[d] Based on observed NO gradients and assuming photochemical steady-state.
[e] From 1-D chemistry-diffusion model based on trace gas measurements.
[f] Based on depth-dependent actinic flux profiles derived from snowpack radiative transfer model and snow-impurity measurements.
[g] Depth-integrated FNOx with measured spectral irradiance.

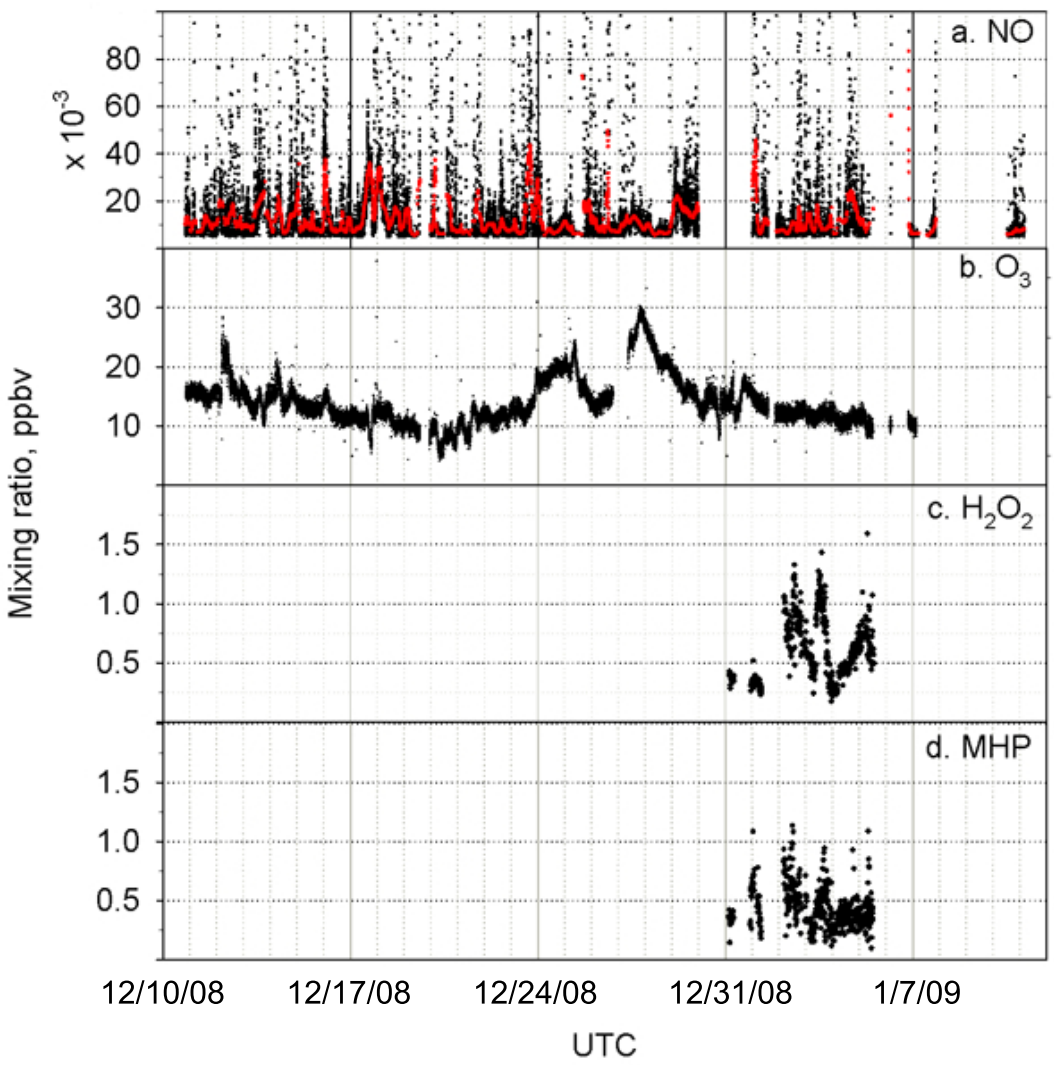

Figure 1. Atmospheric mixing ratios of NO after filtering and O_3 (1 min averages), and of H_2O_2 and MHP (10-minute averages) during austral summer 2008–2009 at WAIS Divide. The 4 h running median of NO is also shown (red symbols).

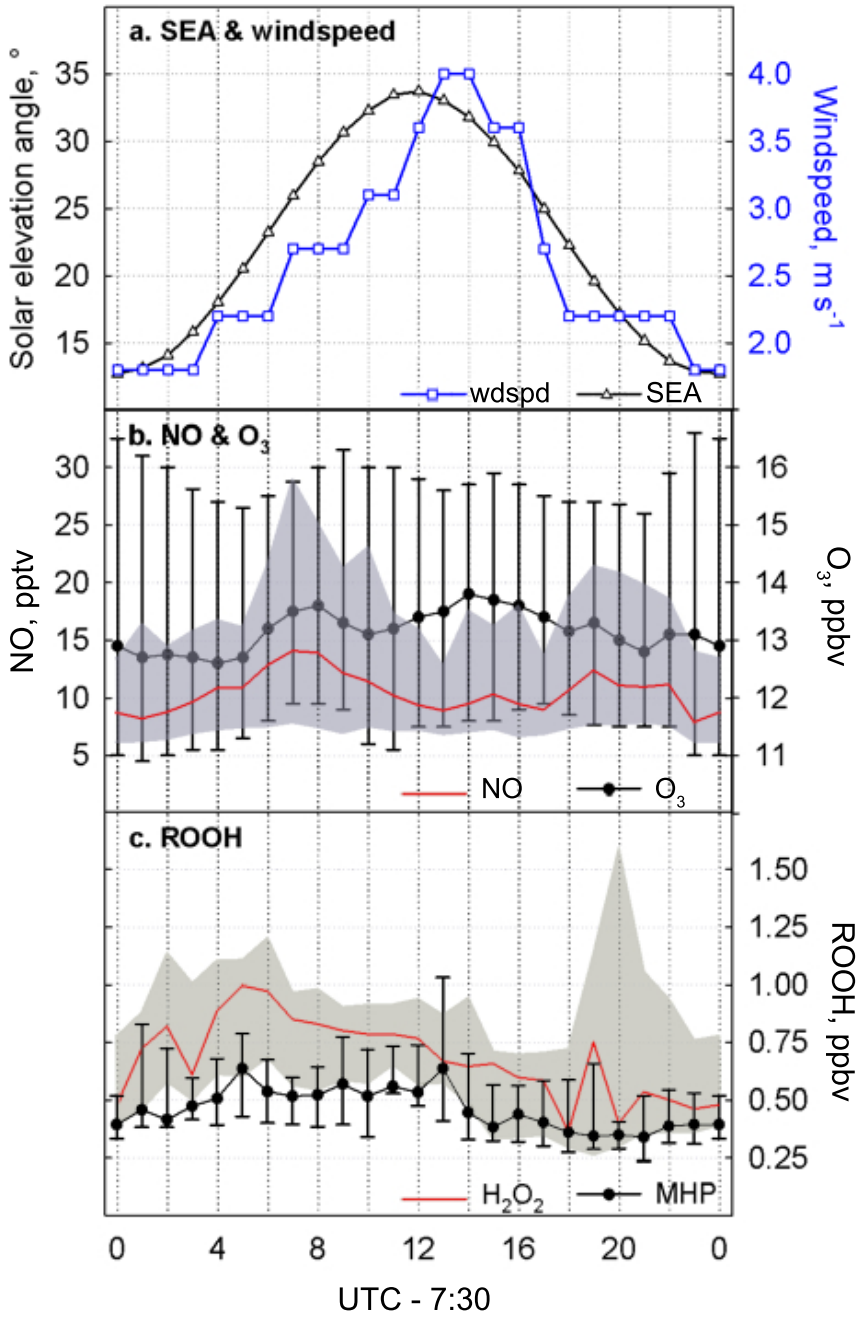

Figure 2. Diel variation of **(a)** average solar elevation angle (SEA) and wind speed, **(b)** median NO (left axis) and O_3 (right axis), and **(c)** median H_2O_2 and MHP. Symbols and lines are 1 h binned values centered on each hour; shaded area and error bars indicate the range centered on each hour; shaded area and error bars indicate the range between the first and third quartiles; local time is UTC − 07:30.

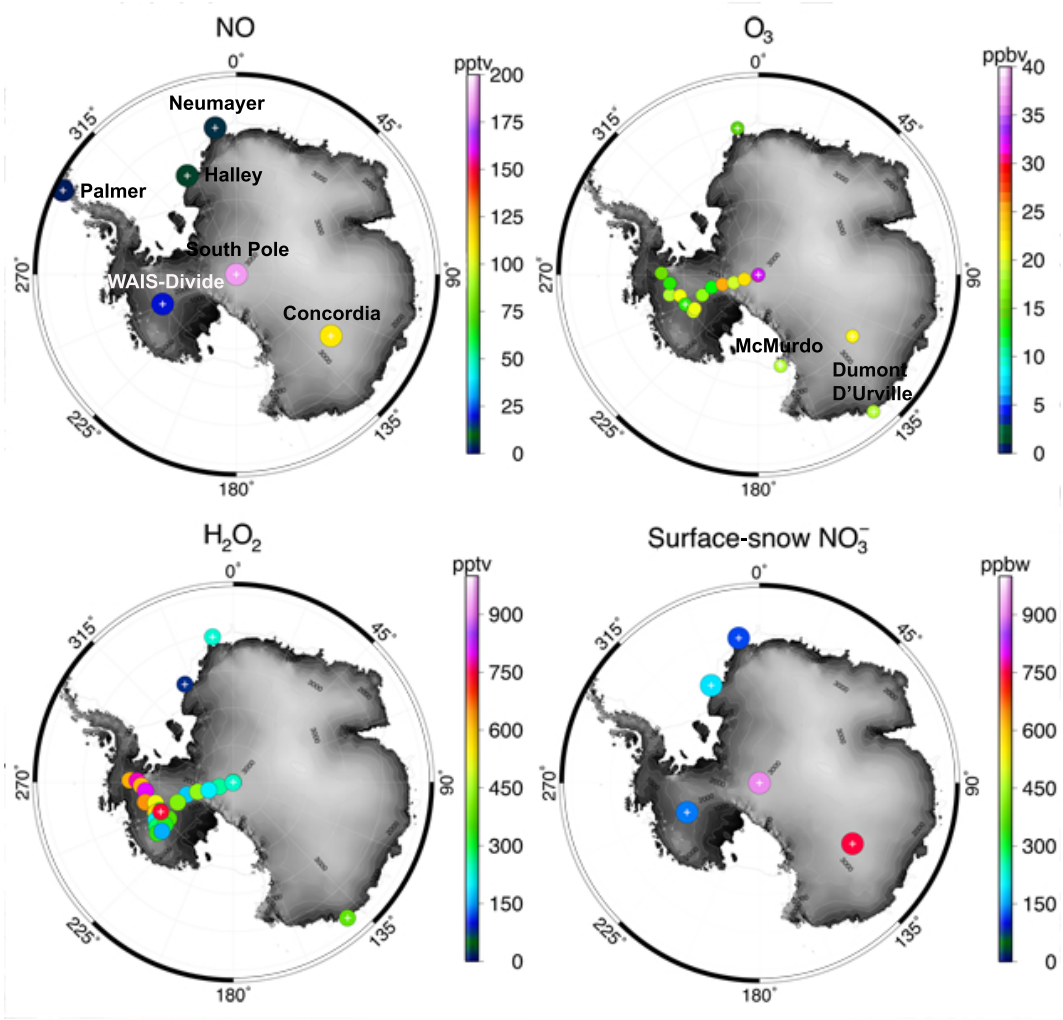

Figure 3. Report of some previous Antarctic measurements of atmospheric NO, surface O_3, H_2O_2, plus NO_3^- in surface snow. Data from Frey et al. (2013), Preunkert et al. (2012), Frey et al. (2009a), Legrand et al. (2009), Frey et al. (2005), Dibb et al. (2004), Davis et al. (2004), Rothlisberger et al. (2000), Jacobi et al. (2000), Jones et al. (1999), Mulvaney et al. (1998), Jefferson et al. (1998), NOAA/GMD, and AWI (http://ds.data.jma.go.jp/gmd/wdcgg/).

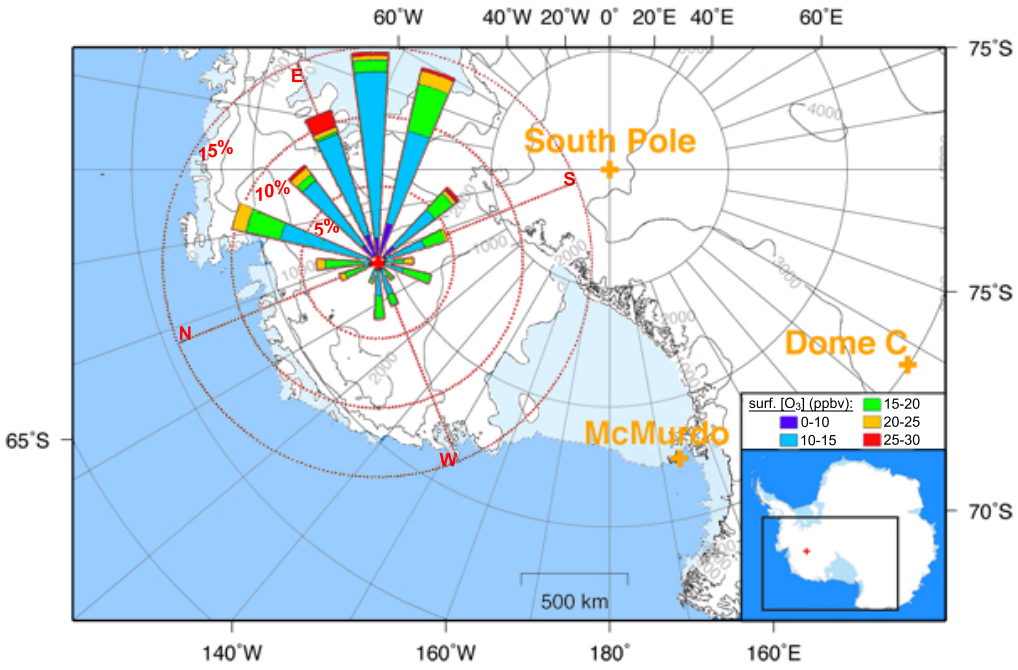

Figure 4. The windrose for WAIS Divide for period of 10 December 2008 to 5 January 2009 and O_3 concentrations from each direction for the same period.

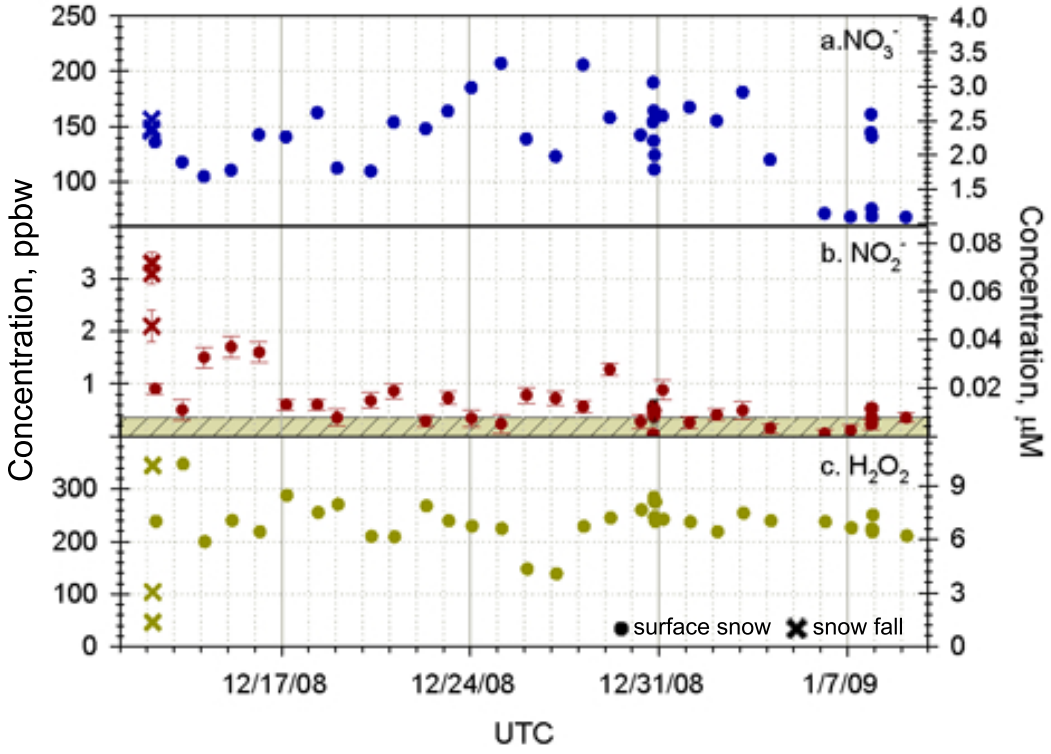

Figure 5. Surface-snow concentrations and snow concentrations from the 12 December 2008 precipitation of (a) NO_3^-, (b) NO_2^-, (c) H_2O_2. The shaded area in (b) represents the NO_2^- LOD.

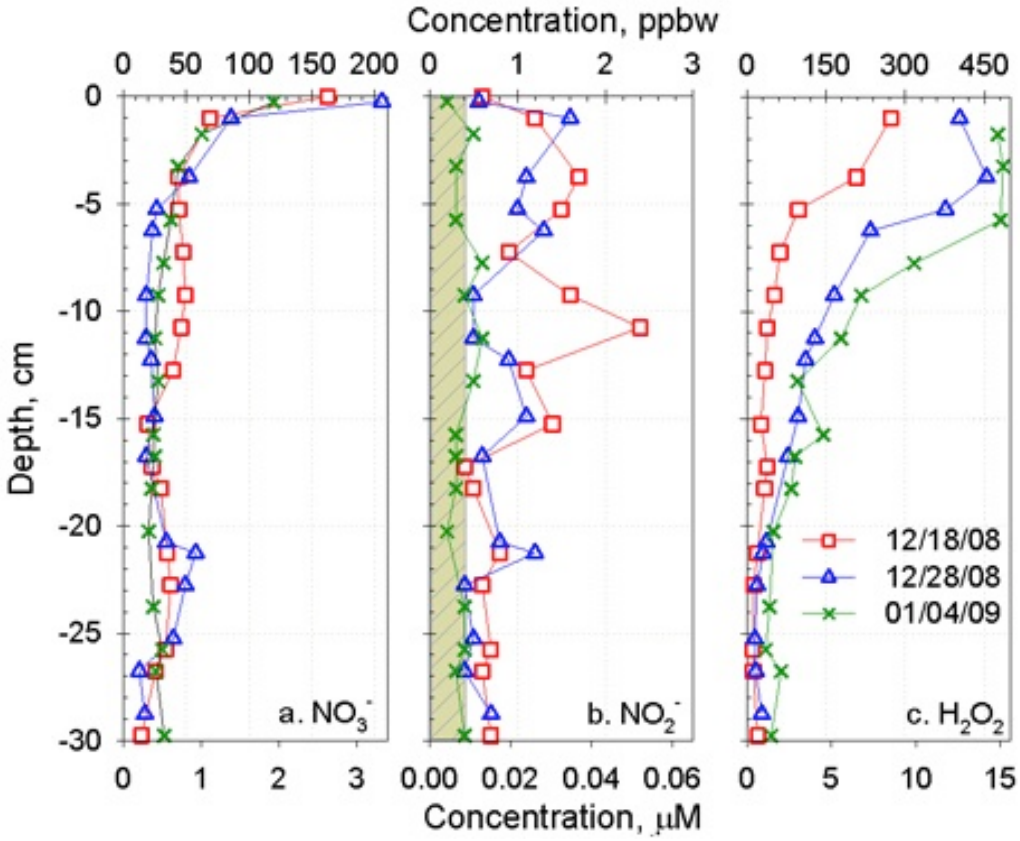

Figure 6. Snow concentrations of (a) NO_3^-, (b) NO_2^-, (c) H_2O_2 measured in the 30 cm-depth snow pits dug on 18 December 2008 (red squares), 28 December 2008 (blue triangles) and 04 January 2009 (green crosses). The shaded area in (b) represents the NO_2^- LOD.

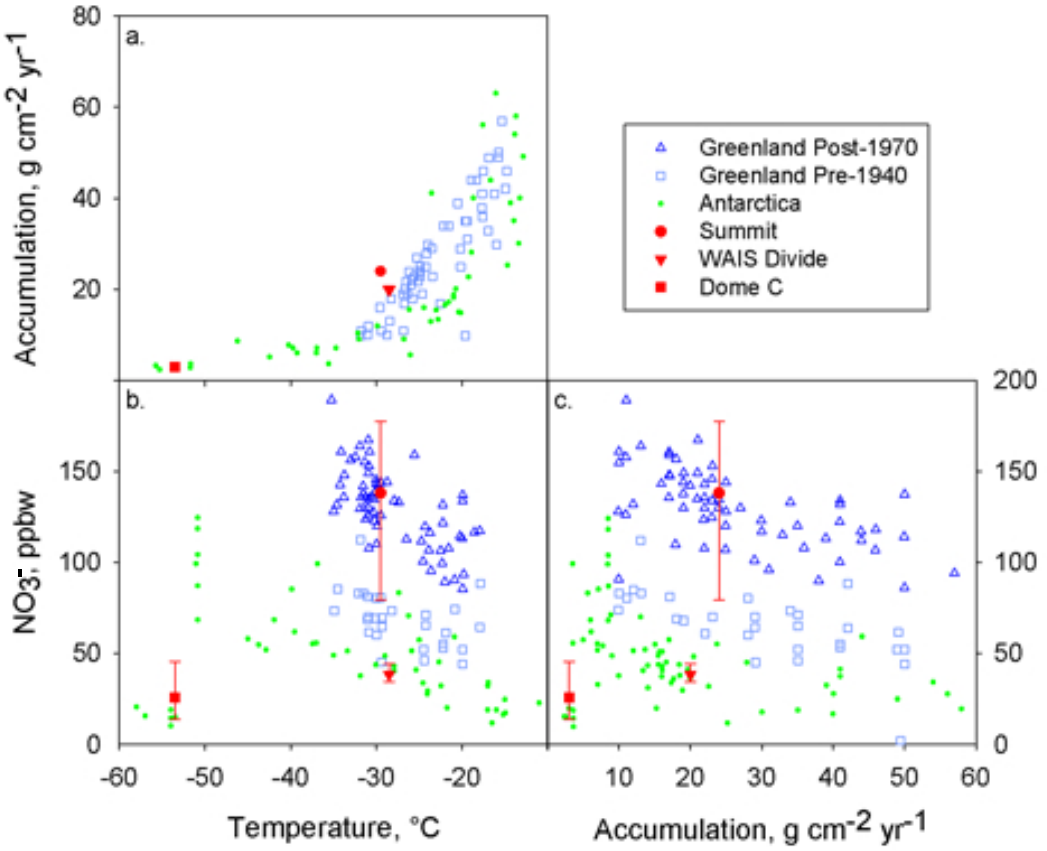

Figure 7. Updated Figs. 2, 3 and 4 from Rothlisberger et al. (2002) with additional measurements from WAIS Divide, Summit, and Dome C (median and range). Data reported from Greenland are NO_3^- concentrations in snow deposited either before 1940 (squares) or after 1970 (triangles). The NO_3^- levels observed in the snow deposited after 1970 over Greenland are influenced by anthropogenic emissions that do not reach the Antarctic continent, whereas the difference between the pre-1940s records and the Antarctic data is likely due to a difference in alkalinity.

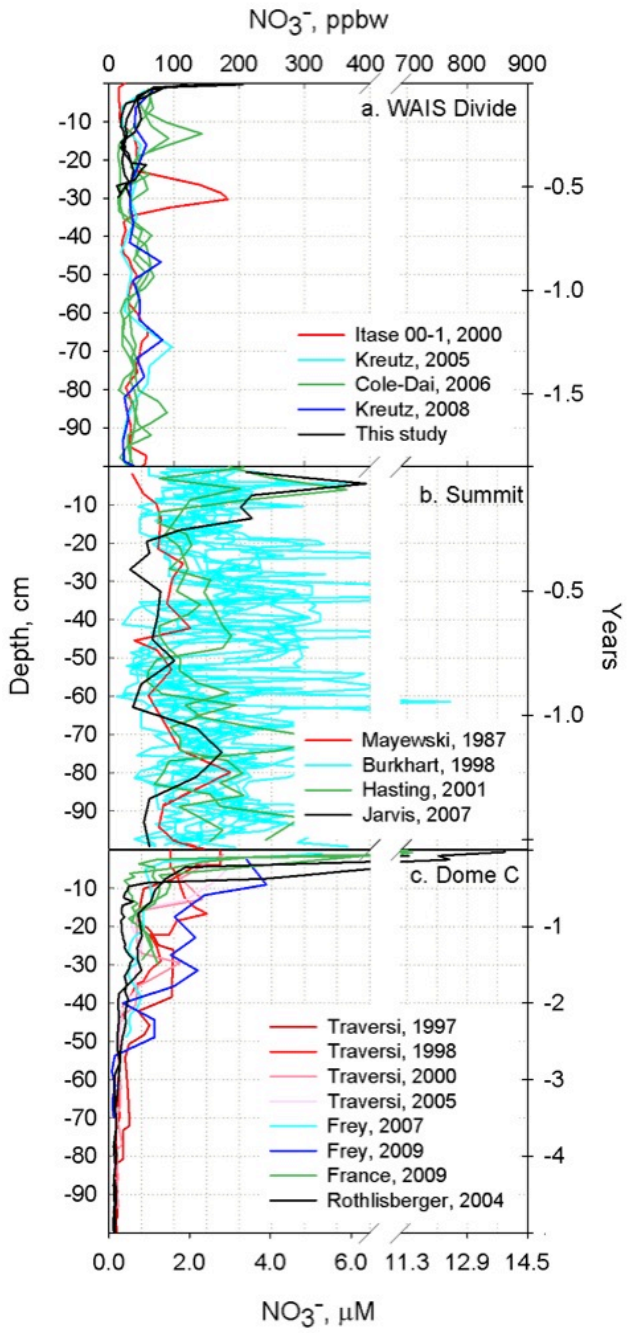

Figure 8. The 1 m NO_3^- profiles from snowpits reported from WAIS Divide, Summit, and Dome C (Frey et al., 2013; France et al., 2011; Traversi et al., 2009; Burkhart et al., 2004; Hastings, 2004; Rothlisberger et al., 2000; Mayewski et al., 1990, Jarvis (unpublished data)).

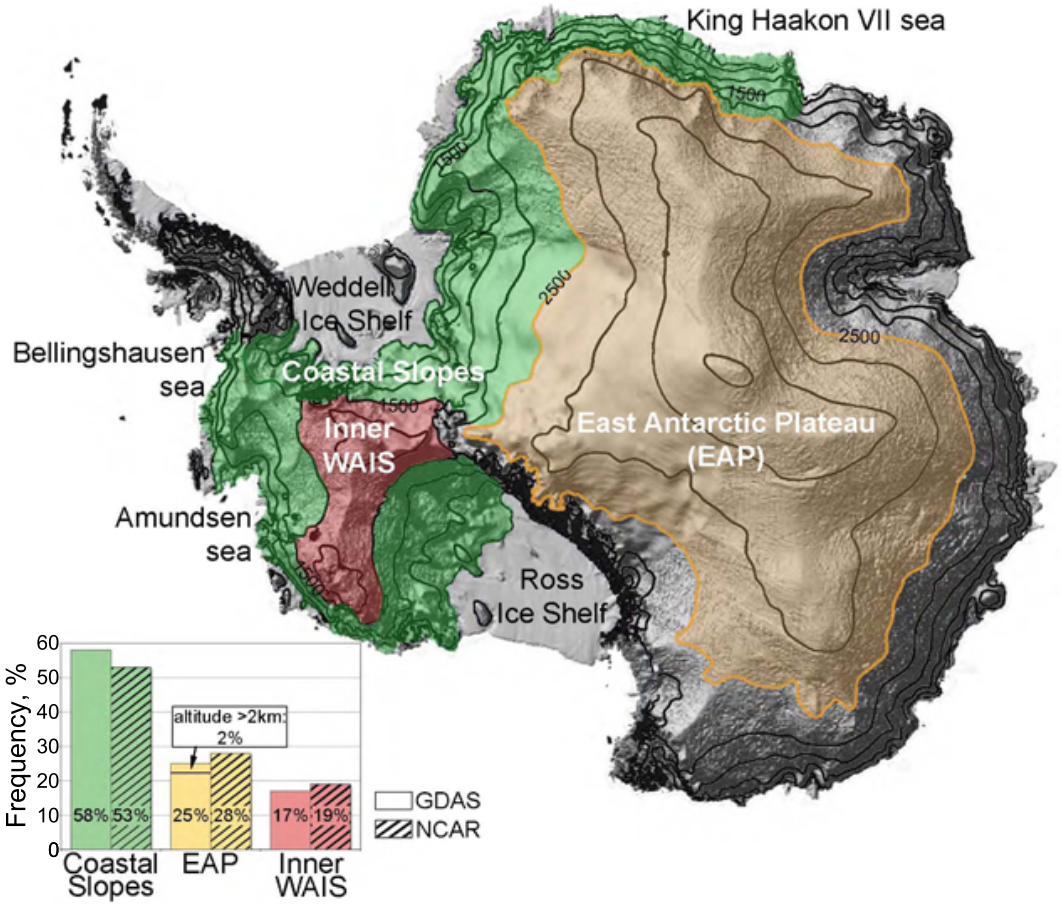

Figure 9. Map of the different origins of air reaching WAIS Divide identified by the 4-day back-trajectory analysis and topography: East Antarctic Plateau (yellow), inner WAIS (red) and the Antarctic coastal slopes (green). Comparison between the results from analyses using the GDAS and NCAR meteorological archived data is shown.

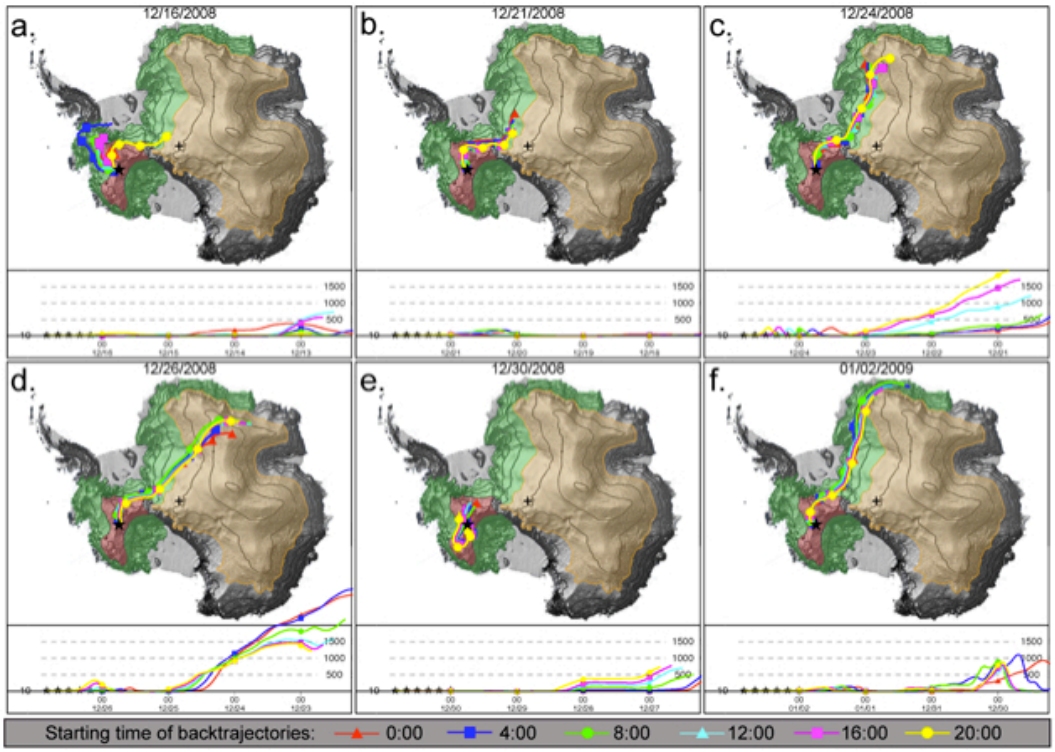

Figure 10. Combined 4-day back-trajectory maps of some specific events identified in Fig. 11. Each daily map contains 6 trajectories of 4-hour intervals and symbols are plotted for every 24 h time step. The different regions of air origin are identified in Fig. 9. Trajectory colors do not correspond to map colors. Trajectory elevations are meters above ground level.

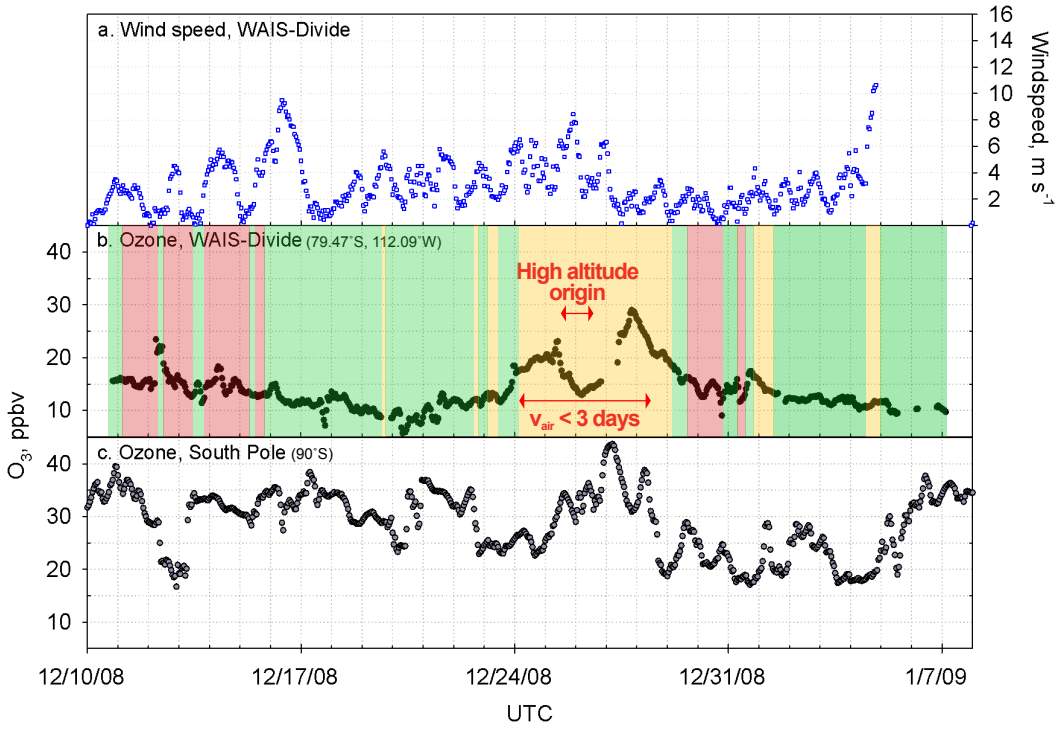

Figure 11. The 1 h averages of observed **(a)** wind speed at WAIS Divide, **(b)** O_3 at WAIS Divide, and **(c)** O_3 at South Pole (data available at: http://ds.data.jma.go.jp/gmd/wdcgg) for austral summer 2008–2009. Air mass origins are reported with the identical color coding used in Fig. 9: East Antarctic Plateau (yellow), inner WAIS (red) and Antarctic coastal slopes (green). Events of air transport less than 3 days between East Antarctic Plateau and WAIS Divide ($v_{air} < 3$ days) and of high-altitude air origin (< 2 km above ground level) are also reported.

CHAPTER 3:

ICE-CORE FORMALDEHYDE AND HYDROGEN PEROXIDE: MARKERS OF THE DECLINE IN ATMOSPHERIC METHANE OVER THE EARLY- TO MID-HOLOCENE, 9,000-6,000 YEARS BP

S. Masclin[1], M. M. Frey[2,1], G. Faluvegi[3], A. N. LeGrande[3], J. R. McConnell[4], D. T. Shindell[3], M. Sigl[4] ,and R. C. Bales[1,5]

[1]Environmental Systems, University of California, Merced, California, USA
[2]British Antarctic Survey, Natural Environment Research Council, Cambridge, UK
[3]NASA Goddard Institute for Space Studies and Columbia Earth Institute, New York, NY USA
[4]Division of Hydrologic Sciences, Desert Research Institute, Reno, Nevada, USA
[5]Sierra Nevada Research Institute, University of California, Merced, California, USA

In preparation for submission to Climate of the Past

1 Abstract

High resolution measurement of formaldehyde (HCHO) and hydrogen peroxide (H_2O_2) from the WAIS Divide deep ice-core are presented for the early- to mid-Holocene (9,735-6,085 ka). The dataset, with average values $\pm\sigma$ of 0.7±0.3 and 20.7±7.8 ppbw, respectively, confirm and complete previous but discontinuous measurements from the Byrd ice-core, the nearest site from WAIS Divide.

Estimation of the past tropospheric concentrations of HCHO and H_2O_2 from ice-core records was performed using the latest findings on the ice-HCHO and ice- H_2O_2 equilibriums. Estimates of tropospheric H_2O_2, 45 ±9 pptv and 28±6 and for 9,000 and 6,000 yr BP respectively, indicate a constant decrease over the early- to mid-Holocene, as does CH_4. The first estimates of atmospheric HCHO from an ice-core record reveal concentrations of 16±2 and 17±2 pptv for the same respective periods, and were input into the steady state equation of HCHO loss and production to assess past concentrations of radical OH. It leads to OH concentrations of and $(2.9\pm0.5)\times10^5$ and $(3.2\pm0.5)\times10^5$ molecule cm^{-3} for 9,000 and 6,000 yr BP, respectively. The resulting concentrations at 9,000 yr BP of HCHO, H_2O_2 and OH match those computed with the GISS GCM ModelE2 within 7%, and discrepancies between the estimates of H_2O_2 and OH concentrations of about 30% and 50%, respectively, are observed at 6,000 yr BP.

Though these results are based on partial ice-core records analyzed at 6,000 yr BP, they can not explain the reconstructed atmospheric CH_4, suggesting that the decline of CH_4 over the mid-early Holocene is mainly source-driven. Meanwhile,

matching atmospheric estimates at 9,000 yr BP indicate a possible contribution of both source and sink for the relatively constant concentrations of CH_4 observed between about 12,000 and 9,000 yr BP.

2 Introduction

Methane (CH_4), a major greenhouse gas that has 21 times the radiative forcing of the more abundant carbon dioxide (Jacobson, 2005), has significantly changed concentrations over time. Paleoatmospheric CH_4 reconstructed from the EPICA ice-core has fluctuated between about 300 and 800 ppbv during glacial and interglacial periods of the past 800,000 years (Loulergue et al., 2008). These variations result from changes in the contributions of natural sources, including wetlands and biomass burning, and sinks, mainly its oxidation with hydroxyl radicals (OH) (Seinfeld and Pandis, 2006):

$$CH_4 + OH + HO_2 \rightarrow HCHO + 2H_2O \quad \text{(R1)}$$

The increase of CH_4 mixing ratios between the Last Glacial Maximum and the pre-industrial era has been investigated by numerous studies (Martinerie et al., 1995; Crutzen and Brühl, 1993; Chappellaz et al., 1993; Thompson et al., 1993). Though an average drop of OH of about 12- 28% is found between the Last Maximum Glacial and the preindustrial Holocene (Kaplan et al., 2006; Valdes et al., 2005; Alexander et al., 2002; Martinerie et al., 1995; Thompson et al., 1993), all these investigations mainly attribute the drop to CH_4 sources, in particular orbitally driven emissions from tropical wetlands. At best, no more than 30% of the CH_4 variation could be caused by its oxidation with OH. While recent studies suggested that these calculations may have overestimated the CH_4 sources to the detriment of the CH_4 sinks (Kaplan et al., 2011, and references therein), Murray et al. (2013) show a negligible effect of OH change in the significant decline of CH_4 over this period, pointing at the uncertainty in modeling the complex photochemistry involved in the past oxidative capacity. The debate still remains and uncertainties on quantifying the relative contributions of CH_4 sources and sinks persist. Acquiring more robust past oxidant records, e.g. from ice cores, would then provide a reliable tool to validate the models and to help reduce these uncertainties (Levine et al., 2011a; Thompson et al., 1993).

The rise of CH_4 over the mid- to late-Holocene, 5,000 years before present (yr BP) to present, has been considerably discussed. The debate on the contributors remains between a CH_4 increase resulting from potential early anthropogenic activities (Mitchell et al., 2013; Ruddiman, 2013) and a rise essentially caused by changes in tropical wetland emissions driven by natural changes in the Earth's orbital configuration (Singarayer et al., 2011; Schmidt et al., 2005).

Little attention has been given to the early- to mid-Holocene, 10,000-6,000 yr BP, also referred as early Holocene climatic optimum since the warmest conditions of the Holocene occurred during this period (Ciais et al., 1992). CH_4 decreased over

this period of about 20% from nearly 700 to 575 ppbv (Sowers, 2010). Based on the GRIP ice-core, Blunier et al. (1995) attributed this decrease to the reduction of wetlands in a dry low-latitude climate up to 5,000 yr BP, reaching conclusion similar to Mayewski et al. (2004). The latter study pointed to rapid climate changes as the cause of the CH_4 fluctuations. They advanced the possibility of a cooling of the Northern Hemisphere from intense volcanic sulfate release into the atmosphere that reduced the Afro-Asian monsoon circulation and accentuated the tropical aridity around 9,000-8,000 yr BP. But little to no attention has been given to the possible contribution of atmospheric oxidants in the CH_4 budget of the early- to mid-Holocene.

This study aims, first, to provide a dataset on preserved, reversibly deposited species, HCHO and H_2O_2, for the early- to mid-Holocene from measurements of the WAIS Divide ice core. Second, the reliability of past atmospheric HCHO, H_2O_2, inferred from the inversion of their ice-core records, and the information they provide on the past oxidative capacity is evaluated. Researchers have questioned the possibility of using HCHO and H_2O_2 as markers of the past oxidative capacity of the atmosphere (Wolff, 2012, and references therein) because of their sensitivity to post-depositional processes. We used in this study the recent findings on the HCHO ice-air equilibrium (Barret et al., 2011b) and the semi-empirical model of H_2O_2 preservation in snow for the WAIS region (Frey et al., 2006) to infer their respective past atmospheric mixing ratios. With short lifetimes of 13 hr and 3 days for HCHO (Riedel et al., 1999) and H_2O_2 (Riedel et al., 2000), respectively, and in the order of seconds for OH, the inferred atmospheric concentrations of these species are valuable at local scale. Nevertheless, they still represent a potential tool to evaluate the global climate model (GCM) ModelE2 from the Goddard Institute for Space Studies (GISS). The interpretation of these atmospheric estimates also provides significant information on the role of the oxidative capacity of the atmosphere in the decline CH_4 between about 9,000 and 6,000 yr BP.

3 Methods

3.1 Ice-core analysis

The 3,405m WDC06A deep ice-core was collected from 2006 to 2011 at the WAIS Divide drilling camp (79.467˚S, 112.085˚W, 1,766m a.m.s.l., http://www.waisdivide.unh.edu).

Present mean ± 1σ annual accumulation of 20.4±3.5 cm (Banta et al., 2008) and a well known ice-flow regime (Morse et al., 2002) make unprecedented high-resolution chemical analysis possible for an Antarctic archive, with an annual signal detectable to depth of at least 2,800m, equivalent to about 30,000 yr BP. The 462.05m ice-core section between depths 1,301.92 to 1,763.97 m, was processed at the National Ice-core Laboratory (NICL, Colorado) prior to its analysis at the Ultra Trace Chemistry Laboratory at the Desert Research Institute (DRI, Reno, Nevada) in March 2011. The section was analyzed by Continuous Flow Analysis-Trace Elements Dual coupled to a single-particle soot photometer (CFA-TED/BC) (Sigl et al., 2013; Banta et al., 2008, and

references therein). This analytical system allows simultaneous quantification of a broad diversity of elemental and ionic species with low limit of detection (LOD) and a very high depth resolution of about 2±2mm (about 100 samples per year).

For this study, a custom fluorescent instrument built under an ITASE grant (OPP-9814810 (Frey et al., 2005)) was added to the analytical line to measure HCHO. Continuous aqueous-phase detection with the Fluor LC 305 fluorescence detector (Linear Instruments) was based on the method described by Dong and Dasgupta (1987) and Sigg et al. (1994), using the so-called Hantzch reaction with HCHO. Briefly, HCHO is derivatized with purified pentane-2,4-dione and ammonium acetate to form the fluorescent compound 3,5-diacetyl-1,4-dihydrolutidine. The ratio between reagent and sample flows in the 0.25 and 0.44 mm ID Tygon tubings, respectively, is maintain constant at ~0.58 by using a peristaltic pump. The reaction occurs in an 85˚C temperature-controlled chemical reactor that was based on the design of Li et al. (2001) and purified pentane-2,4-dione is obtained from distillation of commercial pentane-2,4-dione. The resulting fluorescence is measured with the fluorescence detector for $\lambda_{excitation}$ 420nm and $\lambda_{emission}$ 510nm. H_2O_2 was measured following a similar procedure as described by Frey et al. (2006).

10% of all the ice core sections were reanalyzed using parallel replicate melter sticks to test the accuracy of the analytical system (Sigl et al., 2013). All the instruments were calibrated at the beginning of each daily analysis by running liquid standards made from commercially available HCHO (ACS reagent, 37% in H_2O, Sigma-Aldrich) and H_2O_2 solutions (30% in H_2O, Sigma-Aldrich) (Fig. 1), with 2 to 3 additional controls. The blanks and standards were quantified using DI water for H_2O_2, and commercial bottled Evian water for HCHO, as Evian water is considered CO_2-free (Burkhart et al., 2002; Hutterli et al., 2002). Actual measurements of HCHO from the DI water showed concentrations (± σ) of 0.8±0.7 ppbw with respect to Evian water. The limit of detection, defined as 3-σ of the baseline, for the HCHO and H_2O_2 were 0.29 and less than a ppbw, respectively, comparable to the values obtained by Hutterli et al. (2004) and Li et al., (2001).

Depth profiles of concentration were converted into time series by applying the official depth-age scale WDC06A-7 for the WAIS Divide ice core (Fudge et al., 2013). The depth-age scale of this ice-core section is established from dielectric profiling (DEP) measurements made in the field and on Alternating Current and Direct Current Electrical Conductivity Measurement (AC-ECM) made at the National Ice-core Lab (NICL) (Fudge et al., 2013). Annual layers were identified with an automatic layer picker described by (McGwire et al., 2011), resulting in a 2% uncertainty, about 35 yr at 1763.97 m depth (Fudge et al., 2013).

3.2 Estimates of past atmospheric concentrations from ice-core records

3.2.1 HCHO

The partitioning of HCHO between the gas phase and water or ice has been investigated by several studies (Barret et al., 2011a,b; Betterton and Hoffmann, 1988;

Burkhart et al., 2002) with results reported in terms of the Henry's law constant K_H or of the air-ice partition coefficient K_D. The Henry's law constant is defined as $K_H = \frac{C_{\mathrm{HCHO}(liquid)}}{P_{\mathrm{HCHO}}}$ with $C_{\mathrm{HCHO}(liquid)}$ the concentration of HCHO in the aqueous phase (mol L^{-1}), and P_{HCHO} the partial pressure in the gas phase (atm). Similarly, the air-ice partition coefficient K_D, $K_D = \frac{C_{\mathrm{HCHO}(snow)}}{P_{\mathrm{HCHO}}}$, is the ratio of the HCHO concentration in snow (mol L^{-1}) over the partial pressure of HCHO in the gas phase (atm).

Estimates of these equilibrium coefficients (Barret et al., 2011b; Betterton and Hoffmann, 1988; Burkhart et al., 2002; Hutterli et al., 1999) are summarized in Figure 2 as a function of temperature, with regard to the partitioning coefficients from co-deposition processes that were derived from the Clausius-Clapeyron equation (Jacobson, 2005). Figure 2 also shows the ratios of HCHO measured in air and snow pits during the ITASE traverses above the West Antarctic Ice Sheet during austral summers 2000 to 2003. These measurements, so far unpublished, were carried out by M. Frey, as part of the ITASE grant, over 1-4 days at each of the 21 different locations described in Frey et al (2005). The authors clustered these 21 locations into 3 groups based on different average snow accumulation rate and temperature, as illustrated in Figure 3. With an annual snow accumulation rate of about 20 cm_{weq} yr^{-1} (Banta et al., 2008) and an average annual temperature of -28.5˚C (Orsi et al., 2012), the WAIS divide ice core site is part of group 1.

Within the 1-σ uncertainty, Figure 2 suggests that the K_D estimated for Group 1, fits mostly with the temperature-dependent ice-air equilibrium function developed by Barret et al. (2011b) for atmospheric HCHO mixing ratios lower than 90 pptv. Therefore this equilibrium function was used to infer atmospheric mixing ratios of HCHO from the preserved signal in the WAIS-Divide ice-core.

The HCHO ice-core record, measured in ppbw, was first converted to mole fraction:

$$X_{\mathrm{HCHO}} = \frac{M_{\mathrm{H_2O}} \times C_{\mathrm{HCHO}}}{\rho - \left(M_{\mathrm{HCHO}} - M_{\mathrm{H_2O}}\right) \times C_{\mathrm{HCHO}}} \quad (1)$$

with C_{HCHO} and X_{HCHO} the ice-core concentrations of HCHO in ppbw and molar fraction, respectively, ρ is the density of pure water (1000g L_{-1}), and M_{H_2O} and M_{HCHO} the molar mass of pure water and formaldehyde.

The partial pressure of HCHO ($P_{\mathrm{HCHO}}(X_{\mathrm{HCHO}},T)$, in Pa) was then calculated using Equation 2 which defines the solubility of HCHO in ice (Barret et al., 2011b):

$$P_{\mathrm{HCHO}}\left(X_{\mathrm{HCHO}},T\right) = \left(X_{\mathrm{HCHO}}\right)^{n_s} \times A_0^{'} \times \exp\left(-\frac{\Delta h_{\mathrm{sub}}}{RT}\right) \quad (2)$$

A_0' = 8.82×10^{14} Pa is a constant for the ice-HCHO system, n_s = 1.245±0.05 is the ice vapor depression factor, Δh_{sub} = 42.15±2.38 kJ mol^{-1} is the partial molar enthalpy of HCHO sublimation, and the gas constant R = 8.314J K^{-1} mol^{-1}. The temperature T that controls the air-ice partition equilibrium is paleo-surface temperature computed for the WAIS Divide site (Cuffey et al., manuscript in preparation, 2014) with a heat- and ice-flow model. This model is constrained by the local ice-core record of deuterium ($\delta^{18}O$), the depth-age scale and the measurements of borehole temperature.

An average atmospheric pressure of 780 hPa was used to calculate the paleoatmospheric concentrations of HCHO, [HCHO], in pptv from the estimated partial pressure $P_{HCHO}(X_{HCHO},T)$ (Eq 3). This average was obtained from measurements of surface atmospheric pressure by the closest automatic weather station from the WAIS Divide drilling site (Kominko-Slade AWS, 79.466˚S, 112.106˚W, 1801m a.m.s.l.) between 2006 and 2013.

$$\left[\mathrm{HCHO}\right] = \frac{P_{\mathrm{HCHO}}\left(X_{\mathrm{HCHO}},T\right)}{P} \times 10^{12} \tag{3}$$

3.2.2 H_2O_2

The atmospheric mixing ratios of H_2O_2 over the early to mid Holocene were inferred from the ice-core records of H_2O_2 based on the semi-empirical deposition model (Eq. 4) developed by Frey et al. (2006). This model describes the sensitivity of H_2O_2 preservation to mean annual temperature and accumulation rate, and was tested for 23 shallow ice-cores drilled across the West Antarctic Ice Sheet (WAIS). The resulting atmospheric H_2O_2, [H_2O_2], in pptv, represents a weighted average of tropospheric H_2O_2 mixing ratios during the non-summer period, when snow accumulation rate is highest.

$$\left[\mathrm{H_2O_2}\right] = \frac{C_{\mathrm{H_2O_2}} - a_0 - a_1 \times \exp\left(a_2 \times A\right)}{K_D} \tag{4}$$

$C_{H_2O_2}$ is the ice-core record of H_2O_2 in mol/L and the constants a_0, a_1 and a_2 are 9.67×10^{-7}, -3.46×10^{-7} and -1.3631, respectively (Frey et al., 2006). The accumulation rate A, in cm yr^{-1} was scaled such as $A = \frac{A_z - \overline{A}}{\sigma_A}$ with A_z the accumulation observed at depth z, $\overline{A}$ and σ_A the mean accumulation rate and the standard deviation reported by Frey et al. (2006) across the West Antarctic Ice Sheet.

Finally K_d, the ice-to-air equilibrium partition coefficient, was calculated from the temperature dependence described in Conklin et al. (1993):

$$K_D = \exp\left(0.22109 \times \left(T_s\right)^2\right) - 0.99248 \times T_s + 8.8932 \tag{5}$$

The temperature T_s is scaled on the observations of Frey et al. (2006) such as $T_s = \frac{T - 258.48}{13.87}$.

3.2.3 CH_4

The concentrations of CH_4 over the early- to mid-Holocene were inferred by assuming a direct ice-air transfer and an age difference between the air and the enclosing ice of 207.8 yr (Mitchell et al., 2011). CH_4 records from the ice-core section were obtained from Sowers (2012) using a wet extraction technique described in Mitchell et al. (2011) with a resolution of 2.1±0.8 cm (~25 years). A gravitational fractionation correction of 0.39% was applied to all data assuming a constant 0.303±0.006 $\delta^{15}N$ value. Data were also corrected for +7 ppbv from results of intercalibrations at OSU-PSU. The gas age of these data were based on the WDC06A timescale with an additional 207.8 years accounting for the gas age difference. The latter is assumed constant over the Holocene (Mitchell et al., 2011).

3.2.4 Radical OH

The past concentrations of radical hydroxyl (OH) were inferred from the atmospheric HCHO and CH_4 using the steady-state relationship described by Staffelbach et al. (1991):

$$[\mathrm{OH}] = \frac{[\mathrm{HCHO}] \times j_{\mathrm{HCHO}}}{k_1 \times [\mathrm{CH_4}] - k_2 \times [\mathrm{HCHO}]} \quad (6)$$

The reaction constants for the oxidation of CH_4 and HCHO, k_1 and k_2 respectively, were calculated such $k_1 = 2.4 \times 10^{-12} \times \exp\left(\frac{-1710}{T}\right)$ and $k_2 = 5.5 \times 10^{-12} \times \exp\left(\frac{125}{T}\right)$ (Sander et al., 2011; Staffelbach et al., 1991). The air surface temperature T was calculated from the heat- and ice-flow model (Section 2.2.1). Finally, the photolysis rate constants of HCHO, j_{HCHO}, were calculated with the online interactive TUV model version 4.1 (Lee-Taylor and Madronich, 2002, http://cprm.acd.ucar.edu/Models/TUV/Interactive TUV/). Monthly values were computed assuming present-day conditions, with a total ozone column of 315 ppbv in agreement with values computed by Crutzen and Brühl (1993) between the pre-industrial and the glacial periods.

3.3 GISS GCM ModelE2

Simulations of the past atmospheric composition were run with the NASA GISS GCM ModelE2 for 6,000 and 9,000 yr BP to test the model with our ice-core inversion method. A full description of this model is developed by Schmidt et al. (2014) and

Shindell et al. (2013). Only changes of interest of this study are presented in this section. The physics of the model E2 are based on the GISS ModelE (Schmidt et al., 2006). It has a 2×2.5 degrees horizontal resolution and improved standard vertical resolution of 40 layers covering up to 0.1 hPa. The coupled ocean-atmosphere model uses the Tracers of Chemistry, Aerosols and their Direct and Indirect effects (TCADI). TCADI includes a fully interactive chemistry, aerosols and dust in the troposphere and stratosphere driven by emissions, and a parameterization of indirect effect on clouds. This gas-phase chemistry is updated from the GISS model for Physical Understanding of Composition-Climate Interactions and Impacts (G-PUCCINI) described in Shindell et al. (2006), and is computed in interaction with the physics run by the model (Shindell et al., 2013). Tropospheric chemistry includes basic NO_X-HO_X-O_X-CO-CH_4 chemistry as well as peroxyacyl nitrates and the hydrocarbons terpenes, isoprene, alkyl nitrates, aldehydes, alkenes, and paraffins. Stratospheric chemistry includes chlorine- and bromine-containing compounds, and CFC and N_2O source gases. With an expanded trace-gas photochemistry detailed in Schmidt et al. (2014) and Shindell et al. (2013), the modelE2 includes 156 reactions among 51 species running on a 30-min chemical step time with photolysis rates computed from the Fast-J2 scheme (Schmidt et al., 2014, and references therein).

The outputs of the modelE2 presented in this study are those computed for the closest geographical coordinates to the WAIS Divide ice-core site (79.00" S, 113.75"W).

4 Results

4.1 Ice-core records

Figure 4 shows the high-resolution records of preserved HCHO and H_2O_2 in the WAIS Divide ice core between 1,300 and 1,764m, equivalent to 6,085 and 9,735 yr BP. The average concentration $\pm\sigma$ of HCHO is 0.7±0.3 ppbw ($(24\pm10)\times10^{-3}$ μM) with maximum of 2.8 ppbw (94×10^{-3} μM). Figure 4 shows a good match between these concentrations and the scarce measurements reported from the Byrd ice-core over the same period (Staffelbach et al., 1991) for a site that presents similar conditions of temperature and snow accumulation than the WAIS Divide site (Fig. 3). Difference between both records are about 4% those measured in the Byrd ice-core, except at about 6,680 yr BP where a difference of about 40% is observed, with values of 0.5 ppbv against 0.9 ppbv.

Figure 5 shows that the 1-year average HCHO concentration measured in 1-m snowpits at WAIS Divide during the ITASE Traverse is lower than the concentrations measured over West Antarctica (M. Frey, personal communication, 2006). However, it is still in the range of the concentrations measured at the sites of group 1, which are defined by an annual accumulation rate of 17±4 (range 10-25) cm yr^{-1} and annual mean temperature of -28.1˚C (Frey et al., 2006).

No annual cycle was observed within the HCHO signal. This is consistent with the conclusion of Hutterli et al. (1999) that the HCHO signal in ice is a multi-year

average concentrations of the overlying troposphere recorded through a temperature-dependent atmosphere-snow equilibrium.

Unlike HCHO, the H_2O_2 record exhibits a clear annual cycle, with summer maxima and winter minima, similar to previous observations (Frey et al., 2006). The average concentration of H_2O_2 is 20.7±7.8 ppbw ((0.6±0.2 μM), with maximum of 89 ppbw (2.6 μM). These values are in the range of those previously reported from the Byrd ice-core by Neftel et al. (1986) (Fig. 3). Though three records, at about 7,130, 8,090 and 8,890 m, differ by 60, 40 and 30% respectively, our results confirm the elevated H_2O_2 signal observed in the Byrd ice-core over the early- to mid-Holocene, with less than a 20% difference between both ice-cores. Like HCHO, the average H_2O_2 concentration is closer to the snow-pit concentrations measured at the West Antarctic sites referred as group 1 (Fig. 6).

From 9,735 to 6,085 yr BP, H_2O_2 increases by 2.25×10^{-3} ppbw yr^{-1}, while accumulation rates increase by 1.48×10^{-3} cm yr^{-1}. The corresponding increases are 8.3 ppbw and 5.4 cm yr^{-1}, about 40 and 47%, respectively, of the average values 20.7 ppbw and 11.6 cm yr^{-1}.

Measurements of H_2O_2 in the WAIS ice-core present a good match with the replicate sections (data not shown), while a few disparities were observed in the case of HCHO (Fig. 4). The divergence from the HCHO replicates corresponds to either an experimental error or a drifting of the HCHO detection. Derivation of the signal was essentially observed during the first 2.5 days of analysis, related to modifications of the HCHO analytical instruments. This results in discarding all of the HCHO records between 1300 and 1400 m, but the concentrations from the ice-core replicates.

4.2 Tropospheric mixing ratios

Figure 7 presents the atmospheric mixing ratios of HCHO, H_2O_2, CH_4 and OH inferred from the WAIS Divide ice-core WDC06A (see Section 2.2).

10-year estimates of the atmospheric HCHO revealed maxima values of 55 pptv and an average mixing ratio of 23±10 pptv over the early- to mid-Holocene period, with an error of propagation of about 15%. No specific trend over the early- to mid-Holocene is observed. The average value is slightly lower than current winter concentrations reported at Halley (Salmon et al., 2008) where an average HCHO of 28 pptv was observed between May and September 2004. Our average value does not compare well with the winter mixing ratios observed at Neumayer (Riedel et al., 1999), but the accuracy of these mixing ratios have been discussed in Salmon et al. (2008).

Average $\pm\sigma$ of the inferred past atmospheric mixing ratios H_2O_2 for the early- to mid-Holocene is 40±13 pptv with maxima of 92 pptv, and a 20% error of propagation is calculated for each estimate. This average is slightly lower than the current 54 pptv observed at polar night at Neumayer (Riedel et al., 2000). Unlike HCHO, H_2O_2 presents a constant decrease from 9,735 to 6,095 yr BP of about 0.006 pptv yr^{-1} (R^2=0.6).

CH_4 average concentration $\pm\sigma$ (range) over the early- to mid-Holocene is 634±31 (560-700) ppbv. While the atmospheric CH_4 concentrations are relatively stable between 12,000 to about 9,000 yr BP (data not shown), a constant decrease of 26 pptv yr^{-1}

(R^2=0.77) of CH_4 is observed between 9,000 and 6,000 yr BP. The drop around 8,200 yr BP measured in previous ice cores (Thomas et al., 2007) is clearly observed in the WAIS Divide ice-core record, while the amplitude of this event is significantly reduced in the Dome C ice-core record (Fig. 4). This 200 year event was too short to be fully recorded in the Dome C ice-core, in which the signal amplitude is mainly governed on the bubble close off process that is driven by the low temperature and accumulation rate of the site (Spahni et al., 2003) The detailed record of the cold event of 8,200 yr BP in the WAIS Divide ice-core is not the focus of this research but it illustrates the high-resolution dataset obtained for the Holocene period, comparable to Greenland ice-cores such as GRIP or GISP2 (Spahni et al., 2003).

In general, the atmospheric estimates from the ice-core and their trend match those from the runs of the modelE2 for 6,000 and 9,000 yr BP (Table 1). Estimation of HCHO from both methods give almost identical tropospheric mixing ratios, 16±2 vs. 15 pptv at 6,000 yr BP (7% difference), respectively, and 17 pptv for both at 9,000 yr BP. Estimates of H_2O_2 only match at 9,000 yr BP, with mixing ratios of 45±9 vs. 49 pptv, respectively (14% difference). At 6,000 yr BP, the inferred atmospheric mixing ratios of H_2O_2 is about 63% of those computed with modelE2, 28±6 vs. 43 pptv at 6,000 yr BP, respectively.

Computed CH_4 from the GISS GCM are slightly lower, about 5%, than the concentrations reconstructed from the ice-core for both run periods. The differences are exactly 7% at 6,000 yr BP and 4% at 9,000 yr BP. Finally, the calculated OH radical from the steady state equation differs mainly from the modeE2 estimate at the 6,000 yr BP period, with respective values of 3.2±0.5 vs. 2.1×10^5 molecule cm^{-3} (52% difference). However, both the 9,000 yr BP estimates lead to comparable concentrations of about $2.9\pm0.5\times10^5$ molecule cm^{-3} calculated from the ice-air partitioning equilibrium described in Section 2.3, and 2.7×10^5 molecule cm^{-3} computed with the GISS GCM modelE2. The average of radical OH inferred from the overall ice-core section is $4.7\pm2.7\times10^5$ molecule cm^{-3}.

5 Discussion

5.1 Ice-core records of HCHO and H_2O_2 and atmospheric estimates

A comparison of the HCHO and H_2O_2 estimates from the ice-core and the modelE2 is not possible for the exact year of 6,000 yr BP since the ice-core record starts at an age of 6,085 yr BP for HCHO and 6,095 yr BP for H_2O_2. Analysis of earlier sections was not performed at DRI since it corresponds to the brittle ice zone of the WAIS Divide ice-core (from ~577 to ~1,302 m). Thus, no measurement of photochemical intermediate species is available for earlier period than 6,085 yr BP. The 6,085 yr BP ice-core estimate of atmospheric HCHO, and 6,095 yr BP H_2O_2, are therefore compared to the mixing ratio computed by the modelE2 for 6,000 yr BP, assuming that change in photochemistry is negligible over that relatively short period of time.

Inferred tropospheric HCHO mixing ratios from the ice-core match the values obtained with ModelE2 (Table 1 and Figure 7). Only a difference of 1 pptv is observed around 6,000 yr BP, and both methods show identical mixing ratios for 9,000 yr BP. This does not suggest a significant decrease of HCHO over the early- to mid-Holocene.

The reconstruction of tropospheric HCHO from its preservation into the ice can be discussed here as Wolff (2012), Wolff et al. (2007) and Grannas et al. (2007, and references therein) highlight the impacts of the physical and photochemical post-depositional processes on the preservation of HCHO in snow and ice. The sensitivity study of HCHO preservation in snow by Hutterli (2003) pointed to the potential of using this reversibly deposited species to infer past atmospheric composition if temperature, snow accumulation rate and snowpack ventilation were taken into account. More recent studies (Barret et al., 2011a,b) found that the kinetics of diffusion of HCHO and its thermodynamic equilibrium in ice need to be estimated in order to calculate the partitioning of HCHO between the atmospheric boundary layer and the snow and ice. Their air-ice equilibrium is the best match with the air-ice partitioning coefficients calculated from measurements of HCHO in air and snow at sites similar to WAIS Divide (Fig. 2). Their thermodynamic equilibrium relationship (Eq. 2) may then be used to reverse the preserved HCHO signal in the WAIS Divide ice core, while the kinetic processes can be neglected. Barret et al. (2011a) suggest that HCHO diffuses slowly into ice, between several days to several weeks, but our study aims to provide year-scale atmospheric estimates of HCHO.

The approach we used to calculate the past tropospheric mixing ratios of HCHO does not consider the possible photochemical production of HCHO in snow that contributes to the atmospheric budget (McNeill et al., 2012, and references therein). This production may, however, be negligible since the efficient absorption of UV radiation by snow leads to a negligible photochemical production in firn air when compared to the atmospheric production of HCHO (Hutterli et al., 1999).

When there is no evidence from the ice-core records (Fig. 4) that changes in accumulation or temperature directly impact on the preservation of HCHO in snow and ice, the snow pits data from the ITASE Traverses point to a nonlinear relationship (Fig. 5). This is consistent with the transfer model predictions of Hutterli (2003) and similar to the observations of Frey et al. (2006) for H_2O_2. The results for the WAIS Divide site that are presented in Figure 2 show that the HCHO concentrations in the top 1 m of snow of some sites of group 1 tend to not be at the thermodynamic equilibrium described by Barret et al. (2011b). The top 1 m snowpack of these sites, including WAIS Divide, are super-saturated which indicates a possible surface-snow degassing, and so slightly more HCHO may be preserved in snow than the concentrations predicted by the equilibrium. These observations suggest that the atmospheric HCHO predicted from the thermodynamic equilibrium function developed by Barret et al. (2011b) may be higher than it actually was during the early- to mid-Holocene. Therefore, this points to the need of developing a semi-empirical model of HCHO preservation constrained by the accumulation rate and the mean annual temperature, similar to the one Frey at al. (2006) established for H_2O_2.

The increase of both the ice-core H_2O_2 and accumulation rate over the early- to mid-Holocene (Fig. 4) is consistent with H_2O_2 preservation in snow being sensitive to

snow accumulation rate and particularly to accumulation timing (Frey et al., 2006; Hutterli, 2003). H_2O_2 is taken up by the snowpack during non-summer seasons, when the snow accumulation is highest but atmospheric H_2O_2 mixing ratios are lowest (Frey et al., 2006, and references therein). Then the increase of snow accumulation rate from 9,000 to 6,000 yr BP enhanced the uptake of atmospheric H_2O_2 in snow, contributing to the increase of its records in ice. The rise of ice-core records of H_2O_2 is then unlikely caused by a possible increase of atmospheric H_2O_2 mixing ratios, as confirmed by our atmospheric estimates (Fig. 7).

Both atmospheric H_2O_2 estimates, from the ice-core inversion and the modelE2, show a drop in concentration over the early- to mid-Holocene. Though H_2O_2 inferred from both procedures show more disparities than HCHO, the mixing ratios are still comparable with a difference of about 35% at 6,000 yr BP (28±6 vs. 43 pptv, Table 1), and of about 8% at 9,000 yr BP (45±9 vs. 49 pptv). As with HCHO, more measurement of H_2O_2 in sections above 1300 m depth, in the brittle ice, would be necessary to confirm the low H_2O_2 mixing ratios we inferred, in contrast to slightly higher values computed with ModelE2. Nevertheless, the relatively good consistence between the atmospheric estimates of HCHO and H_2O_2 based on the inversion of the WAIS Divide ice-core and from the GCM model validates the ModelE2 over the early- to mid-Holocene period.

5.2 Evaluation of the atmospheric oxidants

5.2.1 Total ozone column

Prior studies pointed to an inverse relationship between surface H_2O_2 and total ozone column (Lamarque et al., 2011) or stratospheric ozone (Frey et al., 2005). An increase of surface UV radiations from the decrease of total ozone column would enhance the ozone photolysis rate and the photolysis of nitrate in the surface snowpack, increasing the atmospheric NO_X emissions, and resulting in a rise of tropospheric OH and H_2O_2 (Frey et al., 2005). Thus, the atmospheric H_2O_2 and its record into the ice is a potential indicator of changes in the total ozone column.

The decrease of H_2O_2 mixing ratios observed between 9,000 and 6,000 yr BP points then to an increase of the total ozone column over this period. Based on a linear correlation between surface H_2O_2 and total ozone column observed by Frey et al. (2005), the 17 ppbv H_2O_2 decrease observed over these 3,000 yr period would potentially result from a 7 DU increase of the total ozone column.

The rise of total ozone column over this period is also supported by the decrease in UV radiations inferred from the decrease of sunspot numbers reconstructed from dendrochronologically ^{14}C measurements (Solanki et al., 2013), as from ^{10}Be ice-core records. This is also in agreement with the results of Vieira et al., 2011, whom reconstructed Total Solar Irradiance indicates a drop of about 1W/m^2 between 9,000 and 6,000 yr BP.

5.2.2 Radical Hydroxyl

The drop in OH concentrations over the early- to mid-Holocene period is consistent with the results from ModelE2 but not with our estimates based on Equation 6. In fact, when the OH estimates at 9,000 yr BP from both methods match, with a slight difference of 7%, the estimates at 6,000 yr BP show a difference in concentrations of about 52% (Table 1 and Fig. 7).

Three possible sources of error in our OH estimates are discussed here. First, the estimated OH concentrations present a high correlation with the atmospheric HCHO inferred from the ice-core signal that we used in Equation 6 (polynomial regression with R^2=0.972, data not shown). As mentioned above, we have no record prior to 6,085 yr BP and too few around this age. Analysis of HCHO from slightly shallower sections may provide a more-accurate OH estimate for the period of 6,000 yr BP, which might have matched with estimates from ModelE2. Considering the 2.1×10^5 molecules cm^{-3} OH concentrations from the ModelE2 output, and a CH_4 concentration of 577 ppbv, at 6,000 yr BP, an atmospheric HCHO of 11 pptv is estimated. This would lead to an expected HCHO concentration of about 0.4 ppbw (Eq. 2) in the WAIS Divide ice-core at 6,000 yr BP (about 1287.362 m depth).

This possible overestimation of the atmospheric HCHO concentrations at 6,000 yr BP may also be caused by the fact that our air-snow transfer function is temperature driven only, and does not integrate an accumulation rate dependence. Based on similar sensitivities of HCHO and H_2O_2 preservation in snow with temperature and snow accumulation rate on WAIS (Fig. 5 and 6), we compared the potential atmospheric H_2O_2 calculated with equation 4 and a constant accumulation rate, defined as the average of the accumulation rates inferred from the ice core section, with the concentrations presented in Figure 7. Though the results do not change significantly at ~9,000 yr BP, we observed a large increase of atmospheric H_2O_2 over 6,000 yr BP. Therefore, this suggests that the HCHO mixing ratios estimated over the 6,000 yr period from the temperature-dependence function may actually have been lower. Preliminary calculations reveal HCHO mixing ratios of about 10 pptv for this period. This will then lead to OH concentrations of about 2×10^5 molecules cm^{-3}.

A third error may result from our estimate of HCHO photolysis rate, j_{HCHO}, which follows an annual cycle based on present-day conditions (Section 2.2.4). The variability of Total Solar Irradiance (TSI) over the Holocene was recently investigated by several studies. Reconstructing the radiocarbon production from ^{14}C and CO_2 ice-core records Roth and Joos (2013, and references therein) revealed that TSI around 6,000 and 9,000 yr BP was probably lower by about 0.2 and 0.5 W/m^2, respectively, than today's value. The decrease of TSI computed by Vieira et al. (2011) from ^{14}C ice-core records is about 1% between 9,000 to 6,000 yr BP. Based on Madronich et al. (1998), this implies a increase of TOC of about 1%. A sensitivity study on total ozone column and hydroxyl radical concentrations revealed that a possible change of total ozone column in the order of 10 DU has then negligible effect on OH concentrations (~1%) through changes in photolysis rates. Also, it can also be expected that changes in TSI will impact less the high-latitude than the low-latitude regions. Thus, the variability of orbital parameters may

not be the main source of uncertainty in the estimation of tropospheric OH from the steady-state equation of HCHO production and loss.

Although additional data for 6,000 yr BP and both a temperature and accumulation rate dependent semi-empirical model are needed, we suggest that the early- to mid-Holocene was a period when atmospheric concentrations of H_2O_2 and OH decreased in response to a possible rise of the total ozone column. Because the combination of peroxyradicals (HO_2) is the main photolytic source of H_2O_2 while oxidation of carbon monoxide, CH_4 and non-methane hydrocarbons by OH is the main source of HO_2, our results also suggest that atmospheric HO_2 decreased between 9,000 to 6,000 yr BP.

If the CH_4 budget had been sink driven over the early- to mid-Holocene, CH_4 would have therefore increased over this period.

5.3 Impact on the CH_4 budget

The atmospheric concentrations of CH_4, presented in Table 1 and Figure 7, show clearly that it did not increase over the early- to mid-Holocene but it decreased almost constantly. For most of the period posterior to 9,000 yr BP, the OH concentrations calculated from the tropospheric estimates of HCHO and CH_4 are not consistent with the hypothesis of an increase of total ozone column.

If the steady-state assumption between HCHO production and loss (Eq. 6) was applied with the HCHO and OH concentrations from the ModelE2 outputs, it would result in a CH_4 concentration of about 787 ppbv. This represents a difference of 46% with the ModelE2 output and of 36% with the ice-core estimate. It would then imply that CH_4 had increased over the early- to mid-Holocene, which is against our observations. Thus, these results suggest that the oxidation by the radical OH can not directly explain the decline of CH_4 over the early- to mid-Holocene, so it can be assumed that this decline was mainly source driven.

In contrast to the previous finding, a comparable estimate of past atmospheric OH is obtained at 9,000 yr BP from the steady-state relationship of Staffelbach et al. (1991) and from the ModelE2. This suggests that CH_4 sink was more significant, so both source and sink may have controlled the budget of CH_4. From ice-core records presented in previous research (Sowers, 2010; Blunier et al., 1995), 9,000 yr BP corresponds to a near-end period of about 3000 yr when CH_4 concentrations were almost constant at about 700 ppbv. Therefore, it may be possible to extend our previous result and suggest that the relatively stable CH_4 concentrations between about 12,000-9,000 yr BP were source and sink driven. However, it is not possible to assess here the contribution of each control.

6 Conclusions

While the interpretation of reversibly deposited species in ice core has been under significant debate, reliable estimates of atmospheric photochemically reactive species for the early- to mid-Holocene were calculated from the unprecedented high-resolution

records of HCHO and H_2O_2 in the WAIS Divide ice core, and from the recent findings on the air-ice equilibrium functions of these chemical species.

These estimates provide regional- to global-scale data on the past Antarctic boundary layer. They first provide regional-scale information on the tropospheric composition of photochemically active species HCHO, H_2O_2, OH, and HO_2. Second, the interpretation of these estimates provide global-scale information on the changes of total ozone column, and help in defining the contribution of the CH_4 sink to the global decline of CH_4 between 9,000 to 6,000 yr BP is negligible. Because no major source of CH_4 is observed over the Antarctic continent, our result suggests that the global decline of CH_4 during the early- to mid-Holocene was controlled by its sources, mainly the reduction of wetland emissions at lower latitudes. The constant CH_4 concentrations between ~12,000 and ~9,000 yr BP are consistent with the estimates of HCHO and of the oxidative capacity, suggesting a contribution of both sink and source to the regional budget of atmospheric CH_4.

The atmospheric concentrations of HCHO and H_2O_2 inferred from the inversion of the ice-core records are in relatively good agreement with the mixing ratios computed by the ModelE2. This indicates that this global climate model is capable of reconstructing the atmospheric chemistry of the early- to mid-Holocene over West Antarctica. It may then be a reliable tool to infer and interpret the changes in atmospheric chemistry at global scale over this period.

Finally, the study of the preservation of HCHO in snow and ice over the interior of West Antarctica points to a significant sensitivity of deposited HCHO with accumulation rate and mean annual temperature. Though our atmospheric HCHO estimation from the ice-core record is based on a temperature-dependent relationship, it neglects any possible contribution from changes in accumulation rate over time, suggesting a possible misestimation of our calculated mixing ratios. Preliminary calculations suggest an overestimation of ~37% for HCHO and OH computed at 6,000 yr BP. The development of a semi-empirical model constrained by both mean annual temperature and accumulation rate is therefore needed to correctly infer atmospheric concentrations of HCHO from its record in snow and ice.

Acknowledgements. This work was supported by the National Science Foundation, Office of Polar Programs (OPP-0636929). We would like to thank T. Sowers for providing the methane records from the WAIS Divide ice core, and K. M. Cuffey for sharing the modeled surface temperature for the WAIS Divide site. We also would like to acknowledge all the people at DRI involved in the analysis of the WAIS Divide ice core for their constant support.

7 References

Alexander, B., Savarino, J., Barkov, N. I., Delmas, R. J., and Thiemens, M. H.: Climate driven changes in the oxidation pathways of atmospheric sulfur, Geophys Res Lett, 29, 30–1–30–4, 2002.

Banta, J. R., Mcconnell, J. R., Frey, M. M., Bales, R. C. and Taylor, K.: Spatial and temporal variability in snow accumulation at the West Antarctic Ice Sheet Divide over recent centuries, J Geophys Res, 113(D23), 1–8, 2008.

Barret, M., Domine, F., Houdier, S., Gallet, J.-C., Weibring, P., Walega, J., Fried, A., and Richter, D.: Formaldehyde in the Alaskan Arctic snowpack: Partitioning and physical processes involved in air snow exchanges, J Geophys Res- Atmos, 116, D00R03, 2011a.

Barret, M., Houdier, S., and Domine, F.: Thermodynamics of the Formaldehyde-Water and Formaldehyde-Ice Systems for Atmospheric Applications, J Phys Chem A, 115, 307–317, 2011b.

Betterton, E. A. and Hoffmann, M. R.: Henry's law constants of some environmentally important aldehydes, Environ Sci Technol, 22(12), 1415–1418, 1988.

Blunier, T., Chappellaz, J., Schwander, J., Stauffer, B., and Raynaud, D.: Variations in Atmospheric Methane Concentration During the Holocene Epoch, Nature, 374, 46–49, 1995.

Burkhart, J. F., Hutterli, M. A., and Bales, R. C.: Partitioning of formaldehyde between air and ice at -35˚C to -5˚ C, Atmos Environ, 36, 2157–2163, 2002.

Chappellaz, J., Bluniert, T., Raynaud, D., Barnola, J. M., Schwander, J., and Stauffert, B.: Synchronous changes in atmospheric CH_4 and Greenland climate between 40 and 8 kyr BP, Nature, 366, 443–445, 1993.

Ciais, P., Petit, J. R., Jouzel, J., Lorius, C., Barkov, N. I., Lipenkov, V., and Nicolaiev, V.: Evidence for an early Holocene climatic optimum in the Antarctic deep ice-core record, Clim Dynam, 6, 169–177, 1992.

Conklin, M. H., Sigg, A., Neftel, A., and Bales, R. C.: Atmosphere-Snow Transfer Function for H_2O_2: Microphysical Considerations, J Geophys Res, 98, 18 367–18 376, 1993.

Crutzen, P. J. and Brühl, C.: A model study of atmospheric temperatures and the concentrations of ozone, hydroxyl, and some other photochemically active gases during the glacial, the pre-industrial Holocene and the present, Geophys Res Lett, 20, 1047–1050, 1993.

Dong, S. and Dasgupta, P.: Fast fluorometric flow injection analysis of formaldehyde in atmospheric water, Environ Sci Technol, 21(6), 581–588, 1987.

Frey, M. M., Stewart, R. W., Mcconnell, J. R., and Bales, R. C.: Atmospheric hydroperoxides in West Antarctica: Links to stratospheric ozone and atmospheric oxidation capacity, J Geophys Res, 110, 1–17, 2005.

Frey, M. M., Bales, R. C. and Mcconnell, J. R.: Climate sensitivity of the century-scale hydrogen peroxide (H_2O_2) record preserved in 23 ice cores from West Antarctica, J Geophys Res- Atmos, 111(D21), D21301, 2006.

Fudge, T. J., Steig, E. J., Markle, B. R., Schoenemann, S. W., Ding, Q., Taylor, K. C., Mcconnell, J. R., Brook, E. J., Sowers, T., White, J. W. C., Alley, R. B., Cheng, H., Clow, G. D., Cole-Dai, J., Conway, H., Cuffey, K. M., Edwards, J. S., Lawrence Edwards, R., Edwards, R., Fegyveresi, J. M., Ferris, D., Fitzpatrick, J. J., Johnson, J., Hargreaves, G., Lee, J. E., Maselli, O. J., Mason, W., McGwire, K. C., Mitchell, L. E., Mortensen, N., Neff, P., Orsi, A. J., Popp, T. J., Schauer, A. J., Severinghaus, J. P., Sigl, M., Spencer, M. K., Vaughn, B. H., Voigt, D. E., Waddington, E. D., Wang, X. and Wong, G. J.: Onset of deglacial warming in West Antarctica driven by local orbital forcing, Nature, 500(7463), 440–444, 2013.

Grannas, A. M., Jones, A. E., Dibb, J., Ammann, M., Anastasio, C., Beine, H. J., Bergin, M., Bottenheim, J., Boxe, C. S., Carver, G., Chen, G., Crawford, J. H., Domin´e, F., Frey, M. M., Guzman, M. I., Heard, D. E., Helmig, D., Hoffmann, M. R., Honrath, R. E., Huey, L. G., Hutterli, M., Jacobi, H.-W., Klan, P., Lefer, B., McConnell, J., Plane, J., Sander, R., Savarino, J., Shepson, P. B., Simpson, W. R., Sodeau, J. R., Von Glasow, R., Weller, R., Wolff, E. W., and Zhu, T.: An overview of snow photochemistry: evidence, mechanisms and impacts, Atmos Chem Phys, 7, 4329–4373, 2007.

Hutterli, M. A., Rothlisberger, R., and Bales, R. C.: Atmosphere-to-snow-to-firn transfer studies of HCHO at Summit, Greenland, Geophys Res Lett, 26, 1691–1694, 1999.

Hutterli, M. A., Bales, R. C., Mcconnell, J. R., and Stewart, R.W.: HCHO in Antarctic snow: Preservation in ice-cores and air-snow exchange, Geophys Res Lett, 29, 1235, 2002.

Hutterli, M. A.: Sensitivity of hydrogen peroxide (H_2O_2) and formaldehyde (HCHO) preservation in snow to changing environmental conditions: Implications for ice-core records, J Geophys Res, 108, 1–9, 2003.

Hutterli, M. A., Mcconnell, J. R., Chen, G., Bales, R. C., Davis, D. D., and Lenschow, D.: Formaldehyde and hydrogen peroxide in air, snow and interstitial air at South Pole, Atmos Environ, 38, 5439–5450, 2004.

Jacobson, M. Z.: Fundamentals of Atmospheric Modeling, Cambridge University Press, second edition edn., 2005.

Kaplan, J. O., Folberth, G., and Hauglustaine, D. A.: Role of methane and biogenic volatile organic compound sources in late glacial and Holocene fluctuations of atmospheric methane concentrations, Global Biogeochem Cy, 20, GB2016–n/a, 2006.

Kaplan, J. O., Krumhardt, K. M., Ellis, E. C., Ruddiman, W. F., Lemmen, C., and Goldewijk, K. K.: Holocene carbon emissions as a result of anthropogenic land cover change, Holocene, 21, 775–791, 2011.

Lamarque, J.-F., J. R. McConnell, D. T. Shindell, J. J. Orlando, and G. S. Tyndall, Understanding the drivers for the 20th century change of hydrogen peroxide in Antarctic ice-cores, Geophys. Res. Lett., 38, L04810, 2011.

Lee-Taylor, J. and Madronich, S.: Calculation of actinic fluxes with a coupled atmosphere-snow radiative transfer model, J Geophys Res- Atmos, 107, 4796, 2002.

Levine, J. G.,Wolff, E.W., Jones, A. E., Hutterli, M. A.,Wild, O., Carver, G. D., and Pyle, J. A.: In search of an ice-core signal to differentiate between source-driven and sink-driven changes in atmospheric methane, J Geophys Res, 116, n–a–n–a, 2011a.

Li, J., Dasgupta, P., Genfa, Z. and Hutterli, M. A.: Measurement of atmospheric formaldehyde with a diffusion scrubber and light-emitting diode-liquid-core waveguide based fluorometry, Field Anal Chem Tech, 5(1-2), 2–12, 2001.

Loulergue, L., Schilt, A., Spahni, R., Masson-Delmotte, V., Blunier, T., Lemieux, B., Barnola, J.-M., Raynaud, D., Stocker, T. F., and Chappellaz, J.: Orbital and millennial-scale features of atmospheric CH_4 over the past 800,000 years, Nature, 453, 383–386, 2008.

Madronich, S., McKenzie, R. L., Björn, L. O. and Caldwell, M. M.: Changes in biologically active ultraviolet radiation reaching the Earth's surface, Journal of Photochemistry and Photobiology B: Biology, 46(1–3), 5–19, 1998.

Martinerie, P., Brasseur, G., and Granier, C.: The chemical composition of ancient atmospheres – A model study constrained by ice-core data, J Geophys Res- Atmos, 100, 14 291–14 304, 1995.

Mayewski, P. A., Rohling, E. E., Curt Stager, J., Karlén,W., Maasch, K. A., David Meeker, L., Meyerson, E. A., Gasse, F., van Kreveld, S., Holmgren, K., Lee-Thorp, J., Rosqvist, G., Rack, F., Staubwasser, M., Schneider, R. R., and Steig, E. J.: Holocene climate variability, Quaternary Research, 62, 243–255, 2004.

McGwire, K. C., Taylor, K. C., Banta, J. R. and Mcconnell, J. R.: Identifying annual peaks in dielectric profiles with a selection curve, J Glaciol, 57(204), 763–769, 2011.

McNeill, V. F., Grannas, A. M., Abbatt, J. P. D., Ammann, M., Ariya, P., Bartels-Rausch, T., Dominé, F., Donaldson, D. J., Guzman, M. I., Heger, D., Yr BPhan, T. F., Klan, P., Masclin, S., Toubin, C., and Voisin, D.: Organics in environmental ices: sources, chemistry, and impacts, Atmos Chem Phys, 12, 9653–9678, 2012.

Mitchell, L. E., Brook, E. J., Sowers, T., McConnell, J. R., and Taylor, K.: Multidecadal variability of atmospheric methane, 1000-1800 CE, J Geophys Res-Biogeo, 116, –, 2011.

Mitchell, L., Brook, E., Lee, J. E., Buizert, C., and Sowers, T.: Constraints on the Late Holocene Anthropogenic Contribution to the Atmospheric Methane Budget, Science, 342, 964–966, 2013.

Morse, D. L., Blankenship, D. D., Waddington, E. D., and Neumann, T. A.: A site for deep ice coring in West Antarctica: Results from aerogeophysical surveys and thermo-kinematic modeling, Ann Glaciol, 35, 36–44, 2002.

Murray, L. T., Mickley, L. J., Kaplan, J. O., Sofen, E. D., Pfeiffer, M., and Alexander, B.: Factors controlling variability in the oxidative capacity of the troposphere since the Last Glacial Maximum, Atmos Chem Phys Discuss, 13, 24 517–24 603, 2013.

Neftel, A., Jacob, P., and Klockow, D.: Longterm record of H_2O_2 in polar ice-cores, Tellus B, 38, 262–270, 1986.

Orsi, A. J., Cornuelle, B. D. and Severinghaus, J. P.: Little Ice Age cold interval in West Antarctica: Evidence from borehole temperature at the West Antarctic Ice Sheet (WAIS) Divide, Geophys Res Lett, 39(9), L09710, 2012.

Riedel, K., Weller, R., and Schrems, O.: Variability of formaldehyde in the Antarctic troposphere, Phys Chem Chem Phys, 1, 5523–5527, 1999.

Riedel, K.,Weller, R., Schrems, O., and Konig-Langlo, G.: Variability of tropospheric hydroperoxides at a coastal surface site in Antarctica, Atmos Environ, 34, 5225–5234, 2000.

Roth, R. and Joos, F.: A reconstruction of radiocarbon production and total solar irradiance from the Holocene ^{14}C and CO_2 records: implications of data and model uncertainties, Clim. Past, 9, 1879–1909, 2013.

Ruddiman, W. F.: The Anthropocene, Annual Review of Earth and Planetary Sciences, 41, 45–68, 2013.

Salmon, R. A., Bauguitte, S. J. B., Bloss, W., Hutterli, M. A., Jones, A. E., Read, K., and Wolff, E. W.: Measurement and interpretation of gas phase formaldehyde concentrations obtained during the CHABLIS campaign in coastal Antarctica, Atmos Chem Phys, 8, 4085–4093, 2008.

Sander, S., Friedl, R., Barker, J., Golden, D., Kurylo, M., Wine, P., Abbatt, J., Burkholder, J., Kolb, C., Moortgat, G., Huie, R., and Orkin, V.: Chemical Kinetics and Photochemical Data for Use in Atmospheric Studies, Evaluation Number 17, 2011.

Schmidt, G., DTT, S., and Harder, S.: Reply to comment by W.F. Ruddiman on "A note on the relationship between ice-core methane concentrations and insolation", Geophys Res Lett, 32, –, 2005.

Schmidt, G., Ruedy, R., Hansen, J., Aleinov, I., Bell, N., Bauer, M., Bauer, S., Cairns, B., Canuto, V., Cheng, Y., Del Genio, A., Faluvegi, G., Friend, A., Hall, T., Hu, Y., Kelley, M., Kiang, N., Koch, D., Lacis, A., Lerner, J., Lo, K., Miller, R., Nazarenko, L., Oinas, V., Perlwitz, J., Perlwitz, J., Rind, D., Romanou, A., Russell, G., Sato, M., DTT, S., Stone, P., Sun, S., Tausnev, N., Thresher, D., and Yao, M.: Present-day atmospheric simulations using GISS ModelE: Comparison to in situ, satellite, and reanalysis data, J Climate, 19, 153–192, 2006.

Schmidt, G. A., Kelley, M., Nazarenko, L., Ruedy, R., Russell, G. L., Aleinov, I., Bauer, M., Bauer, S. E., Bhat, M. K., Bleck, R., Canuto, V., Chen, Y.-H., Cheng, Y., Clune, T. L., Del Genio, A., de Fainchtein, R., Faluvegi, G., Hansen, J. E., Healy, R. J., Kiang, N. Y., Koch, D., Lacis, A. A., LeGrande, A. N., Lerner, J., Lo, K. K., Matthews, E. E., Menon, S., Miller, R. L., Oinas, V., Oloso, A. O., Perlwitz, J. P., Tausnev, N., Tsigaridis, K., Unger, N., Voulgarakis, A., Yao, M.-S., and Zhang, J.: Configuration and assessment of the GISS ModelE2 contributions to the CMIP5 archive, J. Adv. Model. Earth Syst., pp. n/a–n/a, 2014.

Seinfeld, J. H. and Pandis, S. N.: Atmospheric Chemistry and Physics, From Air Pollution to Climate Change, John Wiley & Sons Inc., 2006.

Shindell, D. n. T., Faluvegi, G., Unger, N., Aguilar, E., Schmidt, G. n. A., Koch, D. n. M., Bauer, S. n. E., and Miller, R. n. L.: Simulations of preindustrial, present-day, and 2100 conditions in the NASA GISS composition and climate model G-PUCCINI, Atmos Chem Phys, 6, 4427–4459, 2006.

Shindell, D. T., Pechony, O., Voulgarakis, A., Faluvegi, G., Nazarenko, L., Lamarque, J. F., Bowman, K., Milly, G., Kovari, B., Ruedy, R., and Schmidt, G. A.: Interactive ozone and methane chemistry in GISS-E2 historical and future climate simulations, Atmos Chem Phys, 13, 2653–2689, 2013.

Sigg, A., Fuhrer, K., Anklin, M., Staffelbach, T. and Zurmuehle, D.: A continuous analysis technique for trace species in ice cores, Environ Sci Technol, 28(2), 204–209, 1994.

Sigl, M., Mcconnell, J. R., Layman, L., Maselli, O., McGwire, K., Pasteris, D., Dahl-Jensen, D., Steffensen, J. P., Vinther, B., Edwards, R., Mulvaney, R., and Kipfstuhl, S.: A new bipolar ice-core record of volcanism fromWAIS Divide and NEEM and implications for climate forcing of the last 2000years, J Geophys Res- Atmos, 118, 1151–1169, 2013.

Singarayer, J. S., Valdes, P. J., Friedlingstein, P., Nelson, S., and Beerling, D. J.: Late Holocene methane rise caused by orbitally controlled increase in tropical sources, Nature, 470, 82–U91, 2011.

Solanki, S. K., Krivova, N. A., and Haigh, J. D.: Solar Irradiance Variability and Climate, Astron. Astrophys., 51, 311–351, 2013.

Sowers, T.: Atmospheric methane isotope records covering the Holocene period, Quaternary Science Reviews, 29, 213–221, 2010.

Sowers, T: Methane Concentrations from the WAIS Divide Ice Core (WDC06A), 60 to 11,300 ybp. [6,000-10,000 ybp]. Boulder, Colorado USA: National Snow and Ice Data Center. 2012.

Spahni, R., Schwander, J., Fluckiger, J., Stauffer, B., Chappellaz, J., and Raynaud, D.: The attenuation of fast atmospheric CH_4 variations recorded in polar ice-cores, Geophys Res Lett, 30, 1571, 2003.

Staffelbach, T., Neftel, A., Stauffer, B., and Jacob, D.: A record of the atmospheric methane sink from formaldehyde in polar ice-cores, Nature, 349, 603–605, 1991.

Thomas, E. R., Wolff, E. W., Mulvaney, R., Steffensen, J. P., Johnsen, S. J., Arrowsmith, C., White, J. W. C., Vaughn, B., and Popp, T.: The 8.2yr BP event from Greenland ice-cores, Quaternary Science Reviews, 26, 70–81, 2007.

Thompson, A., Chappellaz, J., and Fung, I.: The atmospheric CH4 increase since the Last Glacial Maximum, Tellus B, 1993.

Valdes, P. J., Beerling, D. J., and Johnson, C. E.: The ice age methane budget, Geophys Res Lett, 32, L02 704, 2005.

Vieira, L. E. A., Solanki, S. K., Krivova, N. A. and Usoskin, I.: Evolution of the solar irradiance during the Holocene, A&A, 531, A6, 2011.

Wolff, E. W., Hutterli, M. A., and Jones, A. E.: Past atmospheric composition and chemistry from ice-cores – progress and prospects, Environ Chem, 4, 211–216, 2007.

Wolff, E. W.: Chemical signals of past climate and environment from polar ice-cores and firn air, Chem Soc Rev, 41, 6247–6258, 2012.

8 Tables & Figures

Table 1. Comparison of the paleoatmospheric concentrations of OH, HCHO and H_2O_2 inferred from the WAIS Divide ice-core and from the GISS model for early and mid-Holocene periods. Averages over the 10 years surrounding 6,000 or 9,000 yr BP are reported with their standard deviations for the ice-core estimates.

	6000 yr BP		9000 yr BP	
	Ice-core estimate	Model estimate	Ice-core estimate	Model estimate
HCHO, pptv	16±2[a]	15	17±2	17
H_2O_2, pptv	28±6[b]	43	45±9	49
CH_4, ppbv	577±0.1	540	658±1	630
OH, 10^5 molecules cm^{-3}	3.2±0.5[a]	2.1	2.9±0.5	2.7

[a]estimate of the year 6085 yr BP
[b]estimate of the year 6095 yr BP

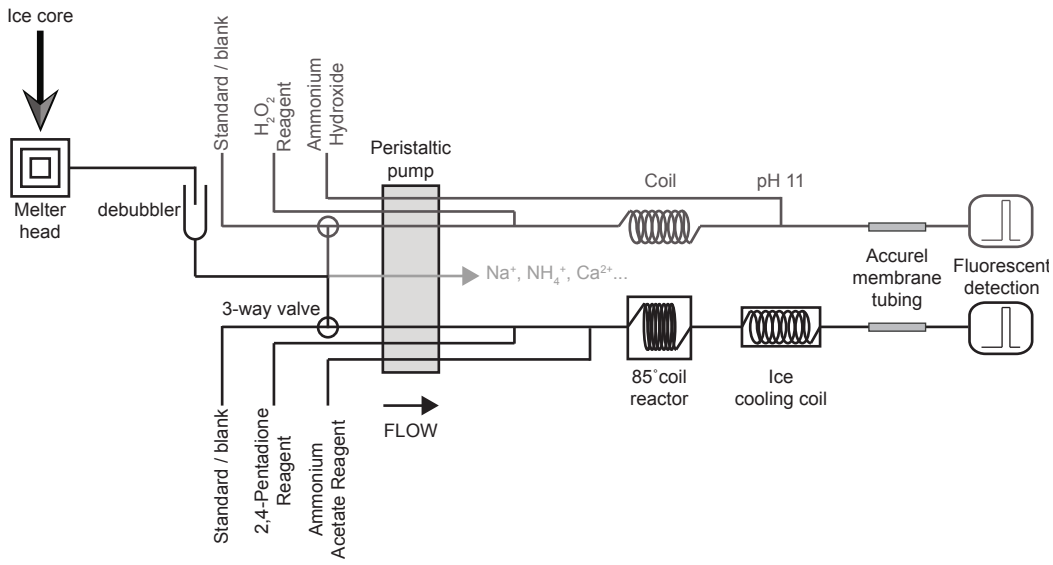

Figure 1. Partial schematics of the CFA system representing the HCHO and H_2O_2 channels custom-built by M. Frey under the ITASE grant (OPP-9814810) and used to analyze the WAIS-Divide ice-core.

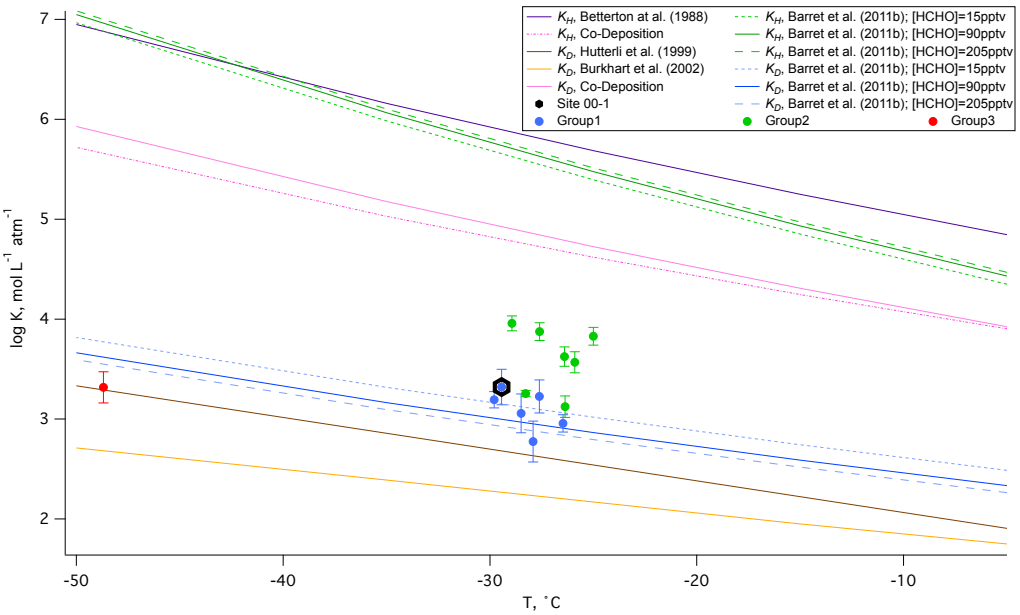

Figure 2. Reports of the air-liquid, K_H, and air-ice equilibrium, K_D, functions investigated by the cited studies, and of the atmosphere-snow partitioning coefficients calculated from measurements of HCHO in air and snow pits over WAIS (M. Frey, personal communication, 2006). The partitioning coefficients from Barret et al. (2011b) are calculated from their formula using the average and range of atmospheric HCHO observed during the ITASE Traverses. The partitioning coefficients of co-deposition are derived from the Clausius-Clapeyron equation for the saturation vapor pressure of water over a liquid surface or ice (Jacobson, 2005). The estimates of the partitioning coefficients from the WAIS measurements are clustered in 3 groups, based on differences in accumulation rates and temperatures (Frey et al., 2006), and the error bars represent the 1-σ uncertainty. With the smallest distance between both locations, the partitioning coefficient for site 00-1 (Group 1) is considered the best estimate for the WAIS Divide ice-core site.

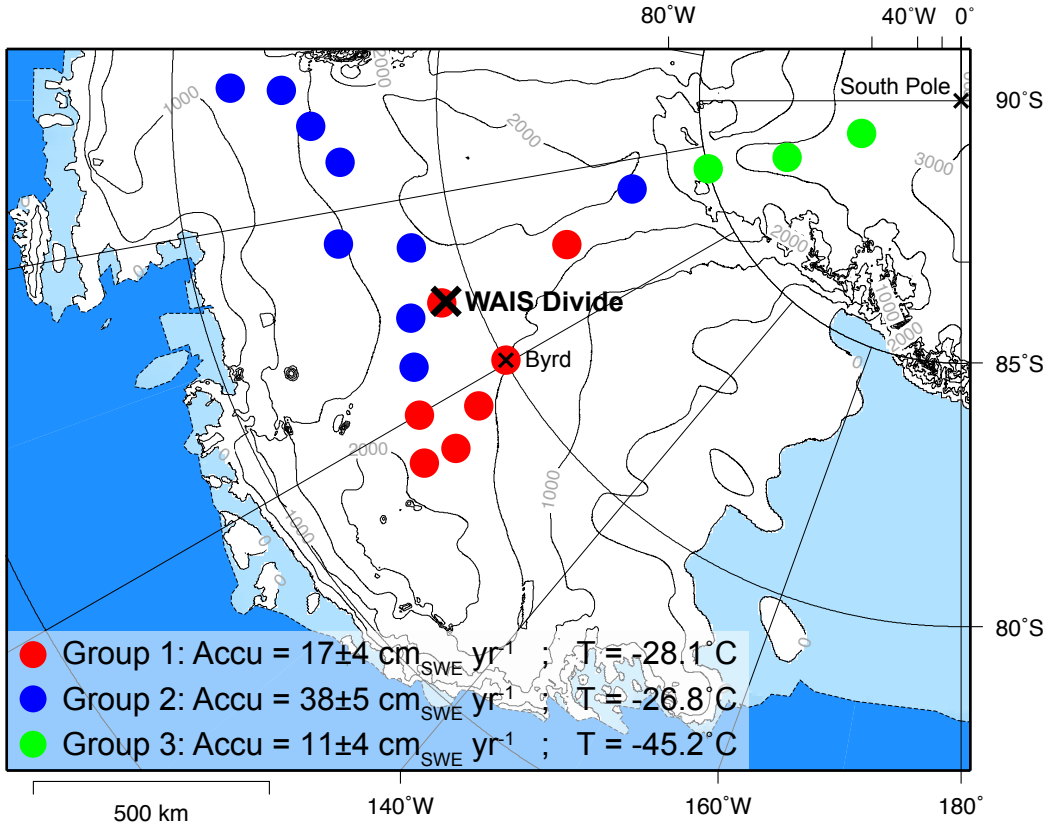

Figure 3. The West Antarctic shallow ice-core sites investigated during the U.S. ITASE traverse 1999-2002. Each site was grouped based on its average annual accumulation rate and temperature (Frey et al., 2006). The WAIS Divide deep ice-core site is also reported, along with Byrd and South Pole stations (black cross).

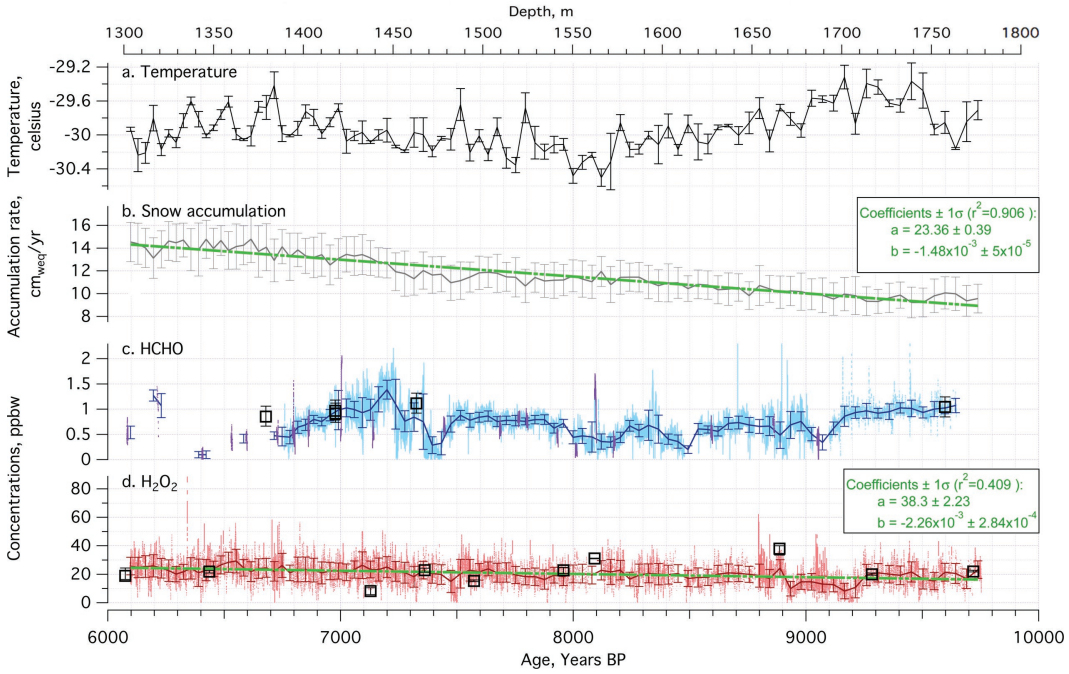

Figure 4. 5 meter averages of a) temperature and b) snow accumulation rates inferred from the WAIS Divide ice-core, and 2 mm resolution ice-core records of c) HCHO (blue dots) and d) H_2O_2 (red dots) measured between depths of 1301.92 and 1763.97 m. HCHO record from the ice-core replicates is shown in purple, and 5 m averages, corresponding to about 40 year averages, are reported for HCHO and H_2O_2 (dark blue and red circles). Bars represent the standard deviation of each average. The linear trends observed for both snow accumulation and H_2O_2 (green lines) are reported with the respective coefficients of correlation and coefficients of regression (y = bx + a). Finally, HCHO and H_2O_2 measured in the Byrd ice-core (79.983˚S, 120.017˚W, 1530m a.m.s.l) (Staffelbach et al., 1991; Neftel et al., 1986) are also reported to compare both site measurements (black squares).

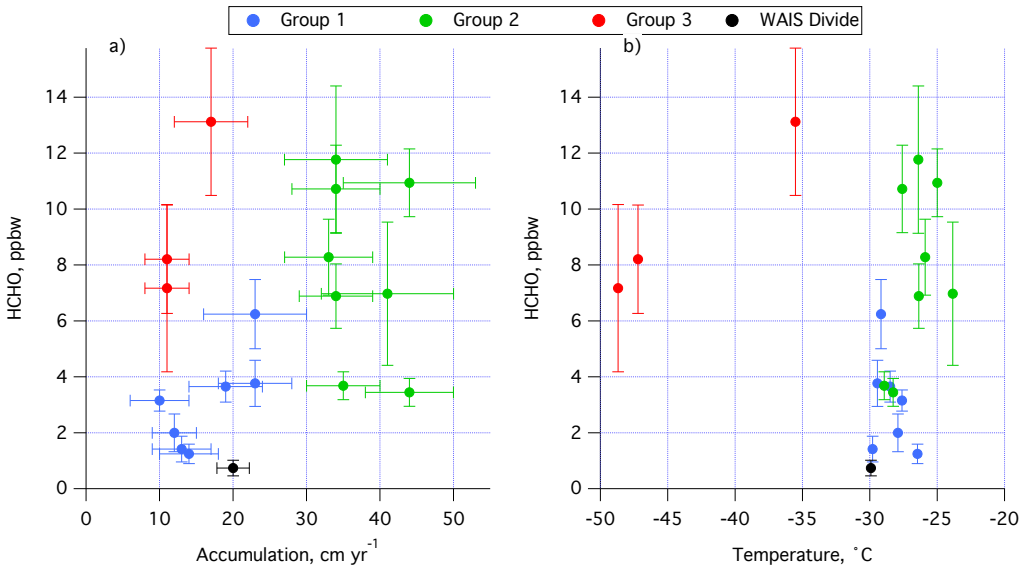

Figure 5. 1-year averages of HCHO, measured in 1-m snow pits over WAIS during the ITASE Traverses 2000 to 2002 (M. Frey, personal communication, 2006), as a function of a) accumulation rate and b) annual mean temperature. Each value of the three groups represents an average over the previous non-summer season. Groups are based on differences in accumulation rates and temperatures between sites (Frey et al., 2006). The average of temperature, accumulation rate and HCHO measured or estimated over the ice-core section is reported for the WAIS Divide site. Error bars represent the 1 σ uncertainty.

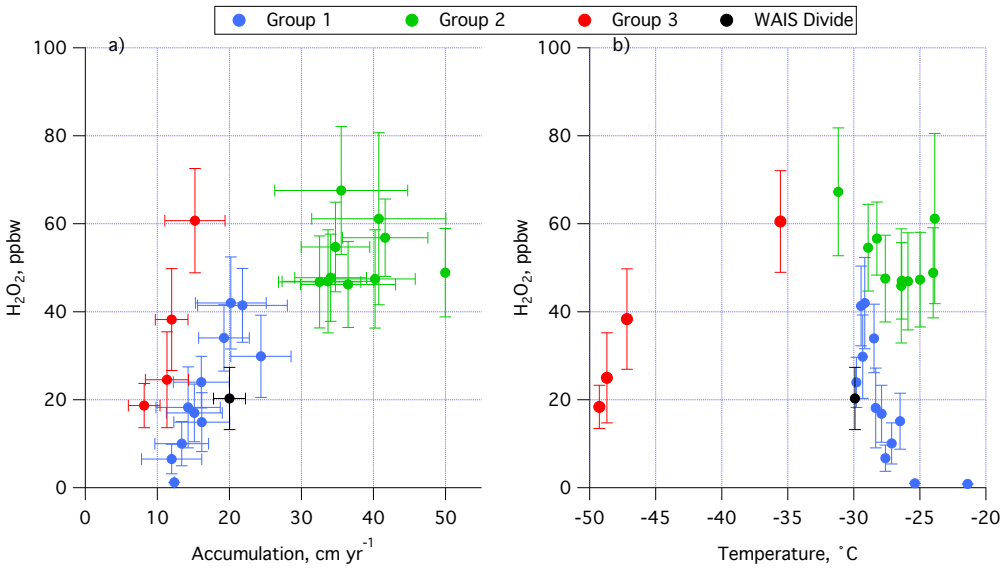

Figure 6. Observed 50-year averages of H_2O_2 between 1911-1960 as a function of a) accumulation rate and b) annual mean temperature from (Frey et al., 2006), within their respective groups. Like Figure 5, the WAIS Divide data points are averages of the measurements or estimates over the ice core section analyzed in this study. Error bars represent the 1 σ uncertainty.

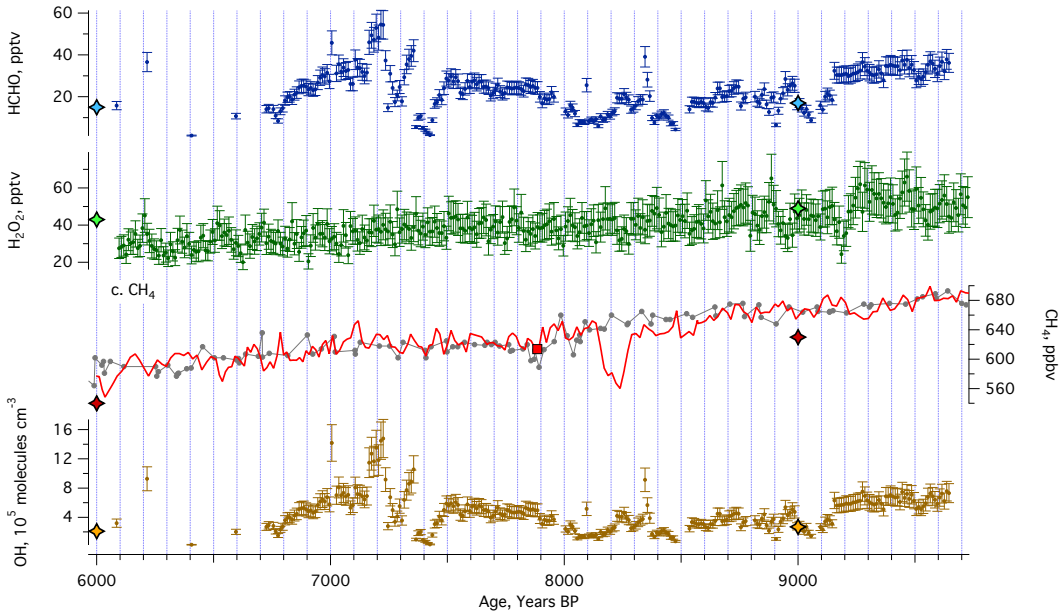

Figure 7. 10-year average data of past atmospheric concentrations of a) HCHO, b) H_2O_2, c) 1-year average CH_4, and d) 10-year average OH inferred from the WAIS Divide ice-core signals over the early to middle Holocene transition. Error bars represent the errors of propagation for each estimate. Atmospheric mixing ratios estimated from the GISS-GCM model are reported for each chemical species (stars). CH_4 records from Dome C (grey line and dots) and from Byrd (red square) are also reported for comparison.

CONCLUSION

The motivation of this research was to determine the sources of the photochemistry above the West Antarctic Ice Sheet (WAIS), by providing new or complementary observations to scarce existing datasets for this region, and use these results to interpret the misknown atmospheric photochemistry of the early-mid Holocene, reconstructed from ice-core analysis. Each chapter of this dissertation addresses one of these specific problems. First, the investigation of the current atmospheric chemistry above WAIS was done by measuring the chemical species involved into the photochemical cycle of NO_X with O_3 (atmospheric NO, O_3 and snow NO_3^- and NO_2^-), which led to identifying the sources of short- and long-lived species above the inner WAIS and quantify their impacts. Second, the potential control of the photochemical sink of CH_4 on its atmospheric budget over the early-to-mid Holocene was evaluated through the ice-core reconstruction of the past oxidative capacity of the atmosphere.

1 The WAIS atmospheric chemistry

The results from the atmospheric and snow measurements at the WAIS Divide site show values of NO, O_3, H_2O_2 and NO_3^- that are more in the range of those measured at coastal sites than those observed above the East Antarctic Plateau. The effective annual estimates of atmospheric HCHO and H_2O_2 from the WAIS Divide ice-core and the GCM model also reveal concentrations closer to those observed currently in winter on the Antarctic coast. These results suggest that local sources from snowpack emissions, and regional sources from the Antarctic coast and the inner WAIS are the main contributors of the photochemistry of the WAIS region.

2 Snowpack emissions and regional sources

The concentrations of NO_3^- in surface snow and in shallow snow pits reveal that possibly 30% of the nitrate deposited in snow will be preserved. A consequent portion of nitrate in surface snow is then expected to be emitting back in the atmosphere, mostly through photolysis. This preservation rate at the WAIS Divide site is significantly lower than at Summit, where most of NO_3^- is redeposited locally. A lower local redeposit is therefore expected for NO_3^- emitted by the surface snowpack of the WAIS region, which may then be removed by lateral export.

The significance of NO_3^- emissions contribution from snowpack was tested by comparing estimates of the potential production rate of NO_X from daily average depth-integrated emission fluxes of NO_X, with NO_X mixing ratios computed from the photostationary state. The comparable values indicate that photolysis of nitrate and nitrite in the surface snowpack is a significant source of NO_X in the WAIS region. Then, NO_3^- could be a

potential marker of the local NO_X concentration above the WAIS if better knowledge and constrain are acquired on its post depositional processes.

The calculations of local production of O_3 indicate that this oxidant is not significantly produced by in situ oxidation of CH_4, and instead point to regional sources. These calculations also assume negligible halogen chemistry in the WAIS atmosphere. This is supported by both the 4-day back-trajectory interpretation and satellite observations. This assumption and the back-trajectory analysis suggest that air masses from the Antarctic coast, where halogen chemistry occurs and depletes the local O_3, may contribute significantly to the budget of O_3 and other long-lived species above the WAIS region.

The results also show a limited contribution of air from the East Antarctic Plateau to the WAIS photochemistry. About 25% of all back-trajectory runs originated from this region during the campaign, but these air masses only raised the O_3 levels of WAIS Divide if they were transported near surface and in under 3 days from the East Antarctic Plateau. Thus, it is suggested that the record in snow and ice of photochemical intermediate species, such as HCHO and H_2O_2, may provide information of past pristine and remote atmosphere relevant for regional scale investigation

3 Estimates of paleoatmospheric HCHO and H_2O_2 from ice-core records

Because of the sensitivity of HCHO and H_2O_2 preservation in snow to changing environmental conditions, several studies pointed at the limitations in using reversibly deposited species as paleoatmospheric proxies. Being the first study using air-snow equilibrium functions developed by recent research, the results show that reliable atmospheric estimates of photochemically active species and radical species, such as OH and HO_2, can be reconstructed from ice-core records. Alike H_2O_2, the results for HCHO and OH of this study indicate that both temperature and snow accumulation rate are essential parameters that have to be taken into account to compute the atmospheric mixing ratios of these species. These atmospheric estimates allow then a more detailed investigation of the regional photochemistry, but also of the global photochemistry though the interactions of OH and HCHO with CH_4, and H_2O_2 with stratospheric O_3.

4 Photochemistry of the early- to mid-Holocene

Comparison between the estimates of atmospheric HCHO and H_2O_2, and the resulting OH assuming a steady state between HCHO loss and production, with the model outputs indicates that photochemistry contributed with the CH_4 sources to the atmospheric CH_4 at 9,000 ka. With a CH_4 concentration mostly constant between 12,000-9,000, it is suggested that both sink and sources were controlling the regional budget of CH_4.

At 6,000 ka, similar concentrations are inferred atmospheric HCHO, and smaller H_2O_2 mixing ratios from the ice-core than from the model are calculated, but both results

present a decrease of H_2O_2 between 9,000-6,000 ka. This decrease may be related to a decrease of total ozone column and a possible decrease of HO_2, the main source of H_2O_2. The resulting drop of OH concentration over the early-mid Holocene is supported by the model outputs but not from the ice-core estimates. This suggests that the CH_4 sink was a negligible driver of the CH_4 decline observed over this period.

5 Future work

This study provides the first observations of atmospheric NO above the West Antarctic Ice Sheet, includes a complementary atmospheric and snow photochemical dataset, and presents atmospheric oxidant and photochemical intermediate species inferred from ice-core records for the early-to-mid Holocene period.

When additional field measurements of photochemical species such as NO_2 or possibly HO_X could definitely help gain a better insight on the regional photochemistry, subsequent research should mainly focus on the air-to-snow transfer of the reversibly deposited species HCHO. The investigation described in Chapter 3 points at the uncertainty in estimating the air-ice equilibrium functions used for the preservation of HCHO in snow and ice. It is suggested here that an approach similar to Frey et al. (2006) should be followed to establish a semi-empirical model of the HCHO preservation in snow relevant for the WAIS Divide site. The model described in Chapter 3 is only temperature dependent, though the preservation of HCHO in snow is also sensitive to accumulation rate. Preliminary calculations based on the temperature and accumulation rate dependence revealed that our estimates of atmospheric HCHO tend to be overestimated at the higher accumulation rate observed around 6,000 yr BP. This further investigation would require the deployment of analytical instruments at the WAIS Divide site to measure concentrations of HCHO in the air, firn air, snow and in 5-6 m shallow ice-cores.